

South Dakota State University

## Open PRAIRIE: Open Public Research Access Institutional Repository and Information Exchange

---

Electronic Theses and Dissertations

---

2018

### Evaluation of the Moisture-Induced Damage Potential of Asphalt Mixes and Asphalt Binder-Aggregate Systems

Rajan Acharya  
South Dakota State University

Follow this and additional works at: <https://openprairie.sdstate.edu/etd>



Part of the [Civil Engineering Commons](#)

---

#### Recommended Citation

Acharya, Rajan, "Evaluation of the Moisture-Induced Damage Potential of Asphalt Mixes and Asphalt Binder-Aggregate Systems" (2018). *Electronic Theses and Dissertations*. 2682.  
<https://openprairie.sdstate.edu/etd/2682>

This Thesis - Open Access is brought to you for free and open access by Open PRAIRIE: Open Public Research Access Institutional Repository and Information Exchange. It has been accepted for inclusion in Electronic Theses and Dissertations by an authorized administrator of Open PRAIRIE: Open Public Research Access Institutional Repository and Information Exchange. For more information, please contact [michael.biondo@sdstate.edu](mailto:michael.biondo@sdstate.edu).

EVALUATION OF THE MOISTURE-INDUCED DAMAGE POTENTIAL OF  
ASPHALT MIXES AND ASPHALT BINDER-AGGREGATE SYSTEMS

BY

RAJAN ACHARYA

A thesis submitted in partial fulfillment of the requirements for the

Master of Science

Major in Civil Engineering

South Dakota State University

2018

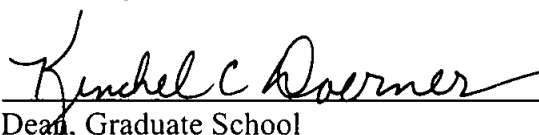
EVALUATION OF THE MOISTURE-INDUCED DAMAGE POTENTIAL OF  
ASPHALT MIXES AND ASPHALT BINDER-AGGREGATE SYSTEMS

RAJAN ACHARYA

This thesis is approved as a credible and independent investigation by a candidate for the Master of Science in Civil Engineering degree and is acceptable for meeting the thesis requirements for this degree. Acceptance of this does not imply that the conclusions reached by the candidate are necessarily the conclusions of the major department.

  
Rouzbeh Ghabchi, Ph.D.  
Thesis Advisor  
08/03/2018  
Date

  
Nadim Wehbe, Ph.D.  
Head, Department of Civil & Environmental Engineering  
August 3, 2018  
Date

  
Kenneth C. Doerner  
Dean, Graduate School  
3 AUG 2018  
Date

This thesis is dedicated to my beloved parents.

## ACKNOWLEDGEMENTS

Firstly, I would like to thank my mentor and thesis advisor, Dr. Rouzbeh Ghabchi for providing me the opportunity to be a part of this study. I would like to sincerely appreciate his guidance, support, and encouragement to complete this study. I would like to express my gratitude to Dr. Ghabchi for his marvelous motivation throughout my graduate study. His endless guidance and support in completing the study tasks and preparing my thesis are highly commendable.

I would like to thank for the financial support received from the Mountain Plains Consortium (MPC) and contributions of the Ingevity Co. which made this study possible. The material donations from Bowes Construction Co. and Jebro Co. are also highly appreciated. I am thankful to Mr. Chamika Prashan Dharmarathna and Mr. Buddhika Prasad Rajapaksha for helping me in the lab. Also, I would like to acknowledge my professors, Dr. Suzette Burckhard, Dr. Jonathan Wood, Dr. Michael Pawlovich, Dr. Allen Jones, and Dr. Cedric Neumann for sharing their knowledge with me through the coursework. I would also like to thank Mr. Zachary Gutzmer for his help with maintaining the laboratory equipment. I am thankful to all of my friends and relatives who supported me through this journey. Also, I am thankful to Ms. Lisa Enstad and other staff at the Department of Civil and Environmental Engineering, Graduate College, International Affairs and other offices in South Dakota State University.

## TABLE OF CONTENTS

ABBREVIATIONS .....	ix
LIST OF FIGURES .....	xii
LIST OF TABLES .....	xv
ABSTRACT .....	xvi
CHAPTER 1 INTRODUCTION .....	1
1.1 Background .....	1
1.2 Research Objectives .....	2
1.3 Study Tasks .....	3
CHAPTER 2 LITERATURE REVIEW .....	5
2.1 Moisture-induced Damage in Asphalt Mixes .....	5
2.2 Moisture-induced Damage Mechanisms .....	5
2.3 Evaluation of Moisture-induced Damage in Asphalt Mixes .....	6
2.3.1 Asphalt Mixes Containing WMA Additives .....	10
2.3.2 Asphalt Mixes Containing RAP .....	11
2.3.3 Asphalt Mixes Containing ASA .....	12
2.4 Evaluation of Moisture-induced Damage in Asphalt Binder-Aggregate Systems .....	14
2.4.1 Asphalt Binders Containing RAP Binders and Aggregates .....	15
2.4.2 Asphalt Binders Containing WMA Additives and Aggregates .....	16
2.4.3 Asphalt Binders Containing Antistripping Agent (ASA) and Aggregates .....	18
CHAPTER 3 MATERIALS AND METHODS .....	19
3.1 Materials .....	19
3.1.1 Aggregates .....	19

3.1.2	Asphalt Binders.....	20
3.1.3	Warm Mix Asphalt (WMA) Additives.....	20
3.1.4	Simulated RAP Binder (S-RAP).....	21
3.1.5	Liquid Antistripping Agent (ASA).....	21
3.1.6	Asphalt Mixes .....	22
3.2	Sample Preparation .....	25
3.2.1	Tensile Strength Ratio (TSR) and Indirect Tension Test (IDT) Samples.	25
3.2.2	Semicircular Bend (SCB) Samples.....	30
3.2.3	Binder Bond Strength (BBS) Samples.....	32
3.3	Laboratory Testing.....	35
3.3.1	Theoretical Maximum Specific Gravity ( $G_{mm}$ ).....	35
3.3.2	Bulk Specific Gravity ( $G_{mb}$ ) .....	37
3.3.3	Tensile Strength Ratio (TSR) Test.....	39
3.3.4	Indirect Tension Test (IDT).....	40
3.3.5	Semicircular Bend (SCB) Test.....	44
3.3.6	Binder Bond Strength (BBS) .....	47
CHAPTER 4 RESULTS AND DISCUSSIONS.....		52
4.1	Asphalt Mix Testing .....	52
4.1.1	Volumetric Tests.....	52
4.1.2	Performance Tests.....	52
4.1.2.1	<i>Tensile Strength Ratio Test (TSR) Results.....</i>	53
4.1.2.2	<i>Indirect Tensile Strength Test (IDT) Result.....</i>	57
4.1.2.3	<i>Semi-Circular Bend (SCB) Test Results .....</i>	62

4.2	Asphalt Binder-Aggregate Testing .....	71
4.2.1	Binder Bond Strength (BBS) Test Results.....	71
4.2.1.1	<i>Moisture-induced damage evaluation in granite-II aggregate with PG 58-28 binder .....</i>	<i>71</i>
4.2.1.2	<i>Moisture-induced damage evaluation in granite-II aggregate with PG 64-22 binder .....</i>	<i>76</i>
4.2.1.3	<i>Moisture-induced damage evaluation in granite-II aggregate with PG 64-34 binder .....</i>	<i>78</i>
4.2.1.4	<i>Moisture-induced damage evaluation in granite-II aggregate with PG 70-28 binder .....</i>	<i>80</i>
4.2.1.5	<i>Moisture-induced damage evaluation in quartzite aggregate with PG 58-28 binder .....</i>	<i>83</i>
4.2.1.6	<i>Moisture-induced damage evaluation in quartzite aggregate with PG 64-22 binder .....</i>	<i>85</i>
4.2.1.7	<i>Moisture-induced damage evaluation in quartzite aggregate with PG 64-34 binder .....</i>	<i>86</i>
4.2.1.8	<i>Moisture-induced damage evaluation in quartzite aggregate with PG 70-28 binder .....</i>	<i>88</i>
4.2.1.9	<i>Moisture-induced damage evaluation in granite-I aggregate with PG 58-28 binder .....</i>	<i>91</i>
4.2.1.10	<i>Moisture-induced damage evaluation in granite-I aggregate with PG 64-22 binder .....</i>	<i>93</i>



4.2.1.11	<i>Moisture-induced damage evaluation in granite-I aggregate with PG 64-34 binder .....</i>	94
4.2.1.12	<i>Moisture-induced damage evaluation in granite-I aggregate with PG 70-28 binder .....</i>	96
CHAPTER 5	CONCLUSIONS AND RECOMMENDATIONS .....	99
5.1	Conclusions.....	99
5.2	Recommendations.....	101

## ABBREVIATIONS

ASA	Antistripping Agent
AST	Asphalt Standard Tester
ASTM	American Society for Testing and Materials
AASHTO	American Association of State Highway and Transportation Officials
APA	Asphalt Pavement Analyzer
AV	Air Voids
AC	Asphalt Cement
AMPT	Asphalt Mixture Performance Tester
CAA	Coarse Aggregate Angularity
DSR	Dynamic Shear Rheometer
DM	Dynamic Modulus
3D	Three Dimensional
EBS	Ethylene Bis Stearamide
ESR	E* Stiffness Ratio
ESAL	Equivalent Single Axle Load
ERR	Energy Release Ratio
FIR	Fatigue Index Ratio
FT	Fischer-Tropsch
GC	Gyratory Compactor
G <sub>mb</sub>	Bulk Specific Gravity
G <sub>mm</sub>	Maximum Specific Gravity
HWTDT	Hamburg Wheel Tracking Device Test
HWT	Hamburg Wheel Tracking

HMA	Hot-Mix Asphalt
HDPE	High-Density Polyethylene
IDT	Indirect Tension
ITS	Indirect Tensile Strength
$J_c$	Critical Strain Energy Release Rate
LVE	Linear Viscoelastic
LWT	Loaded Wheel Tracking
LVECD	Layered Viscoelastic Continuum Model
MTS	Mechanical Testing System
MIST	Moisture-Induced Stress Testing
NMAS	Nominal Maximum Aggregate Size
PAV	Pressure Aging Vessel
PG	Performance Grade
PATTI	Pneumatic Adhesion Tensile Testing Instrument
POTS	Pull Off Tensile Strength
PS	Pull-off Strength
PSR	Pull-of Strength Ratio
PE	Polyethylene
PPA	Poly-phosphoric Acid
PS	Pelletized Surfactant
PAC	Polymerized Asphalt Cement
RAP	Reclaimed Asphalt Pavement
RoAM	Raveling of Asphalt Mixes
RA	Rejuvenating Agent

RAS	Reclaimed Asphalt Shingles
RMS	Retained Marshall Stability
RSM	Response Surface Methodology
SCB	Semicircular Bend
SFE	Surface Free Energy
SB	Styrene-Butadiene
SBS	Styrene-Butadiene-Styrene
SD	South Dakota
SMA	Stone Mix Asphalt
SPT	Simple Performance Test
SP	Superpave <sup>®</sup>
SBR	Styrene-Butadiene Rubber
S-VECD	Simplified Viscoelastic Continuum Model
S-RAP	Simulated RAP
TSR	Tensile Strength Ratio
TB	Terminal Blend
TIR	Toughness Index Ratio
USA	United States of America
UTM	Universal Testing Machine
VR	Viscosity Reducer
VG	Viscosity Grading
VMA	Voids in Mineral Aggregates
WMA	Warm-Mix Asphalt
WTT	Wheel Tracking Test
WB	Water-bearing

## LIST OF FIGURES

Figure 3-1 Collection of HMA-Lime asphalt mix from an overlay project on I-90 near Brandon, SD.....	23
Figure 3-2 Collection of HMA-RAP mix from a parking lot construction project on SDSU's main campus (Brookings, SD).....	23
Figure 3-3 Collection of C-WMA mix from asphalt plant located in Minnesota used for reconstruction of a runway project in (Webster, SD) .....	24
Figure 3-4 Asphalt mix in the oven ready for reheating.....	27
Figure 3-5 Hand mixing of asphalt mix.....	28
Figure 3-6 Compaction of asphalt mix by Superpave® gyratory compactor (SGC).....	28
Figure 3-7 Tensile strength ratio (TSR) sample extraction from SGC mold.....	29
Figure 3-8 Vacuum saturation chamber.....	30
Figure 3-9 Thawing chamber.....	30
Figure 3-10 Rock saw used prepare semicircular specimens .....	31
Figure 3-11 Saw used to cut a notch in semicircular specimens .....	32
Figure 3-12 Semicircular specimens.....	32
Figure 3-13 Preparation of flat pieces from aggregate chunks .....	34
Figure 3-14 Surface preparation .....	34
Figure 3-15 Surface Cleaning .....	35
Figure 3-16 $G_{mm}$ test details (a) $G_{mm}$ test setup (b) loose asphalt mix before testing (c) transferring of the loose mix into the pycnometer .....	36
Figure 3-17 Water tank .....	38
Figure 3-18 Tensile strength ratio (TSR) testing using MTS .....	40

Figure 3-19 Tensile strength ratio (TSR) specimen after testing.....	40
Figure 3-20 Indirect tension (IDT) test plots (a) Typical tensile stress vs deformation plot (b) Typical normalized tensile stress vs strain (%) curve .....	42
Figure 3-21 Semicircular bend (SCB) test using AST.....	45
Figure 3-22 Semicircular (SCB) specimen after testing .....	45
Figure 3-23 Typical load-deformation plots for SCB test conducted on samples with different notch depths .....	46
Figure 3-24 Typical load vs deformation curve with area representing strain energy .....	47
Figure 3-25 Binder bond strength (BBS) test component of PATTI device: (a) PATTI device and quantum gold software; (b) F-2 piston type, talc powder, magnifying lens, pull stub-connector.....	48
Figure 3-26 Typical asphalt binder-aggregate BBS sample .....	49
Figure 3-27 Dry BBS samples inside the environmental chamber at 25°C.....	49
Figure 3-28 Binder bond strength test set up of dry asphalt binder-aggregate sample.....	50
Figure 3-29 Moisture conditioning of BBS samples .....	51
Figure 3-30 Test (BBS test) setup for moisture-conditioned asphalt-aggregate samples.	51
Figure 4-1 Tensile strength (TSR) test result of the asphalt mixes.....	54
Figure 4-2 Photographic view of failure surfaces observed in HMA-Lime mix after conducting TSR test on (a) unconditioned sample (b) moisture-conditioned sample .....	56
Figure 4-3 Photographic view of failure surfaces observed in HMA-RAP mix after conducting TSR test on (b) moisture-conditioned sample.....	57
Figure 4-4 Photographic view of failure surfaces observed in C-WMA mix after conducting TSR test on (a) unconditioned sample (b) moisture-conditioned sample .....	57

Figure 4-5 Typical tensile stress-deformation plot obtained from IDT test .....	58
Figure 4-6 Toughness indices/ratios determined for different mixes .....	60
Figure 4-7 Fatigue indices/ratios determined for different mixes .....	62
Figure 4-8 Strain energy release rate of different asphalt mixes .....	64
Figure 4-9 Visual failure pattern in HMA-Lime after conducting SCB test (a) unconditioned sample (b) moisture-conditioned sample .....	66
Figure 4-10 Visual failure pattern in HMA-RAP after conducting SCB test (a) unconditioned sample (b) moisture-conditioned sample .....	66
Figure 4-11 Visual failure pattern in C-WMA after conducting SCB test (a) unconditioned sample (b) moisture-conditioned sample .....	66
Figure 4-12 Correlations between the SCB, IDT, and TSR test result (a) unconditioned samples (b) moisture-conditioned samples (c) ratio of the parameter for moisture- conditioned to unconditioned samples.....	70
Figure 4-13 Comparison of pull-off strength of different binders with granite-II.....	74
Figure 4-14 Failure modes in BBS test.....	76
Figure 4-15 Comparison of pull-off strength between quartzite and different binders ....	83
Figure 4-16 Comparison of pull-off strength between granite-I and different binders ....	91

## LIST OF TABLES

Table 3-1 Types and the sources of the aggregates collected for BBS test.....	19
Table 3-2 Types of the WMA additive collected for BBS test.....	21
Table 3-3 Type of the ASA collected for preparing samples for BBS test.....	22
Table 3-4 Sources and types of the collected asphalt mixes.....	24
Table 3-5 Sources and location of the plant produced asphalt mixes.....	25
Table 4-1 Summary of the tensile strength ratio (TSR) test result .....	53
Table 4-2 Indirect tension (IDT) test result analysis of the asphalt mixes .....	59
Table 4-3 Critical strain energy release rate ( $J_c$ ) and $J_c$ ratio values from SCB test.....	63
Table 4-4 Binder bond strength test results for various asphalt binders with granite-II...	73
Table 4-5 Binder bond strength test results for various asphalt binders with quartzite....	82
Table 4-6 Binder bond strength test results for various asphalt binders with granite-I....	90
Table 4-7 Resistance to moisture-induced damage based on average PSR.....	98



## ABSTRACT

## EVALUATION OF THE MOISTURE-INDUCED POTENTIAL OF ASPHALT MIXES

## AND ASPHALT BINDER-AGGREGATE SYSTEMS

RAJAN ACHARYA

2018

The current thesis presents the findings of a study conducted on asphalt mixes to evaluate their moisture-induced damage potential through testing of the plant produced asphalt mixes in South Dakota using local aggregates and commonly used asphalt binders. The moisture-induced damage potentials of the asphalt mixes were evaluated by conducting tensile strength ratio (TSR) and modified Semicircular Bend (SCB) tests. The effect of moisture on asphalt binder-aggregate adhesion was evaluated by conducting binder bond strength (BBS) test on binder-aggregate systems. The asphalt mixes tested in this study included a hot mix asphalt (HMA) containing hydrated lime (1% by the weight of aggregates), asphalt mix containing an amine-based warm mix asphalt (WMA) additive (0.5% by the weight of mix), and asphalt mix containing reclaimed asphalt pavement (RAP) (20% by the weight of aggregates). Asphalt binder-aggregate adhesion evaluation plan comprised of testing sixteen types of asphalt binder blends, namely PG 64-34, PG 64-22, PG 58-28, and PG 70-28, blended with simulated RAP binder, an amine-based antistripping agent (ASA), and an amine-based WMA additive. The BBS tests were conducted on combinations of the binder blends with three types of aggregates, namely quartzite, granite-I, and granite-II. A total of forty eight combinations of asphalt binder-aggregate systems were tested. Tensile strength ratio obtained from TSR test, critical strain energy release rate, and energy release ratio (ERR) obtained from modified SCB

test, and pull-off strength obtained from BBS test for unconditioned and moisture-conditioned samples were used to evaluate the moisture-induced damage. The indirect tension (IDT) test results were used to perform a fracture energy analysis of the TSR samples in dry and moisture-conditioned states to explore the feasibility of applying this method for evaluating the moisture-induced damage utilizing parameters such as toughness index, toughness index ratio (TIR), fatigue index and fatigue index ratio (FIR). The result showed that the asphalt mixes tested in this study met the minimum TSR requirement set by the Superpave<sup>®</sup> mix design method. The critical strain energy release rate of HMA for both dry and moisture-conditioned samples were found to be lower than the range recommended by the ASTM D8044-16 standard (ASTM, 2016). For the asphalt mix containing RAP and the asphalt mix containing WMA additive, the critical strain energy release rate values of dry and moisture-conditioned samples were found to meet the minimum values recommended by the ASTM D8044-16 standard (ASTM, 2016). The ERR and FIR values calculated for all mixes were found to be greater than one, indicating no decrease in their resistance to cracking after moisture-conditioning. The TIR values calculated for the mixes were found to be less than one for HMA mixes but greater than one for the mix containing RAP, and the mix containing WMA additive. The pull-off strength ratio (PSR) obtained from BBS tests showed that PG 58-28 binder containing 20% RAP by the weight of the binder with granite-I had a higher moisture-induced damage potential compared to other asphalt binder-aggregate systems tested in the study. The PG 64-34 binder containing 0.5% ASA with granite-I, and PG 58-28 binder containing 0.5% WMA additive with granite-II were found to have higher PSR than the other asphalt binder-aggregate combinations tested in the current study. The

findings of this study are expected to help engineers and the asphalt industry select asphalt binders and aggregates which are more compatible in order to minimize moisture-induced damage in asphalt mixes.

## CHAPTER 1 INTRODUCTION

### 1.1 Background

Moisture-induced damage is known as the degradation of the strength and durability of the asphalt mix in the presence of the water (LaCroix et al., 2016). Moisture-induced damage, described as the loss of bond between binder and aggregate or within asphalt binder/mastic interface itself (Huang et al., 2010), has been considered as one of the commonly occurring distresses in the asphalt pavements (Kim et al., 2008). Field testing of the asphalt mixes to evaluate their moisture-induced damage can take long time with an uncertainty of obtaining consistent results (Kim et al., 2012). Recent developments have enabled the asphalt industry to use various laboratory equipment and test methods for evaluating the performance of asphalt mixes in the laboratory (e.g. Hossain et al., 2014; Ozer et al., 2016; Yang et al., 2016).

The current industry practice used to screen the asphalt mixes for their moisture-induced damage potential is to conduct tests that are not necessarily mechanistic and may not represent field conditions and damage mechanisms (e.g. Ahmad et al., 2014; Tarefder et al., 2017). Therefore, in many cases, these tests underestimate or overestimate the resistance of the asphalt mixes to moisture-induced damage, when compared to field observations (e.g. Tarefder et al., 2015; Wen et al., 2016). Different techniques including digital imaging, surface wave techniques and developing finite element models are applied to analyze and simulate the moisture-induced damage phenomenon in the asphalt mixes (e.g. Barnes et al., 2010; Kim, 2011; Lee et al., 2013). Therefore, the major challenge is to develop methods for evaluating the moisture-induced damage potential in

asphalt mixes which are more mechanistic and can better correlate with the field conditions an asphalt pavement may experience during its service life. During the last two decades, with introduction of different asphalt technologies, new materials and methods for producing asphalt mixes have become available which are economically efficient and environmentally sustainable (e.g. Ghabchi et al., 2015; Ghabchi et al., 2016). Among them, warm mix asphalt (WMA), asphalt mixes containing reclaimed asphalt pavement (RAP), and asphalt mixes containing antistripping agents (ASA) have gained popularity across the pavement industry (Mogawer et al., 2013). However, methods used for evaluation of the moisture-induced damage in asphalt mixes are developed and verified for the traditional HMA mixes. Therefore, evaluation of the moisture-induced damage potential of the WMA mixes and HMA mixes containing RAP and ASA are of significant importance.

In view of the significance and importance of the moisture-induced damage as a costly distress, further research is needed to assess the moisture-induced damage potential of the asphalt mixes by using methods that have a mechanistic base and can represent the failure mechanisms in the field.

## 1.2 Research Objectives

Specific objectives of this study are as follows:

1. Characterize moisture-induced damage potential of asphalt mixes used in South Dakota and Upper Midwest region;

2. Evaluate the effect of using warm-mix asphalt (WMA), anti-stripping agent (ASA), and reclaimed asphalt pavement (RAP) on moisture-induced damage potential of mixes;
3. Evaluate of the moisture-induced damage potential of the asphalt binder-aggregate systems using mechanistic method;
4. Study the feasibility of applying innovate test methods in assessing moisture-induced damage potential of the asphalt mixes.

### 1.3 Study Tasks

Specific tasks to be carried in the study are as follows:

1. Collect three types of plant-produced asphalt mixes, including an HMA mix containing a PG 64-34 asphalt binder and 1% hydrated lime with a nominal maximum aggregate size (NMAS) of 12.5 mm, an asphalt mix containing a PG 58-28 asphalt binder and 20% RAP (NMAS = 12.5 mm), and an asphalt mix containing a PG 64-34 asphalt binder and 0.5% of a chemical WMA additive (NMAS = 12.5 mm). These mixes are commonly used in South Dakota and elsewhere in Upper Midwest region;
2. Compact asphalt mixes, prepare test specimens and conduct TSR tests in accordance with (AASHTO, 2010) on unconditioned and moisture-conditioned specimens;
3. Compact asphalt mixes, prepare test specimens and conduct SCB tests in accordance with (AASHTO, 2013a) on unconditioned and moisture-conditioned specimens;

4. Collect four types of asphalt binders, namely PG 58-28, PG 64-22, PG 64-34, PG 70-28, three types of aggregates, namely granite-I, quartzite, granite-II, and asphalt additives, namely an amine based WMA additive, an amine-based ASA, and a PAV-aged PG58-28 asphalt binder (simulated RAP binder);
5. Conduct BBS tests in accordance with AASHTO TP-XX-11 (AASHTO, 2011) using a pneumatic adhesion tensile testing instrument (PATTI) on unconditioned and moisture-conditioned asphalt binder-aggregate samples;
6. Compare the result of the TSR, SCB, and IDT tests (using fracture energy approach);
7. Evaluate the effect of asphalt binder type, aggregate type, and additive type on adhesion of the asphalt binder with aggregates in moisture-conditioned and unconditioned states;
8. Evaluate the effectiveness of the applied test methods for assessing the moisture-induced damage potential of the aggregates-binder systems and mixes in presence of different additives.

## CHAPTER 2 LITERATURE REVIEW

### 2.1 Moisture-induced Damage in Asphalt Mixes

Moisture-induced damage in an asphalt mix occurs as a result of loss of adhesion between asphalt binder and aggregate or loss of cohesion in asphalt binder in the presence of the water (Caro et al., 2008). The air voids and other discontinuities in the asphalt mix allows water to penetrate in the pavement (Lu et al., 2007). Often the term stripping is used for moisture-induced damage governed by material properties (nature of the asphalt and aggregates, the proportion of the asphalt and aggregate), environmental factors (traffic loading, freeze-thaw action, precipitation, and humidity) and construction factors (air voids, weather condition during the construction) (Cho et al., 2010). Also, other forms of distresses, namely fatigue cracking, potholes, and rutting are accelerated as a result of moisture-induced damage (Huang et al., 2010).

### 2.2 Moisture-induced Damage Mechanisms

To describe the mechanism of the moisture-induced damage, different approaches such as contact angle, pore water pressure, surface energy, spontaneous emulsification, and chemical and mechanical reaction have been suggested and studied by several researchers (e.g. Caro et al., 2008; Cho et al., 2010; Varveri et al., 2015). Moisture-induced damage process is known to be accelerated due to pore water pressure buildup under the wheel load repetitions in combination with environmental factors and interaction of clay minerals in aggregate with water (Cho et al., 2010). Aggregates, due to high surface energy, have high tendency to absorb water than the asphalt binder leading to an adhesive failure of the asphalt binder-aggregate bond in presence of the water (Cho et al.,



2010). Adhesion failure is observed if the contact angle of aggregate-water interface is less than that for asphalt-water interface (Bhasin et al., 2006). Varveri et al. (2015) explained the separation of the aggregates from the binder with mechanisms such as detachment, displacement, spontaneous emulsification, pore pressure development, and hydraulic scouring. According to this study, moisture enters the asphalt binder-aggregate interface by molecular diffusion. Also, detachment occurs by separation of the uncracked binder film from aggregate in the presence of water. Furthermore, displacement occurs by disruption of the asphalt film in presence of water. Moreover, spontaneous emulsification occurs without thermal and mechanical energy exchange. Hydraulic scouring occurs by action of the tire in the saturated pavement leading to abrasion of the asphalt binder from the aggregate, losing the contact and dislodging from the pavement (Varveri et al., 2015).

Mineral additives like hydrated lime contain calcium which reacts with aluminates and silicates of the aggregates forming a strong bond in presence of the water (Varveri et al., 2015). Liquid additives like amine group additives act as Lewis base that acquires some protons from an acidic group of the asphalt binders which is suitable for reducing the surface tension of the asphalt binders. Adhesion at asphalt binder-aggregate interface depends upon pH and chemical reaction between the functional group of the aggregates and asphalt binder (Varveri et al., 2015).

### 2.3 Evaluation of Moisture-induced Damage in Asphalt Mixes

Several studies have been carried out to characterize the moisture-induced damage potential of the asphalt mixes by conducting dynamic modulus test (e.g. Chen et al.,

2008; Jahromi, 2009; Barnes et al., 2010; Huang et al., 2010; Weldegiorgis et al., 2015). The dynamic moduli of the moisture-conditioned HMA samples were found to be lower than those measured for the unconditioned samples. In other studies, various researchers (e.g. Tarefder et al., 2012; Ahmad et al., 2014; Amelian et al., 2014; Kakar et al., 2015; Kim et al., 2015; Varveri et al., 2015; Weldegiorgis et al., 2015) have evaluated moisture-induced damage of HMA mixes by conducting TSR test in accordance with the conditioning method described in AASHTO T 283 (AASHTO, 2010) test method. The tensile strength ratio obtained from TSR test was found to be less than one. Moisture-induced damage was found to decrease the tensile strength of the asphalt mixes.

The HMA samples subjected to long-term conditioning were found to show further decrease in the tensile strength (e.g. Chen et al., 2008; Varveri et al., 2016). Tarefder et al. (2015) found that fair correlation exists between tensile strength ratio obtained from TSR test conducted with AASHTO T 283 method (AASHTO, 2010) of moisture conditioning in the laboratory and permeability of pavements when measured in the field. Additionally, moisture-induced stress tester (MIST) has been used for moisture conditioning of the TSR samples (Ahmad et al., 2017). However, no correlation was found to exist between the permeability of pavements measured in the field and the tensile strength ratio obtained from MIST-conditioned samples (Tarefder et al., 2015).

Digital imaging technique was applied by Amelian et al. (2014) to evaluate the moisture-induced damage potential of the asphalt mixes by boiling water test. It was found that the percentage of the stripping in HMA samples obtained from image analysis is linearly

related to the tensile strength ratio obtained from TSR test. Behiry (2013) after conducting Marshall Stability test on HMA samples found that resilient modulus decreased after moisture conditioning. Some researchers have conducted dynamic shear rheometer test on dry and moisture-conditioned HMA samples and found that the debonding potential of the asphalt mixes increased after moisture conditioning (e.g. Hossain et al., 2014; Ahmad et al., 2017).

Several researchers have conducted Hamburg wheel tracking test (HWT) test to evaluate moisture-induced damage potential of the asphalt mixes (e.g. Mogawer et al., 2011; Cui et al., 2015; Ghabchi et al., 2015; Kim et al., 2015; Wen et al., 2016). They have found that, after attaining stripping inflection point, the moisture-induced damage potential of the HMA samples increases as the creep slope of the of the line obtained by plotting rut depth and number of wheel passes decreases.

A number of laboratory and field studies have been carried out to evaluate the fracture resistance of the asphalt mixes (e.g. Mohammad et al., 2012; Kim et al., 2015; Lopez-Montero et al., 2016; Saha et al., 2016a; Saha et al., 2016b). However, few researchers (e.g. Gong et al., 2012; Yang et al., 2016) have analyzed the moisture-induced damage potential of the asphalt mixes using fracture energy methods. They have found that fracture energy of the hot mix asphalt decreases after moisture conditioning. The SCB test was found to be the most reliable test method to determine the fracture energy of the asphalt mixes (e.g. Gong et al., 2012; Saha et al., 2016a). Kim (2011) found that SCB test is the most accurate laboratory test method for characterizing the fracture energy of the

asphalt mixes. An increase in the strain energy release rate of HMA samples in SCB test was found to result in a reduction in fatigue cracking rate in the field (Mohammad et al., 2012). Huang et al. (2013) after conducting SCB samples, found that different types of asphalt binders have different fracture resistant behavior in the HMA. Asphalt binders with higher performance grades were found to show higher fracture resistance. Ozer et al. (2016) found that fracture resistance increases with an increase in the temperature and applied load.

A number of studies have been conducted by several researchers to simulate the moisture-induced damage of the asphalt mixes using laboratory data and finite element modeling methods (e.g. Kringos et al., 2007; Kringos et al., 2008a; Kringos et al., 2008b; Caro et al., 2010; Kim, 2011; Das et al., 2015). Kringos et al. (2007) simulated the molecular diffusion of the moisture in the asphalt mixes and separation of the mastic from the aggregate created by pumping action of the traffic loads in asphalt pavements. It was found that the physical-mechanical processes such as pumping action facilitates diffusion of the moisture and accelerates the moisture-induced damage. In an another study, Kringos et al. (2008a) applied finite element modeling and concluded that the non-moisture-induced damages like settlements, cracks, and aging can occur before the moisture-induced damage. From the similar study, Kringos et al. (2008b) found that mastic weakening is due to moisture diffusion and erosion of the mastic caused by higher pressure gradients finally causes cohesive failure. Aggregate-mastic bond weakening was observed due to continuous moisture diffusion leading to adhesive failure (Kringos et al., 2008c).

Caro et al. (2010) incorporated the moisture diffusion and mechanical loading in a micromechanical finite element model and found that asphalt samples with higher moisture content have higher deformations, longer cracks, and lower load carrying capacity. Cohesive failure was found to develop at the dry condition and adhesive failure due to effect of moisture conditioning. Kim (2011) found that rate-dependency and temperature-sensitivity of the asphalt binder in a mix can be incorporated in finite element models. The combined effect of the moisture-induced damage and oxidative damage in the asphalt mixes was evaluated by Das et al. (2015) using finite element modeling. Moisture diffusion and oxidation were modeled and their effects on adhesion and cohesion bonding were evaluated. It was found that aging may result in a higher moisture-induced damage potential.

### 2.3.1 Asphalt Mixes Containing WMA Additives

A high variability in moisture-induced damage potential of asphalt mixes containing different types of WMA additives has been reported in the literature (e.g. Xiao et al., 2009; Bennert et al., 2011; Mogawer et al., 2011; Gong et al., 2012; Kim et al., 2012; Lee et al., 2013). Xiao et al. (2009) evaluated the moisture-induced damage potential of the asphalt mixes containing WMA additives, namely Asphamin and Sasobit using ITS and TSR tests. It was found that indirect tensile strength, and tensile strength ratio values were not significantly affected by addition of the WMA additives. In a similar study by Kim et al. (2012), after conducting SCB and TSR tests it was reported that HMA has higher resistance to moisture-induced damage than the asphalt mix containing WMA additives. Both the fracture energy, and tensile strength were found to be higher for HMA

mixes than those for mixes containing WMA additives. Also, the field performance of the asphalt mixes containing WMA additives were found to be poorer than that of the HMA with regard to moisture-induced damage.

In an another study, Mogawer et al. (2011) evaluated the moisture-induced damage potential of the asphalt mixes containing WMA additives, namely Advera, Evotherm, Sasobit, and Sonne by conducting HWT test. The moisture-induced damage potential of the asphalt mixes were found to be insignificantly affected by the addition of the WMA additives. Sasobit was found to increase the moisture-induced damage potential of the asphalt mixes. In a study conducted by Wasiuddin et al. (2008) it was found that addition of aspha-min reduced the moisture-induced damage potential of the asphalt mixes. Ghabchi et al. (2015) after conducting Hamburg wheel tracking test reported that asphalt mixes containing Evotherm WMA additive are resistant to moisture-induced damage. Wen et al. (2016) in a similar study found that, rutting resistance of HMA is same as asphalt mix containing WMA additives. Xiao et al. (2009) reported that the dry and wet ITS values were not affected by the addition of the WMA additives.

### 2.3.2 Asphalt Mixes Containing RAP

A number of studies conducted to evaluate the moisture-induced damage potential of the asphalt mixes containing RAP showed that the results can vary depending on the test methods, RAP source, aggregate type, binder source, and other factors. (e.g. Ghabchi et al., 2014; Cong et al., 2016; Ghabchi et al., 2016; Fakhri et al., 2017a; Fakhri et al., 2017b; Singh et al., 2017).

Mogawer et al. (2013) evaluated the moisture-induced damage potential of asphalt mixes containing RAP by conducting SCB test and found that asphalt mixes without RAP have a higher fracture resistance than the asphalt mixes containing RAP. Yang et al. (2016) after conducting the SCB test, found that fracture resistance of the asphalt mixes containing RAP decreased after moisture conditioning. Ozer et al. (2016), and Singh et al. (2017) conducted SCB tests on asphalt mixes and found an increase in fracture resistance and a decrease in moisture-induced damage potential of asphalt mixes after addition of RAP. In an another study, Ghabchi et al. (2016) evaluated the moisture-induced damage potential of the asphalt mixes containing RAP by TSR and HWT tests. The TSR test results showed that addition of RAP increased the moisture-induced damage of the asphalt mixes. However, from HWT test result it was found that moisture-induced damage decreased with an increase in the RAP content. In a study conducted by Cong et al. (2016), it was found that the both moisture-induced damage potential and rutting resistance of the asphalt mixes increased as a result of addition of RAP to mixes. Fakhri et al. (2017b) after conducting wheel tracking test on the asphalt mixes found that moisture-induced damage potential decreases with addition of RAP in both aged and unaged asphalt mixes.

### 2.3.3 Asphalt Mixes Containing ASA

The asphalt mixes containing liquid antistripping agents, hydrated lime, and fly ash have been studied by a number of researchers in the past (e.g. Chen et al., 2008; Kim et al.,

2008; Jahromi, 2009; Huang et al., 2010; Mogawer et al., 2011; Behiry, 2013; Abuawad et al., 2015; Zhang et al., 2017).

Mallick et al. (2005) conducted indirect tensile strength test on the asphalt mixes containing hydrated lime and found that addition of the hydrated lime decreased the moisture-induced damage potential of the asphalt mixes. LaCroix et al. (2016) in a similar study found that addition of ASA to the asphalt mixes provided a higher resistance to moisture-induced damage than the HMA without any ASA. However, hydrated lime was found to be less effective in reducing moisture-induced damage potential than the liquid ASA. Similar findings were obtained after conducting boiling water test by Nazirizad et al. (2015) on the asphalt mixes containing hydrated lime and liquid ASA.

Chen et al. (2008) studied the effect of adding amine-based ASA on HMA by conducting dynamic modulus test, Superpave<sup>®</sup> IDT creep test, and resilient modulus test. It was found that addition of the amine-based ASA to HMA reduced the moisture-induced damage potential of the asphalt mixes. In an another study, Behiry (2013) evaluated the moisture-induced damage potential of asphalt mixes containing hydrated lime and Portland cement. Addition of the hydrated lime and Portland cement was found to decrease the moisture-induced damage potential of the asphalt mixes. However, hydrated lime was found to be better in increasing the resistance of the mix to moisture-induced damage than the Portland cement. Kim et al. (2008) found that the effect of lime used in the form of dry powder or slurry on moisture-induced damage of the mix is different.



After conducting TSR, HWT, and APA tests on the asphalt mixes, it was found that for an increased number of freeze-thaw cycles, the lime slurry has a better anti-stripping effect than dry lime when added to a mix.

In another study conducted by Jahromi (2009) it was found that adding hydrated lime to mix increased the dynamic modulus value of the HMA. Huang et al. (2010) in a similar study, found that the dynamic modulus and tensile strength of HMA increased after addition of the fly ash kiln dust and lime to the HMA. In other study, Amelian et al. (2014) evaluated the moisture-induced damage potential of the asphalt mixes based on digital image analysis and it was found that the ASA in an asphalt mix effectively reduced the moisture-induced damage potential of the HMA.

#### 2.4 Evaluation of Moisture-induced Damage in Asphalt Binder-Aggregate Systems

A number of researchers have evaluated moisture-induced damage potential of asphalt binder-aggregate systems (e.g. Copeland et al., 2007; Moraes et al., 2011; Apeagyei et al., 2015; Lu et al., 2017). Apeagyei et al. (2015) evaluated moisture-induced damage potential of the asphalt binder-aggregate systems by conducting BBS test on four different aggregates, namely granite, limestone, basalt, and greywacke with asphalt mastics prepared by an asphalt binder with a penetration grade of 40/60. It was found that moisture-induced damage is higher in granite than the limestone due to higher absorption and higher diffusion in the granite-mastic sample. Adhesive failure was found to be observed after moisture-conditioning. In a similar study, Copeland et al. (2007) evaluated moisture-induced damage potential of the PG 52-34, PG 64-28, and PG 70-22 asphalt

binders with and without eight binder modifications. It was found that adhesive strength of the asphalt binders decreases after moisture conditioning. Use of modified binders was not found to necessarily decrease the moisture-induced damage potential.

In an another study, Moraes et al. (2011) conducted BBS test on granite and limestone aggregates with modified asphalt binders and found that pull-off tensile strength (POTS) is higher in unconditioned samples and it decreases after moisture conditioning. The failure mode was found to change from the cohesive to adhesive due to the moisture-induced damage. The POTS values were found to be higher in the modified binders with increased adhesion with the aggregate and cohesion within binder. In a atomistic simulation study conducted by Lu et al. (2017) to evaluate the nanoscale effect of the moisture on asphalt binder-aggregate bond, it was found that chemical properties of the aggregates are more dominant parameters in the separation of the binder and aggregates than chemical properties of the asphalt binder. Limestone was found to be a better aggregate in reducing moisture-induced damage potential than the quartzite due to nonpolar-surface in the limestone and polar silica in the quartz.

#### 2.4.1 Asphalt Binders Containing RAP Binders and Aggregates

Few studies have been conducted in the past to evaluate the moisture-induced damage potential of the binder containing RAP-aggregate systems. Canestrari et al. (2014) conducted BBS tests on an artificial RAP substrate in wet and dry conditions. Basalt and limestone aggregates were tested with the binders, namely base binder, soft binder, medium binder, and hard binder. The percentage reduction in the pull-off tensile strength

was found to be higher to lower in the basalt, limestone, coated basalt and coated limestone in a decreasing order of magnitude. Addition of RAP to the binders was found to decrease the moisture-induced damage potential. The pull off tensile strength was observed to be higher in basalt at dry condition and higher in limestone at wet condition. In an another study, Ghabchi et al. (2014) applied surface free energy approach to evaluate the moisture-induced damage potential of the asphalt binders containing RAP. Two types of asphalt binders, namely PG 64-22 (non-polymer modified) and PG 76-28 (polymer-modified), were tested with limestone, rhyolite, sandstone, granite, gravel, and basalt aggregates. The RAP binder with a concentration of 0%, 10%, 25% and 40% by the weight of asphalt mix was mixed with neat binders. It was found that addition of the RAP increased the non-polar surface free energy (SFE) component, and base SFE component, and decreased the acid SFE component. Work of adhesion was found to increase with an increase in the RAP content. The de-bonding potential of the aggregate in the presence of water was found to reduce with an increase in the RAP content.

#### 2.4.2 Asphalt Binders Containing WMA Additives and Aggregates

Wasiuddin et al. (2008) evaluated the moisture-induced damage potential of asphalt mixes containing WMA additives, namely Sasobit, Aspha-min, and paraffin wax, by determining the adhesion and wettability of the asphalt binder-aggregate systems by applying the SFE method. The amount of the additives were varied for different samples. The PG 64-22, and PG 70-28 binders containing WMA additives were tested with limestone and sandstone aggregates. It was found that, Sasobit reduces the adhesion force between the aggregate and binder with increased wettability. Aspha-min additive was

found to decrease the wettability of the asphalt binder-aggregate systems. The moisture-induced damage potential of the PG 70-28 binder was found to be higher than PG 64-22 containing Sasobit. However, addition of Aspha-min was found to decrease the moisture-induced damage potential of the PG 70-28 binder with aggregates.

In an another study, Wasiuddin et al. (2011) found that PG 64-22 binder containing Sasobit produced a mixed mode of failure without a change in significance strength. However, PG 76-22 binder (polymer-modified binder) exhibited adhesive failure. Alavi et al. (2012) conducted binder bond strength test to evaluate the moisture-induced damage in the granite and rhyolite aggregates with PG 64-22 and PG 76-22 binders blended with WMA additives. The binder containing WMA additive was found to have a higher moisture-induced damage potential than the neat binder. The reduction in temperature was found to be the primary reason for moisture-induced damage in WMA. Use of rhyolite aggregate was found to result in have a higher moisture-induced damage potential than of the granite with non-modified binders.

Recently, Cucalon et al. (2017) evaluated the mastic phase of the HMA and WMA using surface free energy approach. Unaged and PAV-aged samples of PG 64-22 and PG 76-22 binders with and without WMA additives, namely Sasobit, Evotherm, and Rediset were tested with gabbro and limestone aggregates. It was found that moisture-induced damage decreases with the aging of the WMA. Limestone aggregate was found to have a higher resistance to moisture-induced damage than gabbro aggregate. However, in the dry

condition, PG 64-22 binder was found to have higher bond strength than PG 76-22 binder with gabbro, and limestone aggregates.

#### 2.4.3 Asphalt Binders Containing Antistripping Agent (ASA) and Aggregates

Kanitpong et al. (2005) conducted BBS test on the asphalt binder-aggregate systems consisted of a PG 58-28 binder with and without ASA with granite and limestone aggregates. The polymers used for modification were styrene-butadiene (SB), styrene-butadiene-styrene (SBS), and elvaloy. The pull-off strengths of the asphalt binder-aggregate samples were found to decrease after moisture-conditioning. The modified binders were found to have a higher pull-off strength than the base binder. Also, modified binder showed higher bond strength than the binders containing ASA. The pull of strength of the binders containing ASA was nearly the same under dry and wet condition, indicating improvement in adhesion with addition of ASA. In a different study, Wasiuddin et al. (2010) applied surface energy approach to test the asphalt binders and aggregates with and without styrene-butadiene rubber (SBR) using universal sorption device. Sandstone and limestone aggregates were used in the test. Both unconditioned and moisture-conditioned samples were evaluated. It was found that addition of the SBR increased the moisture-induced damage potential. However, due to the acidic nature of the sandstone, adhesion energy was found to increase with addition of SBR, providing a better adhesion than samples prepared using limestone aggregate.

## CHAPTER 3 MATERIALS AND METHODS

### 3.1 Materials

This section presents an overview of the materials tested in the present study including their collection and properties.

#### 3.1.1 Aggregates

Aggregate is the collective term used for defining mineralogical materials, namely sand, gravel, and crushed stone. Due to their availability and desirable physical, chemical, mechanical and mineralogical properties, the aggregates are being used in asphalt mixes for the road construction s. However, the difference in the sources and other properties of the aggregates leads to a difference in their quality, durability, strength, and applicability for being used in asphalt mixes.

In the current study, granite-I, quartzite and granite-II (Table 3-1) aggregates with an approximately 300 mm diameter were collected and cut to the pieces with smaller sizes flat surfaces for preparing samples to conduct BBS tests.

Table 3-1 Types and the sources of the aggregates collected for BBS test

<b>Aggregate</b>	<b>Geological Origin</b>	<b>Quarry Location</b>	<b>Visual Appearance</b>
<b>Granite-I</b>	Igneous, intrusive	Brookings, SD	Reddish brown
<b>Quartzite</b>	Metamorphic	Sioux Falls, SD	Red
<b>Granite-II</b>	Igneous, intrusive	Brookings, SD	Bluish brown

The granite-I had a reddish brown color and granite-II was bluish brown. Granite-I and granite-II consisted of quartz mineral bonded with alumina and silica. Quartzite had a red appearance and consisted of the quartz minerals bonded with silica.

### 3.1.2 Asphalt Binders

Asphalt binder is a dark, black, and viscoelastic hydrocarbon residue obtained by distillation of the crude petroleum (HMA Construction, 2001). Asphalt binder is used as an adhesive to bond the aggregates to each other in the asphalt mix. Asphalt binder due to its viscoelastic nature has a time- and temperature-dependent mechanical behavior. Four different types of asphalt binders, namely PG 58-28, PG 64-22, PG 64-34, and PG 70-28 were collected from a local material supplier in South Dakota and were used for preparing the specimens for conducting BBS tests.

### 3.1.3 Warm Mix Asphalt (WMA) Additives

The WMA additives are added to the asphalt mix to increase its workability at low production and compaction temperatures, compared to those of the HMA. One type of an amine-based chemical WMA additive was collected from its supplier and used in this study. According to its manufacturer, the additive is designed to lower the emissions, thermal segregations, reduce binder content, enable the mix to incorporate higher amount of RAP and RAS in production of asphalt mixes.

Table 3-2 Types of the WMA additive collected for BBS test

<b>WMA additive</b>	<b>Type</b>	<b>Form</b>
<b>Amine-based</b>	Chemical	Liquid

#### 3.1.4 Simulated RAP Binder (S-RAP)

The S-RAP binder used in this study was produced by conducting the short-term and long-term aging procedures on a PG 58-28 asphalt binder in the laboratory in accordance with AASHTO T 240 standard method and AASHTO R 28 standard practice, respectively (AASHTO, 2013). This method represents the laboratory simulation of the asphalt binder aged in a pavement's service life that may be extracted from RAP. The pressure aging vessel (PAV) simulates the in-service aging of 7 to 10 years of an asphalt binder through exposing it to heat and air pressure (Pavement-Interactive, 2018).

#### 3.1.5 Liquid Antistripping Agent (ASA)

Liquid antistripping agent (ASA) is a chemical additive used in the asphalt mixes to increase their resistance to moisture-induced damage. Antistripping agent improves the adhesion of the aggregates and binders. Both liquid and mineral form of the additives are used in practice. Hydrated lime is the most commonly used mineral antistripping agent. The liquid antistripping agent used in the current study is an amine-based chemical collected from its supplier (Table 3-3).



Table 3-3 Type of the ASA collected for preparing samples for BBS test

<b>Antistripping agent</b>	<b>Type</b>	<b>Form</b>
Amine-based	Chemical	Liquid

### 3.1.6 Asphalt Mixes

Asphalt mix is prepared by mixing the aggregates and liquefied asphalt binder at high temperature. Superpave<sup>®</sup> volumetric mix design method is widely-accepted mix design method in practice. Asphalt mix design consists of the selection of the appropriate asphalt binder type, aggregate gradation and determination of an optimum asphalt binder content while meeting the volumetric requirements based on traffic and climate data. Asphalt mixes tested in the current study were produced in asphalt plants and collected from different construction projects. The collected mixes were transported to asphalt laboratory at South Dakota State University (SDSU), then reheated in an oven, compacted and tested in the laboratory. Three types of asphalt mixes were collected for this study: (1) an HMA mix containing a PG 64-34 asphalt binder, mainly quartzite aggregate and 1% hydrated lime (HMA-Lime); (2) an HMA mix containing a PG 58-28 asphalt binder, mainly quartzite and granite-II aggregates, and 20% RAP (HMA-RAP); and (3) a WMA mix containing a PG 64-34 asphalt binder, mainly granite-I and granite-II aggregates, and 0.5% of an amine-based chemical WMA additive (C-WMA). All mixes had a nominal maximum aggregate size (NMAS) of 12.5 mm. The details of collected mixes are presented in Table 3-4. The HMA-Lime was collected in August, 2017 from an asphalt overlay project at I-90 near Brandon, South Dakota (Figure 3-1). The HMA-RAP mix was collected in September, 2017 from a parking lot construction

project in SDSU campus in Brookings, South Dakota (Figure 3-2). The C-WMA mix was collected in October, 2017 from an asphalt plant located in Minnesota used for runway 12/30 reconstruction project in Webster, South Dakota (Figure 3-3).



Figure 3-1 Collection of HMA-Lime asphalt mix from an overlay project on I-90 near Brandon, SD



Figure 3-2 Collection of HMA-RAP mix from a parking lot construction project on SDSU's main campus (Brookings, SD)



Figure 3-3 Collection of C-WMA mix from asphalt plant located in Minnesota used for reconstruction of a runway project in (Webster, SD)

Table 3-4 Sources and types of the collected asphalt mixes

Asphalt Mix Name	Asphalt Mix Type	Binder Grade	NMAS* (mm)	Location
<b>HMA-Lime</b>	HMA+ 1% Hydrated Lime	PG 64-34	12.5 mm	Brandon, South Dakota
<b>HMA-RAP</b>	HMA+ 20% RAP	PG 58-28	12.5 mm	Brookings, South Dakota
<b>C-WMA</b>	HMA+ 0.5% amine-based WMA additive	PG 64-34	12.5 mm	Webster, South Dakota

\*NMAS = Nominal Maximum Aggregate Size

### 3.2 Sample Preparation

This section describes the procedures and standards followed for preparing the samples for the TSR, SCB, and BBS tests. The letters and numbers used for labeling of the prepared samples are shown in Table 3-5.

Table 3-5 Sources and location of the plant produced asphalt mixes

<b>Letter Code</b>		<b>Meaning</b>
<b>B</b>	1	Source1 (I-90 project)
	2	Source2 (Parking lot project)
	3	Source3 (Runway reconstruction project)
<b>M</b>	1	HMA without any additive
	2	HMA containing 20% RAP
	3	HMA containing 0.5% WMA additive
<b>T</b>	1	SCB test
	2	TSR test
	3	BBS test
<b>U</b>		Unconditioned
<b>C</b>		Moisture-conditioned
<b>S</b>	1, 2, 3, ...	Sample/specimen number

#### 3.2.1 Tensile Strength Ratio (TSR) and Indirect Tension Test (IDT) Samples

The plant-produced asphalt mixes collected from the different sources were reheated in the laboratory and used to prepare TSR/IDT test samples. Trial samples were prepared for each asphalt mix to determine the weight required to obtain desired air voids ranging from 6.5% to 7.5% for the test samples. Sample preparation procedure was similar for the trial samples and test samples whereas preparation of test samples needed pre-determined weight. Four trial samples, four test specimens for testing without moisture conditioning,

and four test specimens for testing after moisture-conditioning were prepared for each type of the asphalt mix.

The compaction and testing procedures were followed in accordance with AASHTO T 283 standard (AASHTO, 2010). The TSR/IDT sample preparation consisted of the following steps.

1. Scoop, empty tray, material handling chute, compaction mold and lid of compaction mold were heated in the oven at a temperature of  $165^{\circ}\text{C}$  for half an hour.
2. The weight required to prepare four cylindrical specimens of TSR/IDT test was multiplied by the factor of 1.1 to consider the material loss during handling.
3. Asphalt mix was taken out from the paper bag and required weight was transferred to the metal tray (Figure 3-4).
4. Asphalt mix in the tray was heated in an oven at a temperature of  $165^{\circ}\text{C}$  for at least one hour and hand-mixed every 15 minutes (Figure 3-5).
5. The desired weight of the asphalt mix was transferred to the material handling chute and kept in the oven for 5 minutes.
6. Heated mold having an inner diameter of 150 mm was weighted and a circular paper disc was placed inside the mold.
7. The hot mix in the material handling chute was taken out from the oven and remixed.
8. The asphalt mix of required weight was transferred into the mold from the material handling chute.

9. The asphalt mix in the mold was covered with another circular paper disc and the metal lid was place on top.
10. The mold was placed inside a Superpave<sup>®</sup> gyratory compactor. The compaction mode was set to height. Specimen height was set to 95 mm using digital control on SGC (Figure 3-6).
11. The compacted sample was partially extruded and kept for cooling by fan approximately for 30 minutes, before complete extrusion and transferring it to a flat surface (Figure 3-7).
12. Similar procedure was repeated for preparation of all of the TSR/IDT samples.
13. The samples were labeled and kept in in the room temperature for 24 hours.
14. The dry samples were placed inside an environmental chamber at 25°C.



Figure 3-4 Asphalt mix in the oven ready for reheating



Figure 3-5 Hand mixing of asphalt mix



Figure 3-6 Compaction of asphalt mix by Superpave® gyratory compactor (SGC)



Figure 3-7 Tensile strength ratio (TSR) sample extraction from SGC mold

Moisture conditioning consisted of the following steps.

1. The vacuum saturation was carried out on TSR/IDT specimens by applying the vacuum pressure of 254-660 mm Hg to a sample submerged in the water in a vacuum saturation chamber (Figure 3-8).
2. The specimen was weighed to ensure a saturation between 70% and 80%.
3. After obtaining the desired saturation, the specimens were wrapped in the plastic wrap and kept in an air-sealed plastic bag after adding 10 ml of water to the bag.
4. The samples were transferred to a freezer maintaining a temperature of  $-18^{\circ}\text{C}$ .
5. After 16 hours of keeping the specimens at  $-18^{\circ}\text{C}$ , they were placed inside water bath at a temperature of  $60 \pm 1^{\circ}\text{C}$  for 24 hours (Figure 3-9).
6. The specimens were removed from the water bath and placed inside water at  $25^{\circ}\text{C}$  for 2 hours before testing.





Figure 3-8 Vacuum saturation chamber



Figure 3-9 Thawing chamber

### 3.2.2 Semicircular Bend (SCB) Samples

The plant-produced asphalt mixes collected from different projects were used to prepare SCB test specimens in the laboratory. The sample preparation and conditioning procedures were followed in accordance with ASTM D8044 standard and AASHTO T 283 standard, respectively (AASHTO, 2010; ASTM, 2016). The cylindrical samples were compacted

with a height of 120 mm and a diameter of 150 mm. Then, the semicircular specimens of 57 mm thickness were prepared by wet cutting of the cylindrical samples using a rock saw with a blade of 458 mm diameter and 3 mm thickness (Figure 3-10). Then, notches with a depth of 25.4 mm, 31.75 mm, and 38.1 mm were saw-cut in the mid span of the semicircular samples using another saw with a thinner blade (Figure 3-11). The SCB sample preparation procedure was similar for all of the mixes. Trial semicircular samples with different weights were prepared for each asphalt mix to determine the weight of asphalt mix required to obtain desired air voids ranging from 6.5 to 7.5% for the test specimens. For each type of asphalt mixes, nine semicircular specimens for testing without moisture conditioning, and nine semicircular specimens for testing after moisture conditioning, having different notch depths, were prepared (Figure 3-12).



Figure 3-10 Rock saw used prepare semicircular specimens



Figure 3-11 Saw used to cut a notch in semicircular specimens



Figure 3-12 Semicircular specimens

### 3.2.3 Binder Bond Strength (BBS) Samples

The large stone samples with different mineralogies (granite-I, quartzite and granite-II) were cut into flat pieces of the aggregates using a rock saw (Figure 3-13). The flat surface of the specimens were polished to provide a smooth contact area and were cleaned with distilled water to avoid dust and other contaminants. For surface polishing, an electricity-

operated grinder with an angular velocity of 10,000 rpm was used (Figure 3-14). Sample preparation was carried out as follows.

1. The aggregate sample cut with rock saw having parallel surfaces was immersed in the distilled water for 30 minutes. A brush was used for removing the surface dust 3 times: immediately after submerging, 15 minutes after submerging, and 30 minutes after submerging the specimen in the distilled water. The aggregates sample was removed from water and after 30 minutes resting in room temperature, its surface was cleaned with acetone, and then kept at room temperature for 10 minutes before heating (Figure 3-15).
2. The asphalt binder was heated in an oven at 165°C for 2 hours and mixed every 15 minutes to consistency.
3. The pull stub and aggregate samples were heated at 60°C for half an hour to remove the moisture.
4. The surface of the pull stub was dipped in asphalt binder such that at least 0.8 mm thickness of the binder coated the surface of the pull stub. In order to maintain the binder film thickness of 0.8 mm, 3 tiny metal balls having a diameter of 0.8 mm were sandwiched between the surface of the pull stub, binder and aggregate surface.
5. The pull stub was then pushed and attached to the surface of the aggregate and kept for 24 hours at a temperature of 25°C.
6. The dry samples were kept inside an environmental chamber at 25°C for 2 hours before testing.



Figure 3-13 Preparation of flat pieces from aggregate chunks

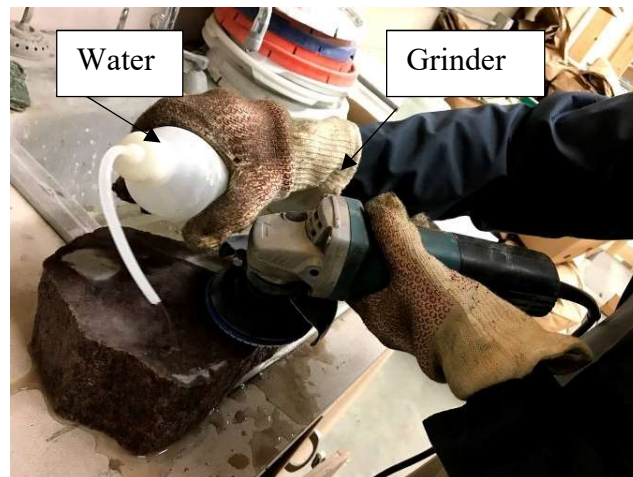


Figure 3-14 Surface preparation

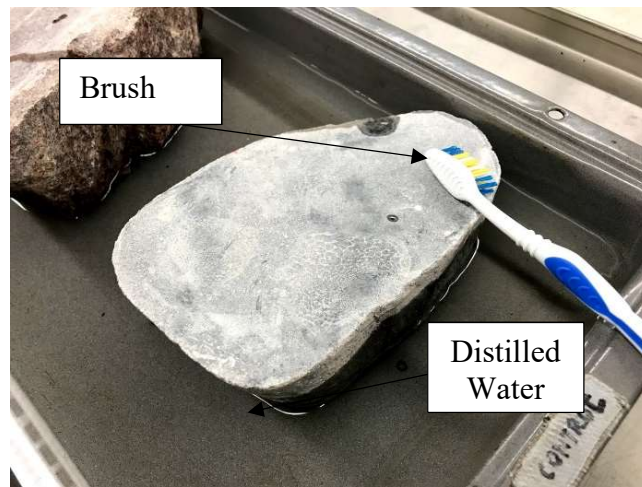


Figure 3-15 Surface Cleaning

Moisture conditioning of the BBS samples consisted of the following steps.

1. The samples were kept at room temperature of 25°C for two hours after preparation.
2. The samples were submerged in water at a temperature of 25°C for 48 hours.
3. Then they were removed and kept inside a freezer at -18°C 16 hours.
4. Then the samples were removed from the freezer and were kept in water at 25°C for 4 hours before testing.

### 3.3 Laboratory Testing

Volumetric tests and performance tests conducted in the current study are described in this section.

#### 3.3.1 Theoretical Maximum Specific Gravity ( $G_{mm}$ )

Theoretical maximum specific gravity test was conducted on the loose asphalt mixes in accordance with AASHTO T 209 specifications (AASHTO, 2013b) (Figure 3-16).



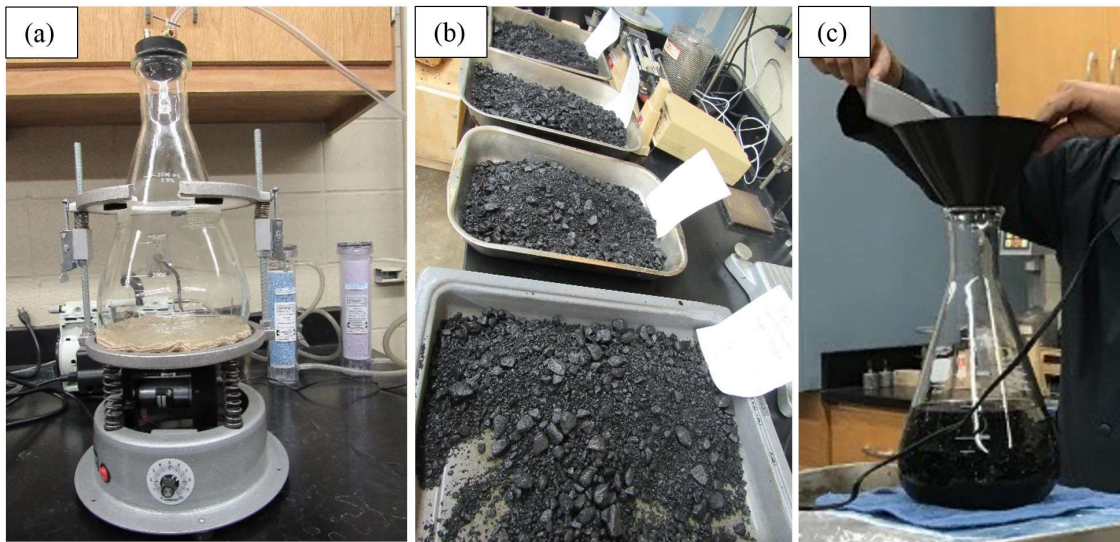


Figure 3-16  $G_{mm}$  test details (a)  $G_{mm}$  test setup (b) loose asphalt mix before testing (c) transferring of the loose mix into the pycnometer

Theoretical maximum specific gravity is needed for calculation of the air voids in the compacted asphalt samples. The test was carried out for all the mixes as follows.

1. Hot and loose asphalt mix was cooled and mixed during cooling in order to maintain a granular form. Then, 3 samples of cool and loose mix with a mass of at least 1500 g each (for NMAAS of 12.5 mm) were placed in the three containers.
2. A glass pycnometer was filled with approximately 2000 ml of water at a temperature between  $24^{\circ}\text{C}$  and  $25.5^{\circ}\text{C}$  and placed on a scale and tared.
3. The loose asphalt mix was placed in the pycnometer using a funnel and its weight was recorded.
4. The pycnometer with the asphalt mix was shaken such that there is about 25 mm of water above the mix.

5. The vacuum pump setup was connected to the pycnometer and de-airing of the loose mix was carried out by vibrating the sample and pycnometer using a mechanical vibrator while the vacuum pressure of between 25 mm Hg to 30 mm Hg was applied for 13 to 15 minutes.
6. After de-airing procedure was complete, the vacuum pressure was released and pycnometer with the asphalt mix was filled with water at a temperature between 24°C and 25.5°C and covered with the glass slide.
7. It was ensured that no bubbles were trapped inside the water, when sliding the glass cover on top of the pycnometer. Then, pycnometer and glass slide were carefully dried using a piece of towel paper and its total weight was recorded.
8. The  $G_{mm}$  value was calculated by the method of mass determination in the air as per as AASHTO T 209 using equation 1.

$$\text{Theoretical maximum specific gravity} = A / (A + D - E) \quad (1)$$

where,

A = mass of oven dry sample in air, g;

D = mass of container filled with water, g; and

E = mass of container filled with sample and water.

### 3.3.2 Bulk Specific Gravity ( $G_{mb}$ )

Bulk specific gravity test was conducted on the compacted asphalt samples (both SCB and TSR samples) in accordance with AASHTO T 166 (AASHTO, 2016). The bulk specific gravity of each sample was determined to calculate their air voids in the compacted asphalt



samples using volumetric relationship. The test was conducted using the water bath with a temperature maintained at 25°C, as follows.

1. The dry weight of the sample was recorded and noted in the measurement sheet.
2. The submerged weight of the sample was recorded after submerging it in the water bath for 4 minutes (Figure 3-17).
3. The submerged sample was removed from the water and its surface was dried by using a wet towel (cotton-nylon) within 30 seconds and its saturated surface-dry (SSD) weight was recorded.



Figure 3-17 Water tank

The bulk specific gravity ( $G_{mb}$ ) was calculated using equation 2.

$$\text{Bulk specific gravity} = A/(B - C) \quad (2)$$

where,

A = mass of the specimen in the air, g;

B = mass of the surface-dry specimen in the air, g; and

C = mass of the specimen in water, g.

Percentage air voids were calculated using equation 3.

$$AV (\%) = (G_{mm} - G_{mb}) \times 100 / G_{mm} \quad (3)$$

### 3.3.3 Tensile Strength Ratio (TSR) Test

The TSR test was conducted on the compacted asphalt samples in accordance with AASHTO T 283 (AASHTO, 2010) using an MTS loading frame (Figure 3-18). The test specimens having a diameter of 150 mm and a height of 95 mm with air voids of  $7.0\% \pm 0.5\%$  were tested. The test was carried out at room temperature (25°C) by applying a monotonical load with a rate of 50 mm/min. The load was applied along the diameter of the specimen fixed in an indirect tension jig mounted in the loading frame until vertical crack separates the samples into two halves and load starts to decline (Figure 3-19). The samples failure surfaces were photographed for visual analysis and rating of the unconditioned and moisture-conditioned samples. The tensile strengths of the moisture-conditioned samples and unconditioned samples obtained after testing were used to calculate the tensile strength ratio. Calculation of the tensile strength of the samples is presented in the next section.



Figure 3-18 Tensile strength ratio (TSR) testing using MTS



Figure 3-19 Tensile strength ratio (TSR) specimen after testing

#### 3.3.4 Indirect Tension Test (IDT)

The IDT test was conducted on the TSR samples and the tensile strength of each samples was measured. Tensile strength of each specimen was calculated after measuring the peak load at failure using equation 4 (AASHTO, 2010).

$$S_t = (2000 P)/(\pi t D) \quad (4)$$

where,

$S_t$  = tensile stress, kPa;

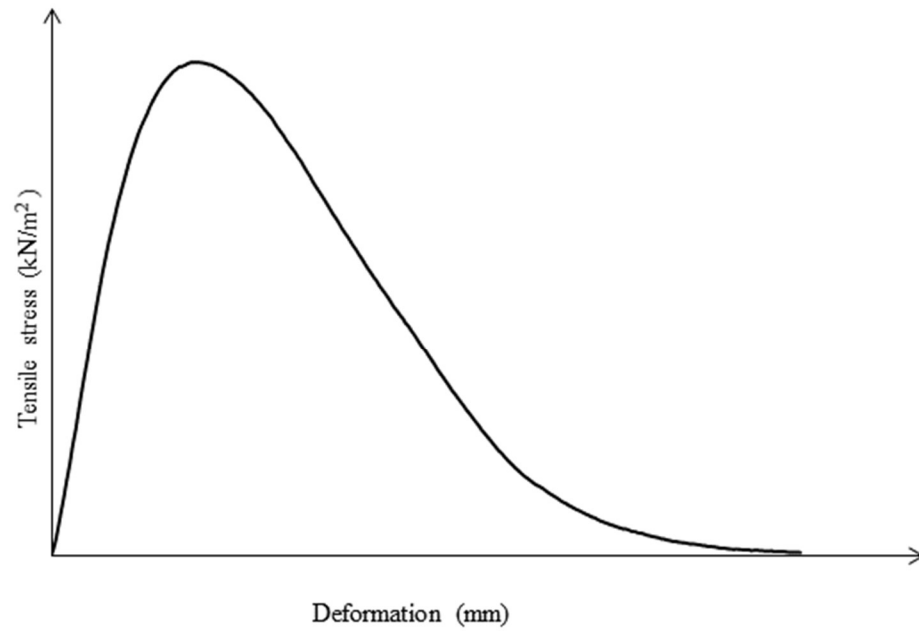
$P$  = maximum load at failure, N;

$t$  = specimen thickness, mm; and

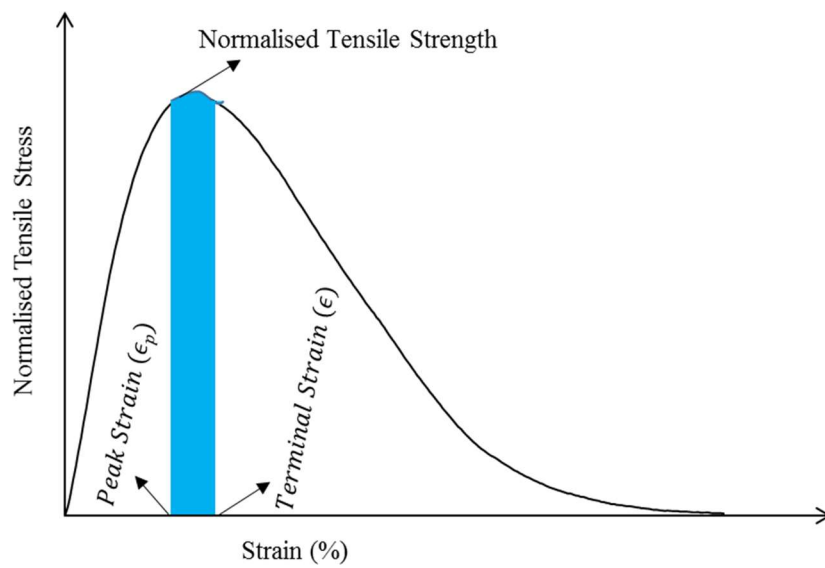
$D$  = specimen diameter, mm.

Additionally, the variation of axial force with axial displacement obtained from the IDT test were plotted and used to calculate the strain energy at failure, toughness index, and fatigue index to analyze the fracture properties of the asphalt mixes (Barman et al., 2018). The indirect tensile stress values were normalized by dividing them to indirect tensile strength (ITS) value, and deformation values were normalized by dividing them to diameter of the specimen (Figure 3-20). The difference in area up to normalized tensile strength with area at terminal strain of 3% was divided by the corresponding difference in the strains to obtain toughness index (Barman et al., 2018). Fatigue index was calculated by dividing the strain energy at failure by the slope of the line connecting the various toughness values at corresponding strains of 3%, 6%, 9%, and 12% (Barman et al., 2018) (Figure 3-20).

Strain energy was determined by calculating the area under the load-deformation plot obtained from IDT test data. Strain energy represents the energy absorbed by the material before the peak load. The toughness index represents the behavior after attaining the peak load. According to Barman et al. (2018) fatigue index represents property of the asphalt mixes both before and after peak load representing both strain energy and toughness index.



(a)



(b)

Figure 3-20 Indirect tension (IDT) test plots (a) Typical tensile stress vs deformation plot

(b) Typical normalized tensile stress vs strain (%) curve

Strain energy at failure was calculated by trapezoidal method of area calculation using equation 5 (Barman et al., 2018). Toughness index, and fatigue index were calculated using equations 6 and 7, respectively (Barman et al., 2018).

$$\text{Strain energy (U)} = \sum_{j=1}^{j=n} (u_{j+1} - u_j) \times \frac{1}{2} (P_{j+1} + P_j) \quad (5)$$

where,

$P_j$  = applied load (kN) at the j load step application;

$P_{j+1}$  = applied load (kN) at the j+1 load step application;

$u_j$  = displacement (m) at the j step; and

$u_{j+1}$  = displacement (m) at j+1 step.

$$\text{Toughness Index (TI)} = \frac{(A_\varepsilon - A_p)}{(\varepsilon - \varepsilon_p)} \quad (6)$$

where,

$A_\varepsilon$  = area under normalized tensile stress-strain (%) curve up to 3% terminal strain

$\varepsilon$  = terminal strain (%)

$A_p$  = area under normalized tensile stress-strain (%) curve up to strain at peak stress ( $\varepsilon_p$ )

$\varepsilon_p$  = terminal strain (%)

$$\text{Fatigue Index (FI)} = (d\text{TI}/d\varepsilon)/U \quad (7)$$

where,

$U$  = Strain energy at failure (kN-m)

### 3.3.5 Semicircular Bend (SCB) Test

The SCB test was conducted at a temperature of 25°C on the laboratory-compacted specimens using an asphalt standard tester (AST) in accordance with ASTM D8044-16 (ASTM, 2016). The semicircular specimens (dry and moisture-conditioned) having notches with depths of 25.4 mm, 31.75 mm, and 38.1 mm were tested. The specimens were tested at a constant monotonic load application rate of 0.5 mm/min (Figure 3-21). The load was applied along the direction of the notch to allow propagation of the cracks along the notch. Figure 3-22 shows a failed SCB specimen after testing. The target temperature was set at 25°C inside the environmental chamber. Before testing, the actual dimensions of the specimen were measured and entered in the software. After conducting the test, the load and deformation data were exported as an MS-Excel file and was used to further analyze the test results. A typical load-deformation output data obtained by conducting the SCB test on samples having different notch depths is shown in Figure 3-23. Cracking analysis was carried out through by calculation of the critical strain energy release rate, J-integral (ASTM, 2016). The area of the load-deformation curve up to peak load was used to calculate total strain energy (U) at failure (Figure 3-24). Trapezoidal method for discrete integration was applied to obtain total strain energy through calculation of the area under the load-deformation curve up to failure, using equation 8 (ASTM, 2016).

$$U = \sum_{j=1}^{j=n} (u_{j+1} - u_j) \times P_j + \frac{1}{2} \times (u_{j+1} - u_j) \times (P_{j+1} - P_j) \quad (8)$$

$P_j$  = applied load (kN) at the j load step application;

$P_{j+1}$  = applied load (kN) at the j+1 load step application;

$u_j$  = displacement (m) at the j step; and

$u_{j+1}$  = displacement (m) at j+1 step.

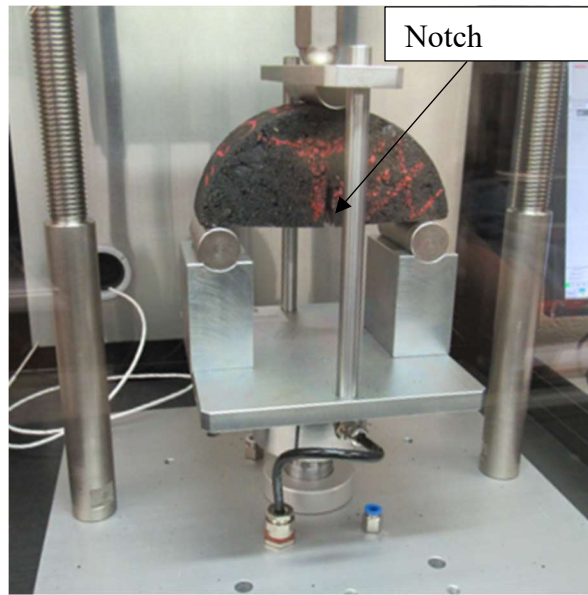


Figure 3-21 Semicircular bend (SCB) test using AST



Figure 3-22 Semicircular (SCB) specimen after testing



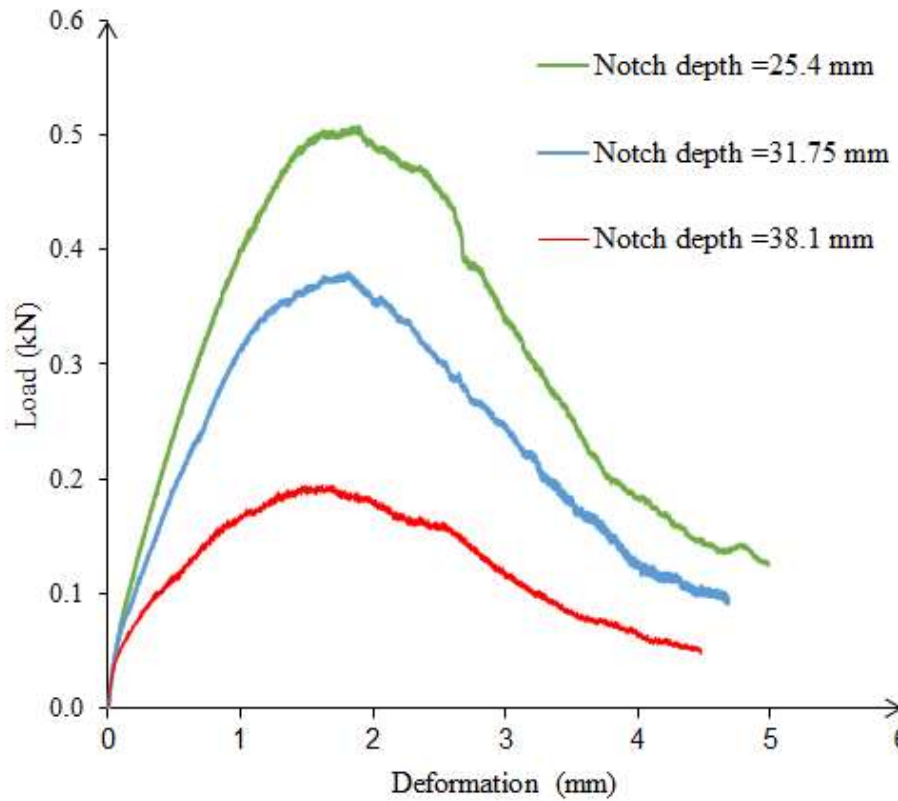


Figure 3-23 Typical load-deformation plots for SCB test conducted on samples with different notch depths

The slope of the linear regression ( $dU/da$ ) developed between the average strain energy at failure and notch depths was divided by average thickness of the specimens to calculate the critical strain energy release rate ( $J_c$ ). Critical strain energy release rate ( $J_c$ ) was calculated using equation 9 (ASTM, 2016).

$$J_c = \frac{-1}{b} (dU/da) \quad (9)$$

where,

$J_c$  = critical strain energy release rate ( $\text{kJ/m}^2$ );

$b$  = sample thickness (m);

$a$  = notch depth (m);

$U$  = strain energy to failure (kJ); and

$dU/da$  = change of strain energy with notch depth.

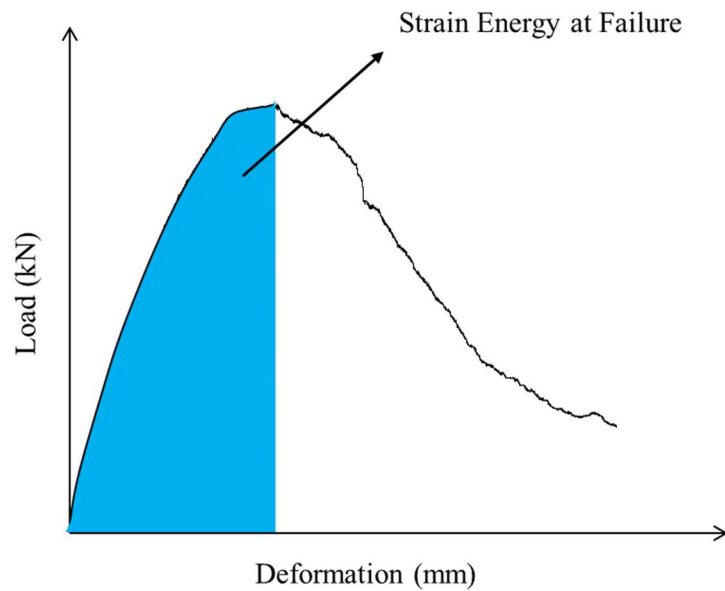


Figure 3-24 Typical load vs deformation curve with area representing strain energy

### 3.3.6 Binder Bond Strength (BBS)

The BBS tests were carried out using a pneumatic adhesion tensile testing instrument (PATTI) on various aggregate-asphalt binder samples to measure their bond strengths (Figure 3-25). PATTI consisted of pull stub, piston, and compressed air supply (Figure 3-25; Figure 3-26; Figure 3-28; Figure 3-29). Before testing the dry samples temperature-controlled environmental chamber was utilized to maintain the temperature at 25°C. The temperature was found to be one of the major factors affecting the bond strength.

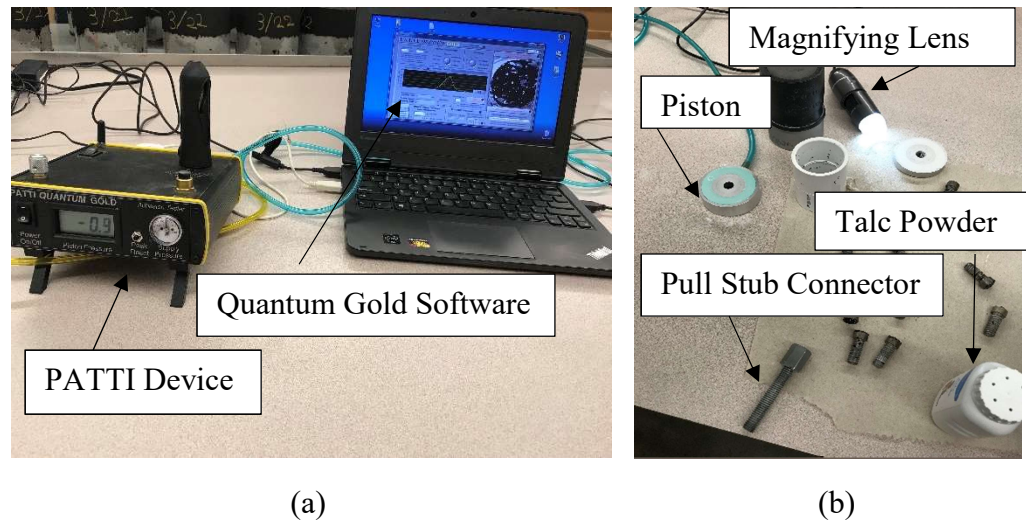


Figure 3-25 Binder bond strength (BBS) test component of PATTI device: (a) PATTI device and quantum gold software; (b) F-2 piston type, talc powder, magnifying lens, pull stub-connector

The piston pressure was maintained at a constant rate of 690 kPa. The diameter of the pull stub was 12.7 mm, and thickness of the asphalt film was 0.8 mm. The testing of the wet samples was carried while the samples were in the water (Figure 3-30). Tensile strength obtained from the PATTI quantum gold software was used for analysis.

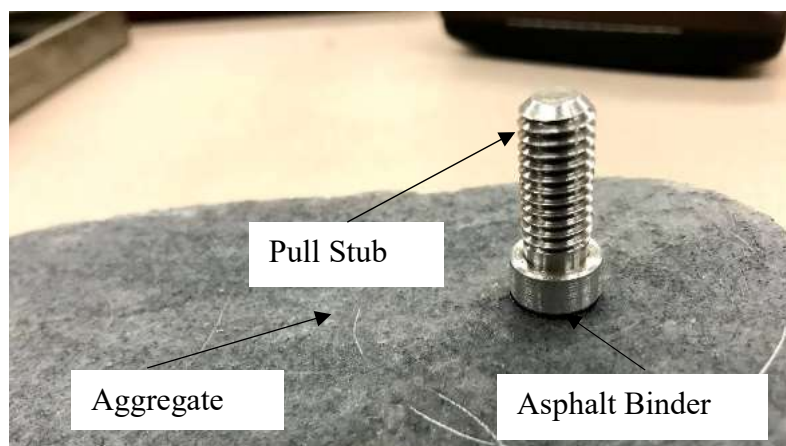


Figure 3-26 Typical asphalt binder-aggregate BBS sample

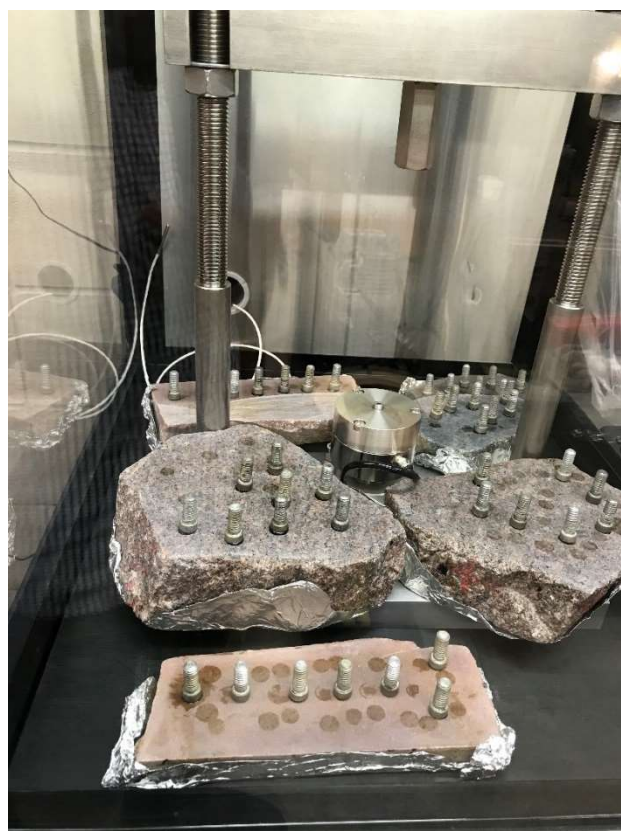


Figure 3-27 Dry BBS samples inside the environmental chamber at 25°C

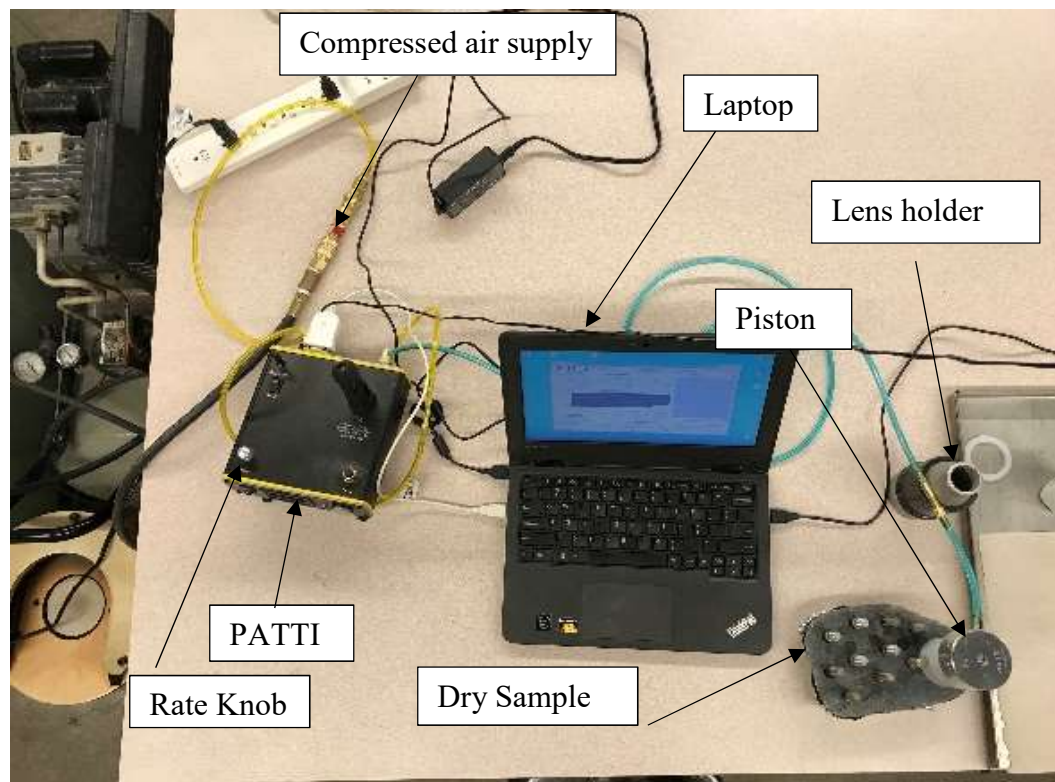


Figure 3-28 Binder bond strength test set up of dry asphalt binder-aggregate sample

The rate knob of the PATTI device was adjusted such that the constant application rate of 1379 kPa with 15% coefficient of variation was maintained (Figure 3-28). Failure occurred when the applied stress exceeded the pull-off strength of the asphalt binder-aggregate. The tensile stress and time was obtained by exporting the test data as a text file.



Figure 3-29 Moisture conditioning of BBS samples

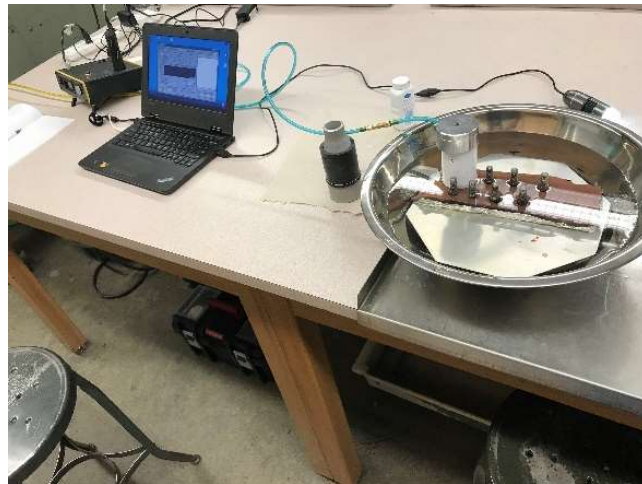


Figure 3-30 Test (BBS test) setup for moisture-conditioned asphalt-aggregate samples



## CHAPTER 4 RESULTS AND DISCUSSIONS

### 4.1 Asphalt Mix Testing

This section describes the result obtained from testing asphalt mixes by conducting volumetric tests, as well as TSR, IDT, and SCB tests.

#### 4.1.1 Volumetric Tests

Two types of volumetric tests, namely the theoretical maximum specific gravity, and bulk specific gravity were conducted on loose asphalt mix and compacted samples, in accordance with AASHTO T 209-10 (AASHTO, 2013b) and AASHTO T 166 (AASHTO, 2016), respectively. The results of the volumetric tests were used to determine the air voids in compacted specimens. Although a very high air voids is detrimental to pavement's durability, keeping the air voids very low is not desirable as some void space is needed for ease of compaction (Asphalt-Magazine, 2018). To simulate the compaction conditions in the field, air voids of the compacted specimens for performance testing were maintained at  $7.0\% \pm 0.5\%$  (AASHTO, 2010). The maximum theoretical specific gravity, bulk specific gravity, and the air voids calculated for all of the asphalt mixes and SCB and TSR test specimens are tabulated and presented in APPENDIX A.

#### 4.1.2 Performance Tests

The result and discussions of TSR test, SCB test, IDT test, and BBS test will be analyzed in this section.

#### 4.1.2.1 Tensile Strength Ratio Test (TSR) Results

The TSR values and tensile strengths of the three types of asphalt mixes are presented numerically and graphically in Table 4-1 and Figure 4-1, respectively.

Table 4-1 Summary of the tensile strength ratio (TSR) test result

Asphalt Mix	HMA-Lime		HMA-RAP		C-WMA	
Performance Grade	PG 64-34		PG 58-28		PG 64-34	
Aggregates	Quartzite		Quartzite, Gravel		Granite, Gravel	
NMAS	12.5 mm		12.5 mm		12.5 mm	
Moisture Condition	Unconditioned	Moisture-conditioned	Unconditioned	Moisture-conditioned	Unconditioned	Moisture-conditioned
Average Tensile Strength (kPa)	915.4	1226.4	858.7	704.9	662.9	631.3
Standard Deviation (kPa)	124.8	70.0	110.4	108.7	36.8	54.5
Coefficient of Variation (%)	13.6	5.7	12.9	15.4	5.6	8.6
Tensile Strength Ratio (TSR)	1.34		0.82		0.95	
Remark	> 0.8		> 0.8		> 0.8	
Visual Rating	1		1		1	



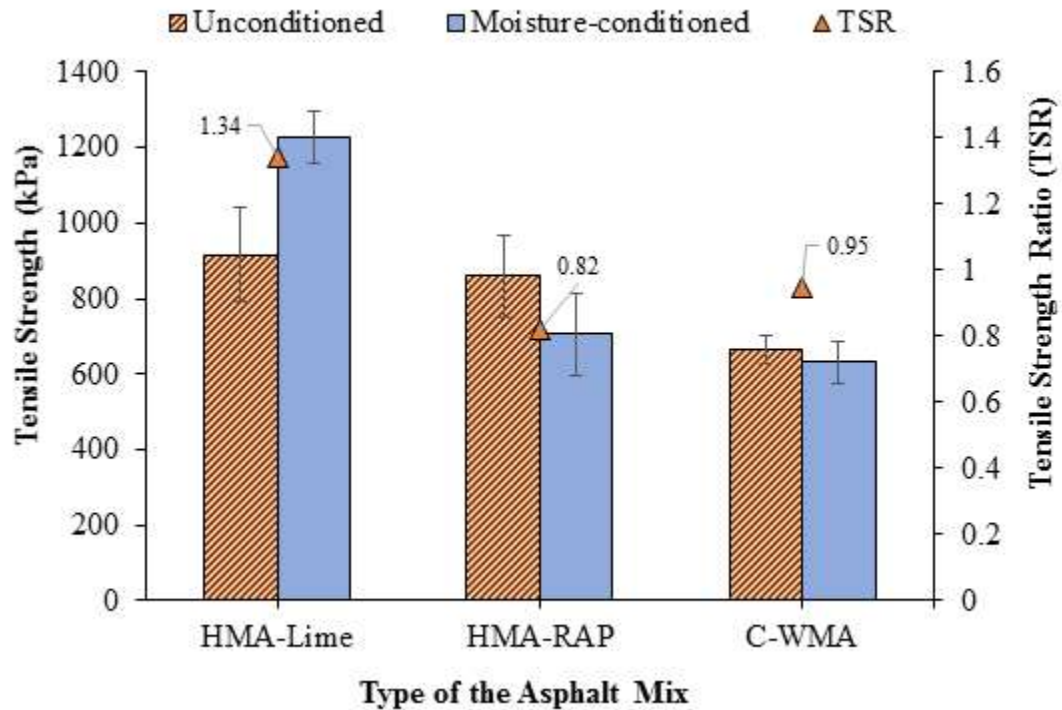


Figure 4-1 Tensile strength (TSR) test result of the asphalt mixes

The TSR values were calculated to find out whether the mixes meet the minimum requirement ( $\text{TSR} \geq 0.8$ ) set by AASHTO Superpave<sup>®</sup> mix design specification (AASHTO, 2012). From Table 4-1 and Figure 4-1, the average tensile strength values of the HMA mix containing 1% hydrated lime (HMA-Lime), HMA mix containing 20% RAP (HMA-RAP), and asphalt mix containing 0.5% chemical WMA additive (C-WMA) in dry condition were found to be 915.4, 858.7, and 662.9 kPa, respectively. The tensile strength values of the HMA-Lime, HMA-RAP, and C-WMA were found to become 1226.4, 704.9, and 631.3 kPa after moisture conditioning, respectively. In order to statistically verify the significance of the differences between the tensile strength between

unconditioned and moisture-conditioned samples, a two tailed t-test ( $\alpha = 0.05$ ) was conducted. The differences between the tensile strength of unconditioned and moisture-conditioned samples were found to be statistically significant ( $\alpha = 0.05$ ) in HMA-Lime. However, no significant differences was observed between the tensile strength of unconditioned and moisture-conditioned samples in the HMA-RAP, and C-WMA mixes. The TSR values calculated for each mix indicate the extent of the moisture-induced damage effect of on loss of tensile strength of the mixes. From Table 4-1 and Figure 4-1 the TSR values of the HMA-Lime, HMA-RAP and C-WMA were found to be 1.34, 0.82, and 0.85, respectively. The TSR values for all of the tested asphalt mixes were greater than 0.8 indicating their satisfactory resistance to moisture-induced damage. It was found that the HMA-Lime had the highest TSR value compared to other mixes.

Interestingly, it can be observed that the HMA-Lime has gained 34% more tensile strength after moisture-conditioning. This can be due to the fact that lime has reacted with the water and other minerals and developed a cementitious compound as a result of hydration, leading to an improved tensile strength. Also, a high TSR value observed for C-WMA mix (0.95) indicates a significant resistance to moisture-induced damage. This can be attributed to the amine-based WMA additive used in this mix which improved the adhesion between asphalt binder and aggregates. Finally, the HMA-RAP with a TSR value of 0.82 was found to have an acceptable resistance to moisture-induced damage ( $\text{TSR} > 0.8$ ). In other studies, incorporation of RAP in asphalt mixes was found to improve the resistance of the mixes to moisture-induced damage (Ghabchi et al., 2016). Overall, one can say that the TSR values can be significantly improved by using hydrated lime in

an asphalt mix. Using an amine-based WMA additive was also found to improve the resistance of tested mixes to moisture-induced damage. The photographic views of the failure surfaces after conducting the TSR tests on HMA-Lime, HMA-RAP and C-WMA mixes (with and without moisture conditioning) are presented in Figures 4-2, 4-3, and 4-4, respectively. Visual ratings (1-4) in accordance with AASHTO T 283 (AASHTO, 2010) specification were assigned as one in each mixes (Ghabchi et al., 2015). The rating of one indicates less damage due to water. In visual rating, very few aggregates were found to be exposed in moisture-conditioned samples and in the dry samples most of the aggregates were found broken. Both cohesive, and adhesive failures were observed. However, the clearly detectable pattern of failure was not observed through visual screening.



Figure 4-2 Photographic view of failure surfaces observed in HMA-Lime mix after conducting TSR test on (a) unconditioned sample (b) moisture-conditioned sample



Figure 4-3 Photographic view of failure surfaces observed in HMA-RAP mix after conducting TSR test on (b) moisture-conditioned sample



Figure 4-4 Photographic view of failure surfaces observed in C-WMA mix after conducting TSR test on (a) unconditioned sample (b) moisture-conditioned sample

#### 4.1.2.2 Indirect Tensile Strength Test (IDT) Result

The load-deformation curves (Figure 4-5) obtained from conducting the indirect tension tests (IDT) were utilized to determine important fracture energy parameters, namely toughness index (TI), fatigue index (FI), toughness index ratio (TIR), and fatigue index ratio (FIR) for asphalt mixes by following the procedure presented by (Barman et al., 2018). These parameters were determined for moisture-conditioned and unconditioned samples to evaluate their moisture-induced damage potentials

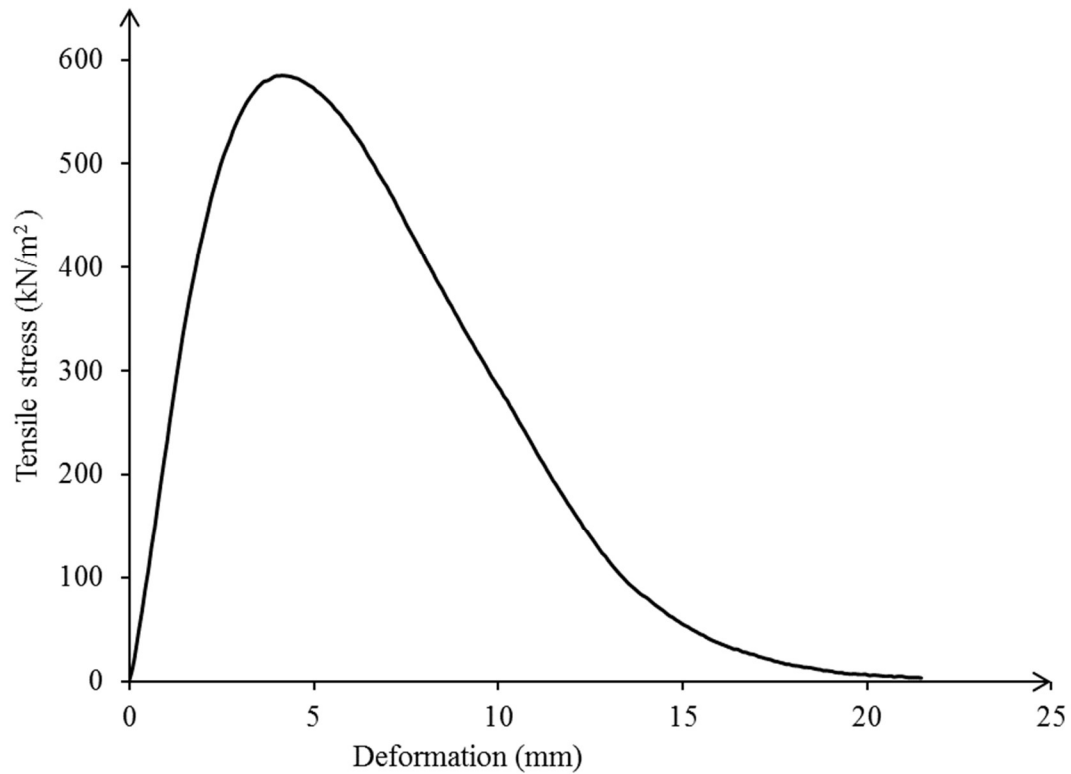


Figure 4-5 Typical tensile stress-deformation plot obtained from IDT test

Table 4-2 presents the values of the fatigue index, toughness index, fatigue index ratio, and toughness index ratio calculated for all mixes tested herein. Also, Figures 4-6 and 4-7 graphically summarize of the toughness indices/ratios and fatigue indices/ratios of the asphalt mixes (unconditioned and moisture-conditioned), respectively. Higher toughness and fatigue indices represent higher resistance to fracture and higher fatigue resistance, respectively.

Table 4-2 Indirect tension (IDT) test result analysis of the asphalt mixes

Mix type	Moisture Condition	Toughness Index			Slope (dTI/dε)	Average Strain Energy at Failure (kN-m)	Fatigue Index (kN-m)	Toughness Index Ratio (TIR)	Fatigue Index Ratio (FIR)
		Terminal Strain (%) (ε)	Average Toughness Index (TI)	Standard Deviation					
HMA-Lime	Unconditioned	3	0.89	0.02	-0.08	0.040	0.52	0.90	1.27
		6	0.42						
		9	0.24						
		12	0.16						
	Moisture-conditioned	3	0.80	0.08	-0.07	0.047	0.66		
		6	0.30						
		9	0.18						
		12	0.12						
HMA-RAP	Unconditioned	3	0.91	0.01	-0.08	0.039	0.50	1.01	1.23
		6	0.49						
		9	0.29						
		12	0.21						
	Moisture-conditioned	3	0.92	0.03	-0.07	0.045	0.62		
		6	0.69						
		9	0.41						
		12	0.29						
C-WMA	Unconditioned	3	0.91	0.08	-0.07	0.039	0.59	1.02	1.02
		6	0.75						
		9	0.48						
		12	0.33						
	Moisture-conditioned	3	0.93	0.05	-0.06	0.038	0.60		
		6	0.80						
		9	0.54						
		12	0.37						

As it is evident from Table 4-2, TI, TIR, FI and FIR were determined for both unconditioned and moisture-conditioned samples in order to study the effect of moisture-induced damage on fracture parameters. It is important to note that the toughness indices were determined at a terminal strain of 3%.

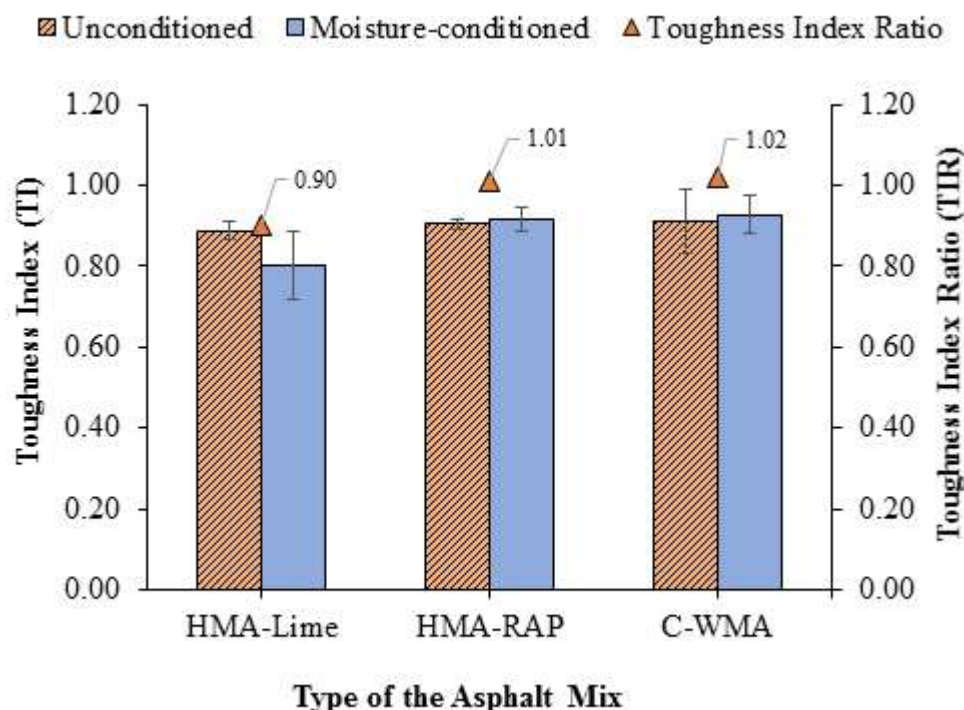


Figure 4-6 Toughness indices/ratios determined for different mixes

From Figure 4-6 and Table 4-2 it can be observed that the toughness indices for unconditioned and moisture-conditioned specimens of all three mixes were relatively close. For example, the toughness indices (TIs) for HMA-Lime in unconditioned and moisture-conditioned states were found to be 0.89 and 0.80, respectively, yielding a toughness index ratio (TIR) of 0.90. In other words, the strain energy absorption of the HMA mix containing hydrated lime was found to decrease by 10% after moisture conditioning. The TI values for HMA-RAP in unconditioned and moisture-conditioned states were found to be 0.91 and 0.92, respectively, yielding a TIR of 1.01. In other words, the strain energy absorption of the HMA mix containing 20% RAP remained almost unchanged after moisture conditioning. Finally, the TI values for C-WMA in

unconditioned and moisture-conditioned states were found to be 0.91 and 0.93, respectively, yielding a TIR of 1.02. This means that, the strain energy absorption of the mix containing a chemical WMA additive remained almost unchanged after moisture conditioning. These findings are consistent with those obtained from TSR tests, suggesting high resistance of these mixes to moisture-induced damage. In order to statistically determine the significance of the differences between the TI values in unconditioned and moisture-conditioned samples, a two tailed t-test ( $\alpha = 0.05$ ) was conducted. The difference between the toughness index of unconditioned and moisture-conditioned samples was found to be statistically significant ( $\alpha = 0.05$ ) in HMA-Lime.

However, no significant difference was observed between the toughness index of unconditioned and moisture-conditioned samples in the HMA-RAP, and C-WMA mixes. Fatigue index (FI) and the fatigue index ratio (FIR) are two other parameters obtained by analyzing the IDT test results. From Table 4-2 and Figure 4-7 it is evident that the FI values for HMA-Lime in unconditioned and moisture-conditioned states were 0.52 and 0.66, respectively, yielding an FIR value of 1.27. In other words, the fatigue resistance of the HMA mix containing 1% hydrated lime increased by 27% after moisture-conditioning. Also, the FI values for unconditioned and moisture-conditioned samples of the HMA-RAP were found to be 0.50 and 0.62, respectively, resulting in an FIR value of 1.23. In other words, the fatigue resistance of the HMA mix containing 20% RAP increased by 23% after moisture-conditioning. Finally, the FI values for C-WMA in unconditioned and moisture-conditioned states were found to be 0.59 and 0.60, respectively, yielding an FIR value of 1.02. It means that, the fatigue resistance of the



mix containing 0.5% of a chemical WMA additive remained almost unchanged after moisture-conditioning. These results, although indicate a resistance of the asphalt mixes to moisture-induced damage they are not ranking the mixes in the same order as the TSR test ranked them.

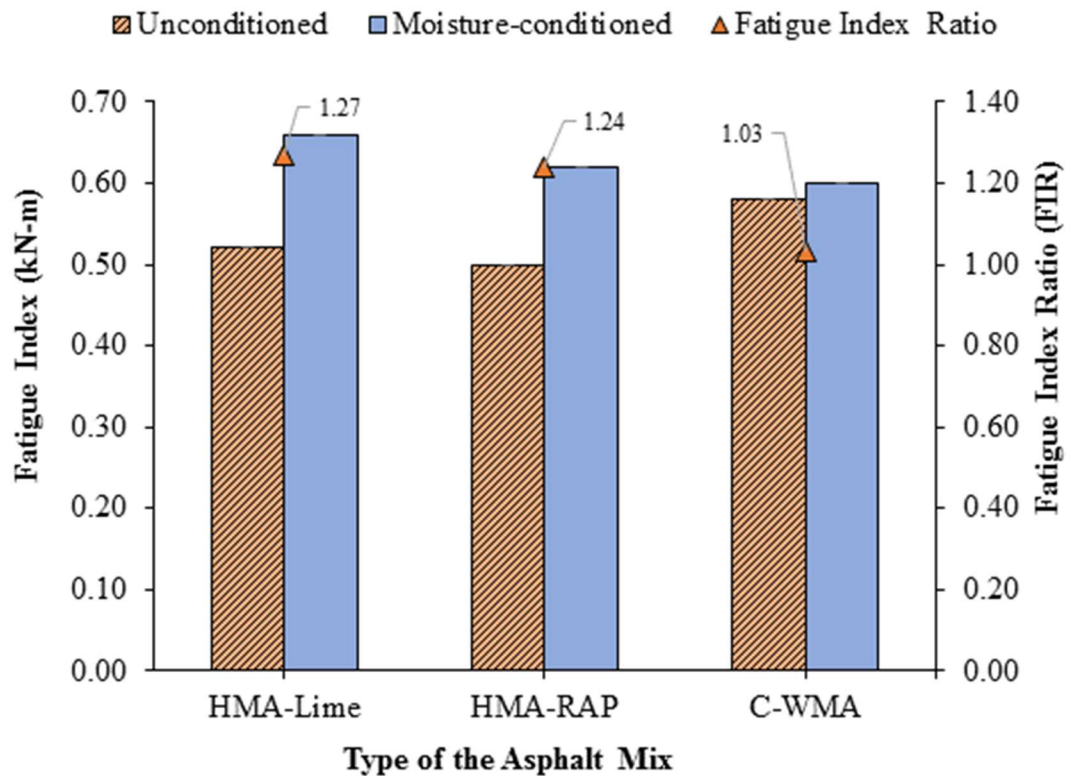


Figure 4-7 Fatigue indices/ratios determined for different mixes

#### 4.1.2.3 Semi-Circular Bend (SCB) Test Results

The SCB tests were conducted on asphalt mixes to obtain and compare their cracking resistance through determining the critical strain energy release rate ( $J_c$ ) for each mix.

According to ASTM D8044-16 standard test method (ASTM, 2016), the  $J_c$  values of 0.5

$\text{kJ/m}^2$  to  $0.6 \text{ kJ/m}^2$  are typically recommended for asphalt mixes having an acceptable resistance to cracking. Therefore, a higher strain energy release rate is desirable for an asphalt mix in order to exhibit a better resistance to cracking. Table 4-3 and Figure 4-8 present the critical strain energy release rate ( $J_c$ ) values calculated for the HMA-Lime, HMA-RAP and C-WMA mixes in unconditioned and moisture-conditioned states and their ratios, in numerical and graphical formats, respectively. Variation of strain energy with notch depth ( $dU/da$ ) utilized in calculation of the  $J_c$  values for tested mixes are presented in APPENDIX B.

Table 4-3 Critical strain energy release rate ( $J_c$ ) and  $J_c$  ratio values from SCB test

Asphalt Mix	HMA-Lime		HMA-RAP		C-WMA	
Performance Grade	PG 64-34		PG 58-28		PG 64-34	
Aggregates	Quartzite		Quartzite, Gravel		Granite, Gravel	
NMAS	12.5 mm		12.5 mm		12.5 mm	
Moisture Condition	Unconditioned	Moisture-conditioned	Unconditioned	Moisture-Conditioned	Unconditioned	Moisture-conditioned
Critical Strain Energy Release Rate ( $\text{kJ/m}^2$ )	0.27	0.32	0.39	1.04	0.59	0.68
Energy Release Ratio	1.19		2.64		1.15	

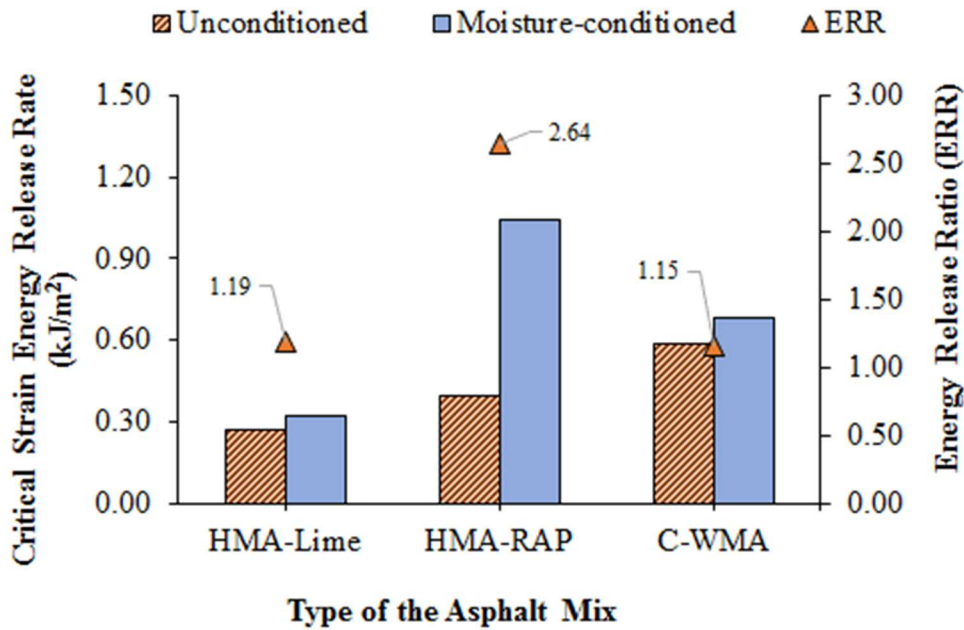


Figure 4-8 Strain energy release rate of different asphalt mixes

From Table 4-3 and Figure 4-8 it is evident that, critical strain energy release rate of the HMA-Lime was found to increase by 19% after moisture conditioning, yielding an energy release ratio (ERR) of 1.19. In other words, strain energy absorption of the HMA-Lime mix increased after moisture-conditioning, leading to a higher cracking resistance possibly due to reaction between hydrated lime, water and the minerals. In other studies, incorporation of hydrated lime in asphalt mixes was found to improve cracking resistance of the asphalt mixes (Abuawad et al., 2015). However,  $J_c$  value of HMA-Lime in the unconditioned and moisture-conditioned samples were found to be  $0.27 \text{ kJ/m}^2$ , and  $0.32 \text{ kJ/m}^2$ , respectively, less than the minimum value of  $J_c$  ( $0.5 \text{ kJ/m}^2$ ) required (ASTM, 2016). Also from Table 4-3 and Figure 4-8 it can be observed that, the ERR value of the

HMA-RAP mix was found to be 2.64 with critical strain energy release rate of 0.39 kJ/m<sup>2</sup>, and 1.04 kJ/m<sup>2</sup> for unconditioned and moisture-conditioned samples, respectively. In other words, strain energy absorption was found to increase by 164% which is very unlikely. It can be said that cracking resistance of the HMA-RAP was not decreased after moisture conditioning. The critical strain energy release rate of HMA-RAP, after moisture-conditioning met the minimum  $J_c$  value requirement of 0.5 kJ/m<sup>2</sup> set by ASTM D8044 (ASTM, 2016). In a different study, addition of RAP was found to increase the resistance of the asphalt mixes to moisture-induced damage (Ghabchi et al., 2014).

However, some studies also found that inclusion of RAP in mixes can decrease the resistance of mixes to moisture-induced damage (Fakhri et al., 2017a). Finally, the  $J_c$  value for C-WMA in unconditioned and moisture-conditioned states were found to be 0.59, and 0.68 respectively, yielding an ERR of 1.15. This means that, the strain energy absorption of the mix containing chemical WMA additive increased by 15% after moisture conditioning. The C-WMA mix was found to pass the minimum  $J_c$  criteria set by ASTM D8044 (ASTM, 2016). Visual inspection of the SCB samples after testing revealed that, very few aggregates were exposed, an indication of minimum moisture-induced damage. (Figure 4-9; Figure 4-10; Figure 4-11)



(a)



(b)

Figure 4-9 Visual failure pattern in HMA-Lime after conducting SCB test (a)  
unconditioned sample (b) moisture-conditioned sample



(a)



(b)

Figure 4-10 Visual failure pattern in HMA-RAP after conducting SCB test (a)  
unconditioned sample (b) moisture-conditioned sample



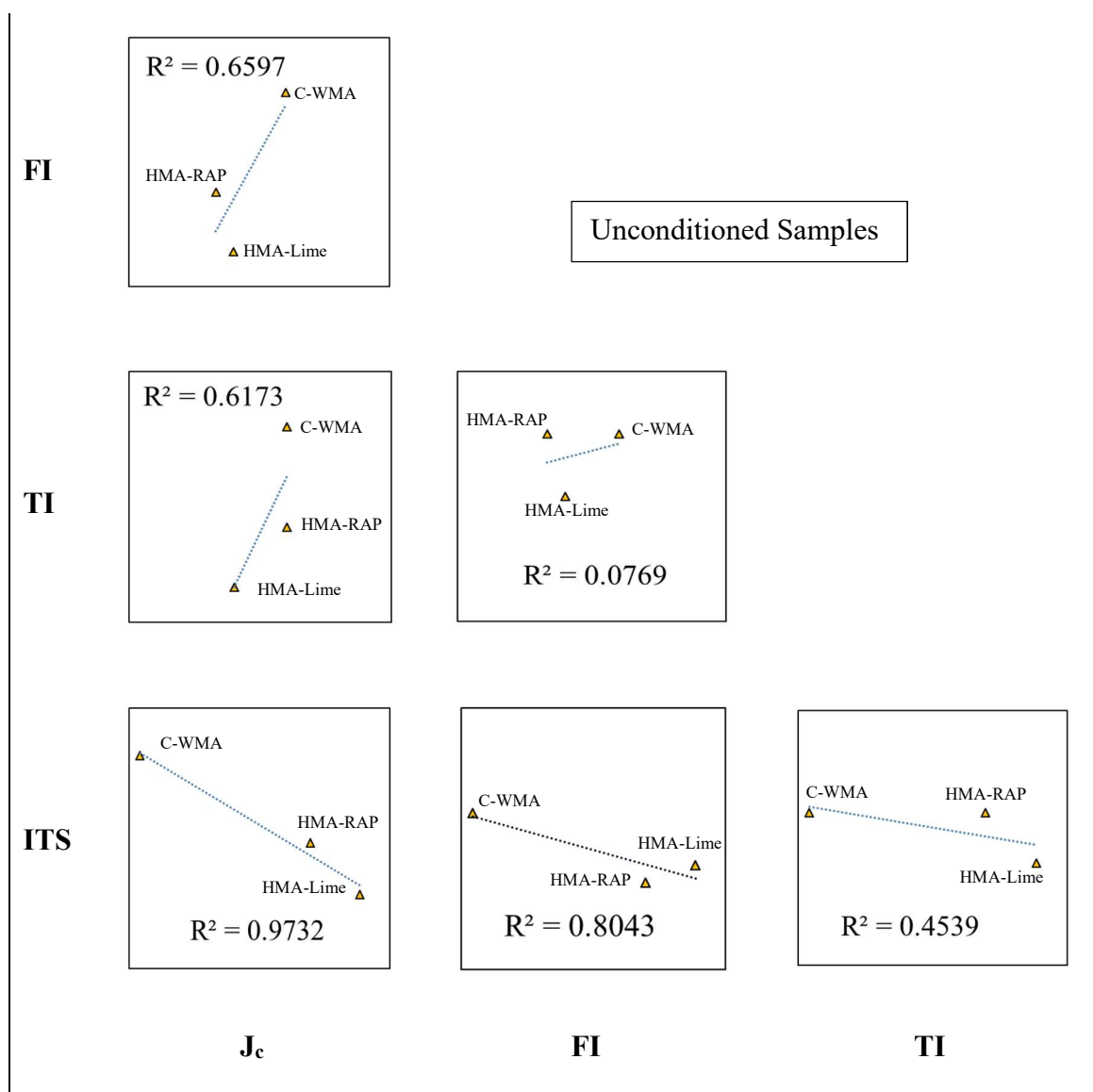
(a)



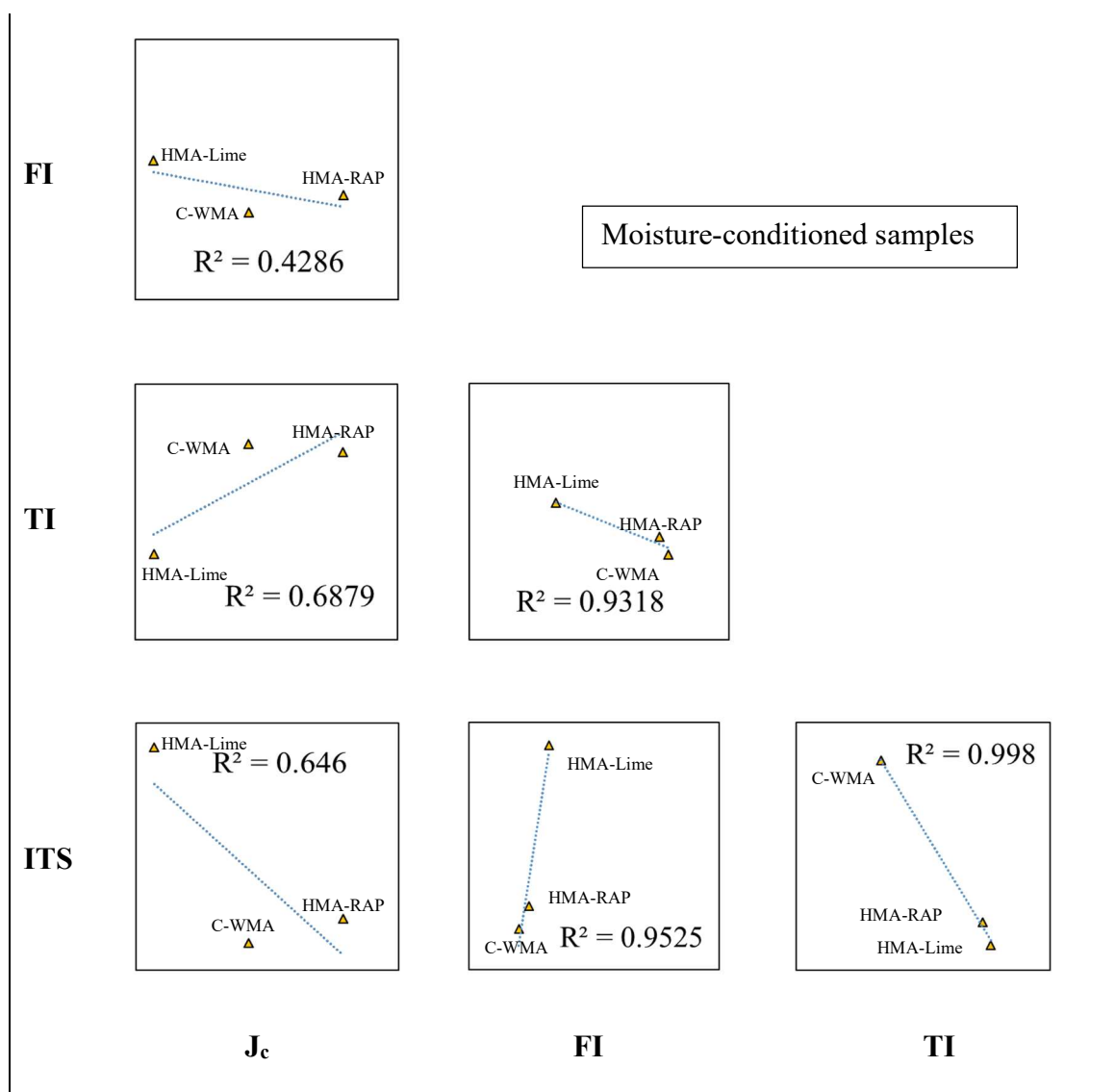
(b)

Figure 4-11 Visual failure pattern in C-WMA after conducting SCB test (a)  
unconditioned sample (b) moisture-conditioned sample

A relative comparison between the tensile strength (ITS), fatigue index (FI), toughness index (TI), and critical strain energy release rate ( $J_c$ ) was made by developing linear correlations. Figure 4-12 presents the linear regression models developed between ITS, FI, TI and  $J_c$  values of the asphalt mixes in dry and moisture-conditioned states. Also the coefficient of determination for each model is displayed in Figure 4-12. The correlation between the TSR, ERR, FIR, TIR is also included in the Figure 4-12.

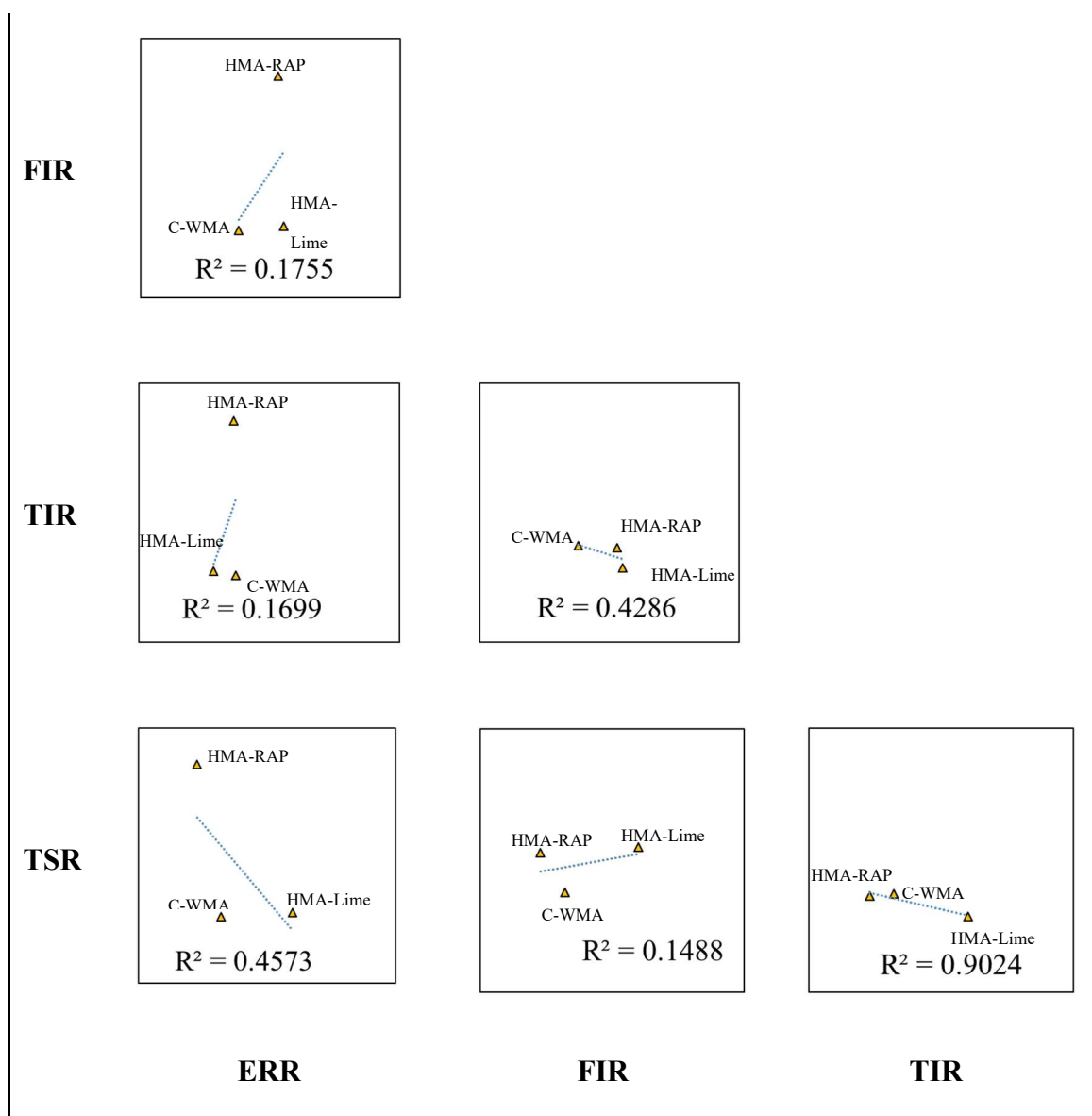


(a)



(b)





(c)

Figure 4-12 Correlations between the SCB, IDT, and TSR test result (a) unconditioned samples (b) moisture-conditioned samples (c) ratio of the parameter for moisture-conditioned to unconditioned samples

A higher  $R^2$  value suggests that a better correlation exists between each pair of the parameters. The parameters FI, and ITS were found to be better correlated in both unconditioned and moisture-conditioned samples. The TI was found to be better correlated with FI, and ITS, only in the moisture-conditioned samples. However, the  $J_c$  was found to be better correlated with ITS, only in the unconditioned samples. Only the TSR and TIR showed higher correlation while comparing the various moisture to dry parameter ratios. Very less correlation was observed between the IDT test result and SCB test result.

## 4.2 Asphalt Binder-Aggregate Testing

### 4.2.1 Binder Bond Strength (BBS) Test Results

The BBS tests were conducted on asphalt binder-aggregate samples which consisted of 4 types of asphalt binders, namely PG 58-28, PG 64-22, PG 64-34, and PG 70-28 and three types of aggregates, namely granite-II, quartzite and granite-I. The BBS tests were conducted on both moisture-conditioned and unconditioned samples.

#### *4.2.1.1 Moisture-induced damage evaluation in granite-II aggregate with PG 58-28 binder*

Table 4-4 and Figure 4-13 present a summary of the pull-off strength (POS) values obtained by conducting BBS tests on granite-II samples prepared with asphalt binders (PG 58-28, PG 64-22, PG 64-34, and PG 70-28) without any additives and those blended with 20% S-RAP, 0.5% WMA additive and 0.5% ASA with and without moisture conditioning. Also, the pull-off strength ratios (PSR) calculated by dividing the POS

values of moisture-conditioned samples to those of dry ones are presented in Table 4-4 and Figure 4-13. In addition, the failure modes, namely adhesive and cohesive, along with the standard deviation (SD) and coefficient of variation (COV) values for BBS tests are presented in Table 4-4. Statistical analysis was conducted using two-tailed t-test to examine the statistical significance of the difference between the average POS values with 95% confidence. Figure 4-14 shows the examples of failure mode determination. A summary of the statistical analysis for determination of significance of difference between the average pull-off strength values at 95 % confidence interval is presented in APPENDIX C.

Table 4-4 Binder bond strength test results for various asphalt binders with granite-II

Aggregate: Granite-II										
Binder Type	Additive	Unconditioned				Moisture-conditioned				Average *PSR
		Average *POS (kPa)	*SD (kPa)	*COV (%)	Failure Type (Visual)	Average *POS (kPa)	*SD (kPa)	*COV (%)	Failure Type (Visual)	
PG 58-28	Neat (0%)	756.36	39.99	5.30	100% cohesive	361.97	54.47	15.00	100% adhesive	0.48
	S-RAP (20%)	785.31	22.06	2.80	100% cohesive	364.04	28.27	7.80	98% adhesive	0.46
	WMA (0.5%)	508.83	20.68	4.00	100% cohesive	637.77	56.54	8.80	99% adhesive	1.25
	ASA (0.5%)	676.38	92.39	13.70	100% cohesive	606.74	57.23	9.40	91% cohesive	0.9
PG 64-22	Neat (0%)	854.95	121.35	14.20	100% cohesive	483.32	19.31	4.00	100% adhesive	0.56
	S-RAP (20%)	1399.64	66.19	4.70	100% cohesive	703.27	76.53	10.80	99% adhesive	0.5
	WMA (0.5%)	902.52	77.22	8.50	100% cohesive	708.78	86.87	12.30	94% adhesive	0.79
	ASA (0.5%)	1161.77	55.16	4.70	100% cohesive	670.17	38.61	5.70	58% adhesive	0.58
PG 64-34	Neat (0%)	461.95	42.75	9.20	100% cohesive	257.17	18.62	7.30	100% adhesive	0.56
	S-RAP (20%)	683.27	71.71	10.50	100% cohesive	381.28	21.37	5.70	100% adhesive	0.56
	WMA (0.5%)	641.90	29.65	4.70	100% cohesive	495.04	51.02	10.40	97% adhesive	0.77
	ASA (0.5%)	444.02	51.02	11.50	100% cohesive	516.42	48.95	9.50	95% cohesive	1.16
PG 70-28	Neat (0%)	831.51	39.30	4.80	100% cohesive	538.48	64.81	12.10	97% adhesive	0.65
	S-RAP (20%)	997.67	57.23	5.80	100% cohesive	690.17	89.63	13.00	85% adhesive	0.69
	WMA (0.5%)	800.48	97.22	12.10	100% cohesive	830.13	67.57	8.20	75% adhesive	1.04
	ASA (0.5%)	837.71	71.71	8.60	100% cohesive	648.80	56.54	8.70	87% adhesive	0.77

\*SD:Standard Deviation\*COV:Coefficient of Variation\*POS:Pull-off Strength\*PSR:Pull-off Strength Ratio

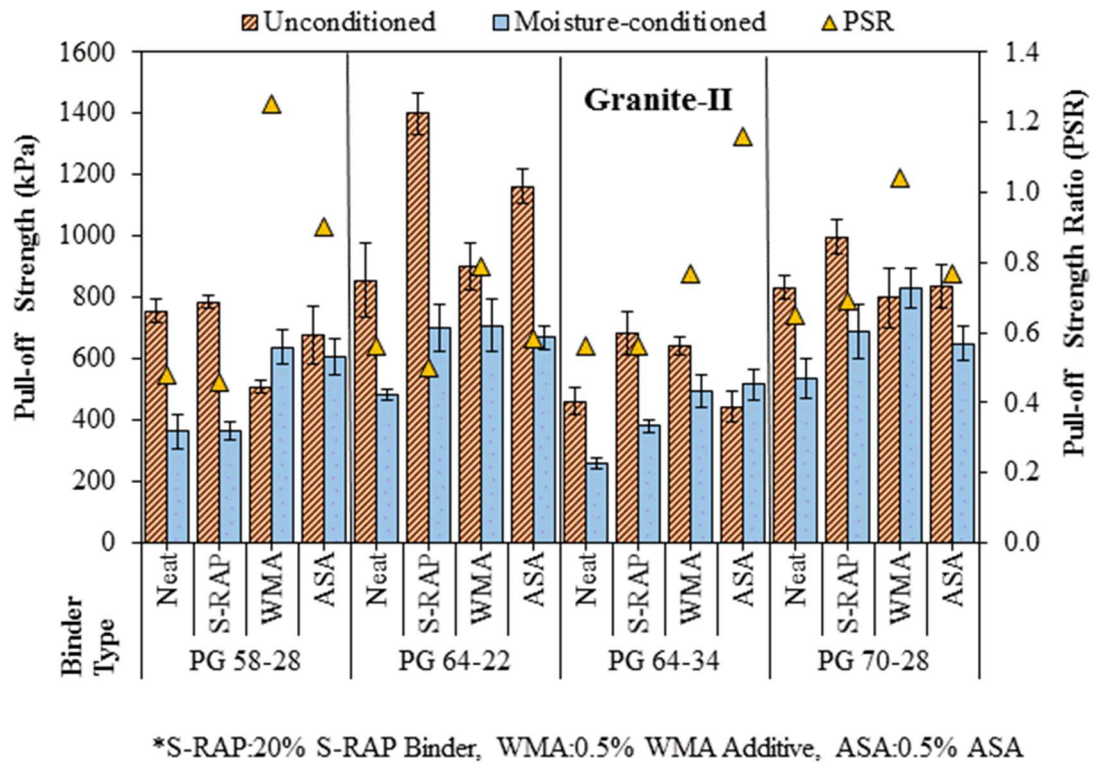


Figure 4-13 Comparison of pull-off strength of different binders with granite-II

From Table 4-4 it is evident that the dry pull-off strength ( $POS_{dry}$ ) of the neat PG 58-28 binder with granite-II (756.4 kPa) slightly increased (3.8%) as a result of addition of 20% S-RAP binder to the blend. The  $POS_{dry}$  values of the PG 58-28 binder blends containing 0.5% WMA additive and 0.5% ASA with granite-II, however, were found to be 32.7% and 10.6% less than that of the neat binder. This clearly shows that the adhesion of the asphalt binder and aggregate in dry condition can be affected by the binder type and aggregate mineralogy. Therefore, selection of the additive type should be made based on the aggregate type and binder properties to maximize adhesion. Adhesion is known to play an important role in determining the durability of a mix in the field (Zhang et al., 2017). Also, from Table 4.4 and Figure 4-13, it is evident that pull-off strength of the

moisture-conditioned sample ( $POS_{wet}$ ) of the neat PG 58-28 binder with granite-II (362.0 kPa) remained almost unchanged (0.6% increase) as a result of addition of 20% S-RAP binder to the blend. Also, the  $POS_{wet}$  values of the PG 58-28 binder blends containing 0.5% WMA additive and 0.5% ASA with granite-II, were found to be 76.2% and 67.6% higher than that of the neat binder. In other words, while addition of S-RAP did not significantly affect the adhesion of the PG 58-28 binder to granite-II after moisture conditioning, addition of an amine-based WMA additive and ASA to the binder significantly increased the  $POS_{wet}$  values compared to that of neat PG 58-28 binder.

In order to compare the effect of moisture-conditioning on the POS values, a parameter, namely pull-off strength ratio (PSR) was calculated by dividing  $POS_{wet}$  to  $POS_{dry}$  for each asphalt binder blend-aggregate system tested herein. The PSR value is analogous to TSR value and is desirable to be higher in order to represent a mix with a better resistance to moisture-induced damage. From Table 4-4 and Figure 4-13 it was found that the PSR value of neat PG 58-28 asphalt binder with granite-II (0.48) did not significantly improve by adding 20% S-RAP to the binder blend. However, PSR values calculated for binder blends containing WMA additive and ASA were found to be 1.25 and 0.9, exhibiting significant improvement. Therefore, it can be concluded that the amine-based additives (WMA and ASA) significantly improved the resistance of the tested PG 58-28 asphalt binder with granite-II aggregate to moisture-induced damage. It is important to note that, the mode of failure was recorded by visual observation and calculation of the adhesive and cohesive areas from pictures taken from the failure surfaces after BBS tests (Figure 4-14).

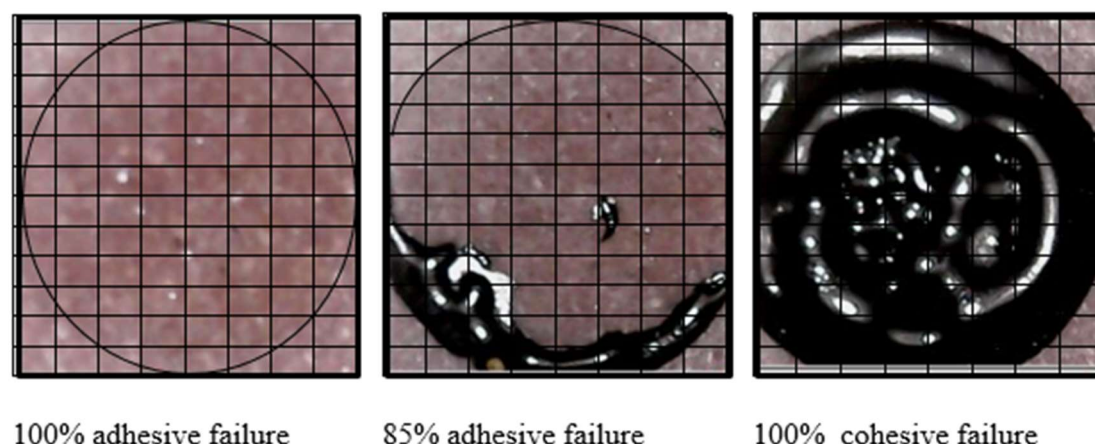


Figure 4-14 Failure modes in BBS test

From Table 4-4, the failure mode for all blends of the unconditioned PG 58-28 binder-granite-II samples were found to be cohesive (i.e., adhesive POS > cohesive POS).

However, the pull-off failure mode of the neat PG 58-28 binder and blends containing 20% S-RAP and 0.5% WMA additive with granite-II aggregate mainly changed to adhesive failure, after moisture-conditioning of the samples. In other words, moisture-conditioning had a detrimental effect on the adhesion of binder and aggregates. However, addition of the ASA to PG 58-28 binder resulted in a cohesive failure after moisture conditioning, indicating an improved adhesion with granite-II as a result of using ASA in binder blend.

#### *4.2.1.2 Moisture-induced damage evaluation in granite-II aggregate with PG 64-22 binder*

From Table 4-4 it is clearly seen that the dry pull-off strength ( $POS_{dry}$ ) of the neat PG 64-22 binder with granite-II (854.95 kPa) increased (63.7%) as a result of addition of 20% S-RAP binder to the blend. The  $POS_{dry}$  values of the PG 64-22 binder blend containing

0.5% WMA additive and that containing 0.5% ASA with granite-II, were found to be 5.56% and 35% higher than that of the neat binder, respectively. Also, from Table 4.4 and Figure 4-13, it is evident that the moisture-conditioned pull-off strength ( $POS_{wet}$ ) of the neat PG 64-22 binder with granite-II (483.32 kPa) was found to increase by 45.5% as a result of addition of 20% S-RAP binder to the blend.

Also, the  $POS_{wet}$  values of the PG 64-22 binder blend containing 0.5% WMA additive and that 0.5% ASA with granite-II, were found to be 46.6% and 38.7% higher than that of the neat binder. In other words, addition of S-RAP, amine-based WMA additive, and ASA to the blend increased the adhesion of the PG 64-22 binder to granite-II after moisture conditioning with significant increase in the  $POS_{wet}$  values compared to that of neat PG 64-22 binder. From Table 4-4 and Figure 4-13 it was found that the PSR value of neat PG 64-22 asphalt binder with granite-II (0.56) did not significantly improve the adhesion by adding 20% S-RAP to the binder blend. Also, the binder blend containing ASA did not significantly improve the adhesion. However, the PSR value calculated for the binder blend containing WMA additive was found to be 0.79, exhibiting a significant improvement in resistance to moisture-induced damage compared to neat binder (0.56). Therefore, it can be concluded that the amine-based WMA additive significantly improved the resistance of the tested PG 64-22 asphalt binder with granite-II aggregate. From Table 4-4, the failure mode for all blends of the unconditioned PG 64-22 binder-granite-II samples were found to be cohesive (i.e., adhesive  $POS >$  cohesive  $POS$ ). However, the pull-off failure mode of the neat 64-22 binder and blends containing 20% S-RAP, 0.5% ASA and 0.5% WMA additive with granite-II aggregate mainly changed to



adhesive failure, after moisture-conditioning of the samples. It is important to note that addition of the WMA additive to PG 64-22 binder resulted in an adhesive failure after moisture conditioning while the PSR values were found to improve by addition of WMA additive to blend (0.5 to 0.79). Even though the addition of 0.5% ASA did not increase the PSR value, it resulted in a change in failure mode in the moisture-conditioned samples from 100% adhesive for neat binder to 58% adhesive and 42% cohesive for the blend containing ASA. In other words, moisture-conditioning had an adverse effect on the adhesion of binder and aggregates that addition of the ASA partially mitigated it.

#### *4.2.1.3 Moisture-induced damage evaluation in granite-II aggregate with PG 64-34 binder*

From Table 4-4 the dry pull-off strength ( $POS_{dry}$ ) of the neat PG 64-34 binder with granite-II (461.95 kPa) significantly increased (43.9%) after addition of 20% S-RAP binder to the blend. The  $POS_{dry}$  values of the PG 64-34 binder blends containing 0.5% WMA additive and those with 0.5% ASA with granite-II were found to be 38.9% higher and 3% less (statistically the same) than that of the neat binder. It is apparent that the selection of the additive type should be made based on both the aggregate type and binder properties to have better durability. The Table 4.4 and Figure 4-13, show that the moisture-conditioned pull-off strength ( $POS_{wet}$ ) of the neat PG 64-34 binder with granite-II (257.17 kPa) was found to increase by 48.3% after addition of 20% S-RAP binder to the blend. Also, the  $POS_{wet}$  values of the PG 64-34 binder blends containing 0.5% WMA additive and that containing 0.5% ASA with granite-II, were found to be 92.5% and 100.8% higher than that of the neat binder. In other words, addition of S-RAP, amine-

based WMA additive, and ASA to PG 64-34 binder increased its adhesion to granite-II after moisture conditioning with significant increase in the  $POS_{wet}$  values compared to that of neat binder. From Table 4-4 and Figure 4-13 it is clear that the PSR value of neat PG 64-34 asphalt binder with granite-II (0.56) did not significantly improve either by addition of 20% S-RAP (0.69) or by addition of 0.5% WMA additive (0.77) to the binder blend.

However, PSR value calculated for binder blends containing 0.5% ASA (1.16) was found to exhibit significant increase in PSR value compared to that of the neat binder.

Therefore, one can say that the amine-based ASA significantly improved the resistance of a mix of PG 64-34 asphalt binder with granite-II to moisture-induced damage. Also, from Table 4-4, it is evident that the failure mode for all blends of the unconditioned PG 64-34 binder- granite-II samples were found to be cohesive (i.e., adhesive  $POS >$  cohesive  $POS$ ). However, the pull-off failure mode of the neat PG 64-34 binder and blends containing 20% S-RAP and 0.5% WMA additive with granite-II aggregate mainly changed to adhesive failure, after moisture-conditioning of the samples. However, addition of the ASA to PG 64-34 binder resulted in a cohesive failure after moisture conditioning, indicating an improved adhesion with granite-II as a result of using an ASA in binder blend.

#### *4.2.1.4 Moisture-induced damage evaluation in granite-II aggregate with PG 70-28 binder*

From Table 4-4 it is evident that the dry pull-off strength ( $POS_{dry}$ ) of the neat PG 70-28 binder with granite-II (831.51 kPa) significantly increased (19.9%) as a result of addition of 20% S-RAP binder to the blend. The  $POS_{dry}$  values of the PG 70-28 binder blends containing 0.5% WMA additive and 0.5% ASA with granite-II, however, were found to be 3% less (statistically the same) and 0.74% higher (statistically the same) than that of the neat binder. Table 4.4 and Figure 4-13, clearly show that the moisture-conditioned pull-off strength ( $POS_{wet}$ ) of the neat PG 70-28 binder with granite-II (538.48 kPa) was found to increase by 28.2% as a result of addition of 20% S-RAP binder to the blend.

Also, the  $POS_{wet}$  values of the PG 70-28 binder blends containing 0.5% WMA additive and those with 0.5% ASA with granite-II, were found to be 54.2% and 20.5% higher than that of the neat binder. In other words, addition of S-RAP, amine-based WMA additive, and ASA to the binder increased the adhesion of the PG 70-28 binder to granite-II after moisture conditioning with significant increase in the  $POS_{wet}$  values compared to that of neat binder. From Table 4-4 and Figure 4-13 it was found that the PSR value of neat PG 70-28 asphalt binder with granite-II (0.65) did not significantly improve by adding 20% S-RAP to the binder blend. Also, incorporating ASA in the binder blend did not significantly improve the adhesion. However, PSR value calculated for binder blends containing WMA additive was found to be 1.04 exhibiting improvement resistance to moisture-induced damage and a significant increase in PSR with respect to the neat binder. Therefore, it can be concluded that the amine-based additive (WMA) significantly

improved the resistance to moisture-induced damage of the tested PG 70-28 asphalt binder with granite-II aggregate. The mode of failure recorded by visual observation and calculation of the adhesive and cohesive areas from pictures taken from the failure surfaces showed that the failure mode for all blends of the unconditioned PG 70-28 binder- granite-II samples were found to be cohesive (i.e., adhesive POS > cohesive POS). However, the pull-off failure mode of the neat 70-28 binder and blends containing 20% S-RAP, 0.5% ASA and 0.5% WMA additive with granite-II aggregate mainly changed to adhesive failure, after moisture-conditioning of the samples.

Table 4-5 Binder bond strength test results for various asphalt binders with quartzite

Aggregate: Quartzite										
Binder Type	Additive	Unconditioned				Moisture-conditioned				Average *PSR
		Average *POS (kPa)	*SD (kPa)	*COV (%)	Failure Type (Visual)	Average *POS (kPa)	*SD (kPa)	*COV (%)	Failure Type (Visual)	
PG 58-28	Neat (0%)	794.97	53.09	6.30	100% cohesive	519.18	44.13	8.50	94% adhesive	0.65
	S-RAP (20%)	698.44	50.33	7.20	100% cohesive	486.08	55.16	11.40	92% adhesive	0.70
	WMA (0.5%)	602.60	33.78	5.60	100% cohesive	555.72	73.08	13.20	100% cohesive	0.92
	ASA (0.5%)	574.33	79.98	14.00	100% cohesive	691.54	88.94	12.90	100% cohesive	1.20
PG 64-22	Neat (0%)	996.98	88.94	9.00	100% cohesive	599.84	80.67	13.40	72% adhesive	0.60
	S-RAP (20%)	1238.30	70.33	5.70	100% cohesive	544.00	74.46	13.60	80% adhesive	0.44
	WMA (0.5%)	855.64	105.49	12.30	100% cohesive	741.19	26.20	3.60	69% adhesive	0.87
	ASA (0.5%)	1150.05	117.90	10.20	100% cohesive	666.03	44.82	6.70	87% cohesive	0.58
PG 64-34	Neat (0%)	493.66	25.51	5.10	100% cohesive	276.48	34.47	12.50	98% adhesive	0.56
	S-RAP (20%)	655.00	37.92	5.80	100% cohesive	514.35	55.85	10.90	82% adhesive	0.79
	WMA (0.5%)	588.12	79.29	13.50	100% cohesive	566.75	45.51	8.00	80% adhesive	0.96
	ASA (0.5%)	476.43	62.05	13.00	100% cohesive	495.04	53.78	10.80	88% cohesive	1.04
PG 70-28	Neat (0%)	796.34	37.92	4.80	100% cohesive	721.19	45.51	6.30	75% adhesive	0.91
	S-RAP (20%)	1157.63	31.03	2.70	100% cohesive	746.70	77.91	10.40	50% adhesive	0.65
	WMA (0.5%)	783.93	79.29	10.20	100% cohesive	834.27	84.12	10.10	69% adhesive	1.06
	ASA (0.5%)	883.91	50.33	5.70	100% cohesive	671.55	76.53	11.40	80% cohesive	0.76

\*SD:Standard Deviation\*COV:Coefficient of Variation\*POS:Pull-off Strength\*PSR:Pull-off Strength Ratio

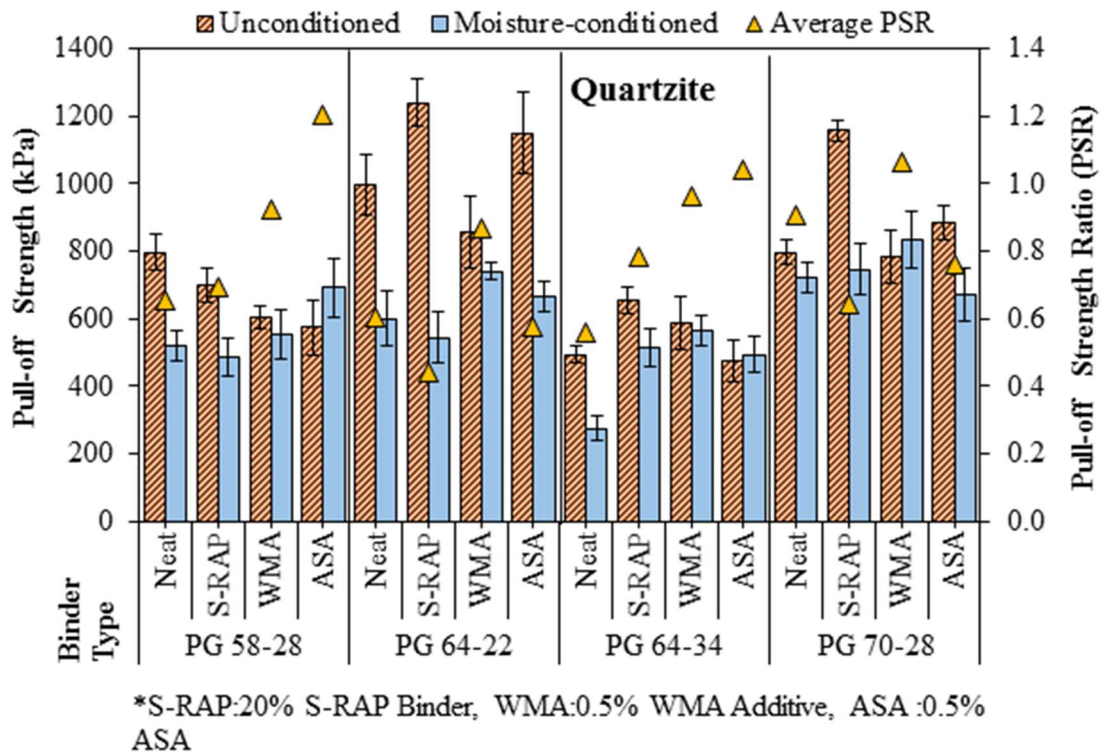


Figure 4-15 Comparison of pull-off strength between quartzite and different binders

#### 4.2.1.5 Moisture-induced damage evaluation in quartzite aggregate with PG 58-28 binder

From Table 4-5 it can be observed that the dry pull-off strength ( $POS_{dry}$ ) of the neat PG 58-28 binder with quartzite (794.97 kPa) decreased by 12.2% as a result of addition of 20% S-RAP binder to the blend. The  $POS_{dry}$  values of the PG 58-28 binder blend containing 0.5% WMA additive and 0.5% ASA with quartzite, however, were found to decrease by 24.2% and 27.8% compared to that of the neat binder. In other words, quartzite unlike the granite-II with same binder as well. Also, from Table 4-5 and Figure 4-15, it is apparent that the moisture-conditioned pull-off strength ( $POS_{wet}$ ) of the neat

PG 58-28 binder with quartzite (519.18 kPa) remained almost unchanged (6% increase) as a result of addition of 20% S-RAP binder to the blend. Also, the  $POS_{wet}$  value of the PG 58-28 binder blends containing 0.5% WMA additive and 0.5% ASA with quartzite, were found to be 7.0% and 33.2% higher than that of the neat binder. In other words, while addition of S-RAP, and 0.5% WMA additive did not significantly affect the adhesion of the PG 58-28 binder to quartzite after moisture conditioning, addition of ASA to the binder significantly increased the  $POS_{wet}$  values compared to that of neat PG 58-28 binder. From Table 4-5 and Figure 4-15 it is evident that PSR value of the neat PG 58-28 asphalt binder with quartzite (0.65) did not significantly improve by adding 20% S-RAP to the binder blend.

However, PSR values calculated for binder blends containing WMA additive and ASA were found to be 0.92 and 1.2, exhibiting significant improvement in adhesion. Therefore, it can be concluded that the amine-based additives (WMA and ASA) significantly improved the resistance of the tested PG 58-28 asphalt binder with quartzite aggregate. Also, from Table 4-5, the failure mode for all blends of the unconditioned PG 58-28 binder-quartzite samples were found to be cohesive (i.e., adhesive  $POS >$  cohesive  $POS$ ). However, the pull-off failure mode of the neat PG 58-28 binder and blends containing 20% S-RAP with quartzite aggregate mainly changed to adhesive failure, after moisture conditioning of the samples. In other words, moisture conditioning had a detrimental effect on the adhesion of binder and aggregates. However, addition of the 0.5% WMA additive, and 0.5% ASA to PG 58-28 binder resulted in a cohesive failure

after moisture conditioning, indicating an improved adhesion with quartzite as a result of using WMA additive, and ASA in the binder blend.

#### *4.2.1.6 Moisture-induced damage evaluation in quartzite aggregate with PG 64-22 binder*

From Table 4-5 it was observed that the dry pull-off strength ( $POS_{dry}$ ) of the neat PG 64-22 binder with quartzite (996.98 kPa) increased (24.2%) as a result of addition of 20% S-RAP binder to the blend. The  $POS_{dry}$  values of the PG 64-22 binder blend containing 0.5% WMA additive and that containing 0.5% ASA with quartzite, were found to be 14.8% less and 15.4% higher than that of the neat binder. Also, from Table 4.5 and Figure 4-15, it is evident that the moisture-conditioned pull-off strength ( $POS_{wet}$ ) of the neat PG 64-22 binder with quartzite (599.84 kPa) was found to be decrease by 9.3% as a result of addition of 20% S-RAP binder to the blend. Also, the  $POS_{wet}$  values of the PG 64-22 binder blend containing 0.5% WMA additive with quartzite was found to be 23.6% higher than that of the neat binder. However, addition of 0.5% ASA to the neat binder was not found to have a significant effect on increasing adhesion.

In other words, adhesion of the PG 64-22 binder to quartzite was found to increase as a result of adding an amine-based WMA additive to the blend, and resulted in an increase in the  $POS_{wet}$  value compared to that of neat PG 64-22 binder. From Table 4-5 and Figure 4-15 it was also found that the PSR value of neat PG 64-22 asphalt binder with quartzite (0.6) decreased after addition of 20% S-RAP to the binder blend (0.44). Also, the PSR value of the binder blend containing ASA (0.58) was not found to be significantly



different than that of the neat binder with quartzite (0.60). However, the PSR value calculated for the binder blend containing WMA additive was found to be 0.87, exhibiting significant improvement compared to that of the neat binder with quartzite. Therefore, it can be concluded that the amine-based additive (WMA) significantly improved the resistance of the tested PG 64-22 asphalt binder with quartzite aggregate to moisture-induced damage. From Table 4-5, the failure mode for all blends of the unconditioned PG 64-22 binder-quartzite samples were found to be cohesive (i.e., adhesive POS > cohesive POS). However, the pull-off failure mode of the neat 64-22 binder and blends containing 20% S-RAP, and 0.5% WMA additive with quartzite aggregate mainly changed to adhesive failure, after moisture-conditioning of the samples. The failure mode of the binder blend containing 0.5% ASA, remained cohesive after moisture-conditioning, an indication of an improved adhesion of the binder with aggregate as a result of using ASA in the blend.

#### *4.2.1.7 Moisture-induced damage evaluation in quartzite aggregate with PG 64-34 binder*

The Table 4-5 shows that the dry pull-off strength (POS<sub>dry</sub>) of the neat PG 64-34 binder with quartzite (493.66 kPa) significantly increased (32.7%) after addition of 20% S-RAP binder to the blend. The POS<sub>dry</sub> values of the PG 64-34 binder blends containing 0.5% WMA additive and those with 0.5% ASA, with quartzite were found to be 19% higher (significantly the same) and 3% lower (statistically the same) than that of the neat binder. This implies that the selection of the additive type should be made based on both the aggregate type and binder properties to have better durability. From Table 4-5 and

Figure 4-15, it is very interesting to know that the moisture-conditioned pull-off strength ( $POS_{wet}$ ) of the neat PG 64-34 binder with quartzite (276.48 kPa) was found to be increased by 86.03%, 104.98%, and 79.06% with addition of 20% S-RAP binder, 0.5% WMA additive, and 0.5% ASA respectively. In other words, addition of S-RAP, addition of amine-based WMA additive and ASA to the binder increased the adhesion of the PG 64-34 binder to quartzite after moisture conditioning with significant increase in the  $POS_{wet}$  values compared to that of neat PG 64-34 binder. The pull-off strength ratio (PSR) was desirable to be higher in order to have a better resistance to moisture-induced damage. From Table 4-5 and Figure 4-15 it is evident that the PSR value of neat PG 64-34 asphalt binder (0.56) with quartzite significantly improved by adding 20% S-RAP to the binder blend, which is different with the result obtained for granite-II, and granite-I.

Also, PSR values calculated for binder blends containing WMA additive, and binder blend containing ASA with quartzite were found to be 0.96, and 1.04 exhibiting significantly higher improvement in adhesion. Therefore, it is credible to say that the amine-based additives WMA, and ASA significantly improved the adhesion of the tested PG 64-34 asphalt binder with granite-II aggregate. Additionally, addition of 20% S-RAP in the neat PG 64-34 binder blend was found to improve the adhesion with quartzite. The examples of mode of failure are presented in Figure 4-14. From Table 4-5, it is evident that the failure mode for all blends of the unconditioned PG 64-34 binder-quartzite samples were found to be cohesive (i.e., adhesive  $POS >$  cohesive  $POS$ ). However, the pull-off failure mode of the neat PG 64-34 binder and blends containing 20% S-RAP and 0.5% WMA additive with quartzite aggregate mainly changed to adhesive failure, after

moisture-conditioning of the samples. Hence, it is apparent to say that moisture-conditioning had a detrimental effect on the adhesion of binder and aggregates. However, addition of the ASA to PG 64-34 binder resulted in a cohesive failure after moisture conditioning, indicating an improved adhesion with quartzite as a result of using ASA in binder blend.

#### *4.2.1.8 Moisture-induced damage evaluation in quartzite aggregate with PG 70-28 binder*

From Table 4-5 it is evident that the dry pull-off strength ( $POS_{dry}$ ) of the neat PG 70-28 binder with quartzite (796.34 kPa) highly increased (45.4%) as a result of addition of 20% S-RAP binder to the blend. The  $POS_{dry}$  values of the PG 70-28 binder blends containing 0.5% WMA additive and 0.5% ASA with quartzite, however, were found to be 1% lower (significantly the same) and 11% higher than that of the neat binder. It is apparent to say that the adhesion of the asphalt binder and aggregate in dry condition can be affected by the binder type and aggregate mineralogy. Therefore, selection of the additive type should be made based on the aggregate type and binder properties to have a better durability with respect to adhesion. Table 4.5 and Figure 4-15, shows that the moisture-conditioned pull-off strength ( $POS_{wet}$ ) of the neat PG 70-28 binder with quartzite (721.19 kPa) was found to be increased by 3.5% (significantly the same) as a result of addition of 20% S-RAP binder to the blend. Also, the  $POS_{wet}$  values of the PG 70-28 binder blends containing 0.5% WMA additive and 0.5% ASA with quartzite, were found to be 15.7% higher and 6.8% lower (significantly the same) than that of the neat binder. In other words, addition of amine-based WMA additive increased the adhesion of

the PG 70-28 binder to quartzite after moisture conditioning with significant increase in the  $POS_{wet}$  values compared to that of neat PG 70-28 binder. In order to compare the effect of moisture-conditioning on the POS values, pull-off strength ratio (PSR) was calculated by dividing  $POS_{wet}$  to  $POS_{dry}$  for each asphalt binder blend-aggregate system tested herein. From Table 4-5 and Figure 4-15 it was found that the PSR value of neat PG 70-28 asphalt binder (0.91) with quartzite did not significantly improved by adding 20% S-RAP to the binder blend. Also, the addition of 0.5% ASA (0.76) did not significantly improved the adhesion. However, PSR values calculated for binder blends containing WMA additive, was found to be 1.04 exhibiting significant improvement.

Therefore, it can be concluded that the 0.5% WMA additive significantly improved the resistance of the tested PG 70-28 asphalt binder with quartzite aggregate. From Table 4-5, and Figure 4-14 it is clear that the failure mode for all blends of the unconditioned PG 70-28 binder-quartzite samples were found to be cohesive (i.e., adhesive POS > cohesive POS). However, the pull-off failure mode of the neat 70-28 binder and blends containing 20% S-RAP, and 0.5% WMA additive with quartzite aggregate mainly changed to adhesive failure, after moisture-conditioning of the samples. It is important to note that the addition of 0.5% ASA in the PG 70-28 with PSR less than that of neat binder with quartzite aggregate showed cohesive failure after moisture conditioning. From Table 4-5 it is apparent to say that while improving the adhesion strength by addition of the 0.5% ASA, reduction in the cohesion strength of the PG 70-28 binder had occurred.

Table 4-6 Binder bond strength test results for various asphalt binders with granite-I

Aggregate: Granite-I										
Binder Type	Additive	Unconditioned				Moisture Conditioned				Average *PSR
		Average *POS (kPa)	*SD (kPa)	*COV (%)	Failure Type (Visual)	Average *PS (kPa)	*SD (kPa)	*COV (%)	Failure Type (Visual)	
PG 58-28	Neat (0%)	752.22	33.78	4.50	100% cohesive	667.41	44.13	6.60	100% adhesive	0.89
	S-RAP (20%)	773.59	104.80	13.60	100% cohesive	170.30	13.10	7.60	100% adhesive	0.22
	WMA (0.5%)	651.55	61.36	9.40	100% cohesive	708.78	39.99	5.70	60% cohesive	1.09
	ASA (0.5%)	640.52	61.36	9.60	100% cohesive	480.56	25.51	5.30	97% adhesive	0.75
PG 64-22	Neat (0%)	974.92	44.82	4.60	100% cohesive	468.15	40.68	8.70	100% adhesive	0.48
	S-RAP (20%)	1362.40	125.48	9.20	100% cohesive	469.53	18.62	4.00	99% adhesive	0.34
	WMA (0.5%)	877.01	80.67	9.20	100% cohesive	721.19	99.28	13.70	87% adhesive	0.82
	ASA (0.5%)	1336.89	138.58	10.40	100% cohesive	449.54	40.68	9.10	99% adhesive	0.34
PG 64-34	Neat (0%)	506.08	43.44	8.60	100% cohesive	366.11	36.54	9.90	100% adhesive	0.72
	S-RAP (20%)	717.06	36.54	5.10	100% cohesive	286.82	21.37	7.50	100% adhesive	0.40
	WMA (0.5%)	629.49	91.70	14.60	100% cohesive	452.30	43.44	9.70	100% adhesive	0.72
	ASA (0.5%)	429.54	37.92	8.80	100% cohesive	550.20	22.75	4.10	92% cohesive	1.28
PG 70-28	Neat (0%)	841.85	76.53	9.10	100% cohesive	384.73	48.26	12.50	100% adhesive	0.46
	S-RAP (20%)	1016.98	75.15	7.40	100% cohesive	595.02	46.19	7.80	100% adhesive	0.59
	WMA (0.5%)	783.24	96.53	12.30	100% cohesive	504.70	63.43	12.60	99% adhesive	0.64
	ASA (0.5%)	990.09	129.62	13.10	100% cohesive	595.71	57.23	9.60	97% adhesive	0.60

\*SD:Standard Deviation\*COV:Coefficient of Variation\*POS:Pull-off Strength\*PSR:Pull-off Strength Ratio

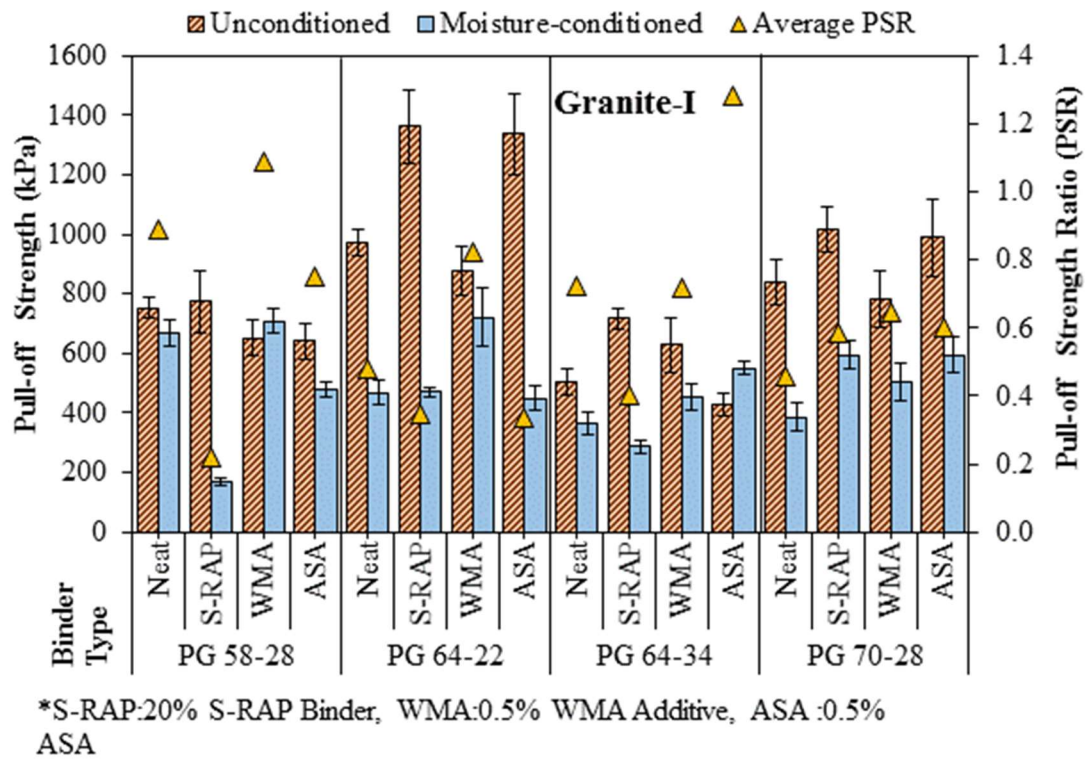


Figure 4-16 Comparison of pull-off strength between granite-I and different binders

#### 4.2.1.9 Moisture-induced damage evaluation in granite-I aggregate with PG 58-28 binder

From Table 4-6 it is evident that the dry pull-off strength ( $POS_{dry}$ ) of the neat PG 58-28 binder with granite-I (752.22 kPa) increased by 2.8% (significantly the same) as a result of addition of 20% S-RAP binder to the blend. The  $POS_{dry}$  values of the PG 58-28 binder blends containing 0.5% WMA additive and 0.5% ASA with granite-I, however, were decreased by 13.4% and 14.8% than that of the neat binder. This clearly shows that the adhesion of the asphalt binder and aggregate in dry condition can be affected by the binder type and aggregate mineralogy. Also, from Table 4.6 and Figure 4-16, it is evident that the moisture-conditioned pull-off strength ( $POS_{wet}$ ) of the neat PG 58-28 binder with

granite-I (667.41 kPa) highly decreased (74.5%) as a result of addition of 20% S-RAP binder to the blend. Also, the  $POS_{wet}$  value of the PG 58-28 binder blend containing 0.5% ASA with granite-I, were found to be 6.2% higher (significantly the same) than that of the neat binder. However, for addition of the 0.5% WMA additive the  $POS_{wet}$  value of the PG 58-28 binder blend with granite-I was found to be increased by 28% than that of neat binder. In other words, while addition of S-RAP, and 0.5% ASA significantly affect the adhesion of the PG 58-28 binder to granite-I after moisture conditioning, addition of WMA additive to the binder,  $POS_{wet}$  values compared to that of neat PG 58-28 binder significantly remained unchanged.

From Table 4-6 and Figure 4-16 it is evident that PSR value of neat PG 58-28 asphalt binder with granite-I (0.89) was not found to be significantly improved by adding 20% S-RAP to the binder blend. Also, addition of ASA to the neat PG 58-28 binder with granite-I did not increase the PSR value (0.75). However, PSR values calculated for binder blend containing WMA additive was found to be 1.2, exhibiting significant improvement in adhesion. Therefore, it can be concluded that the addition of amine-based WMA additive significantly improved the resistance of the tested PG 58-28 asphalt binder with granite-I aggregate. From Table 4-6, and Figure 4-14, it is visible that the failure mode for all blends of the unconditioned PG 58-28 binder-granite-I samples were found to be cohesive (i.e., adhesive  $POS >$  cohesive  $POS$ ). However, the pull-off failure mode of the neat PG 58-28 binder, blends containing 20% S-RAP, and blends containing 0.5% ASA with granite-I aggregate mainly changed to adhesive failure, after moisture-conditioning of the samples. However, addition of the 0.5% WMA additive to PG 58-28 binder

resulted in a cohesive failure after moisture conditioning, indicating an improved adhesion with granite-I as a result of using WMA additive in the binder blend.

#### *4.2.1.10 Moisture-induced damage evaluation in granite-I aggregate with PG 64-22 binder*

From Table 4-5 it is observed that the dry pull-off strength ( $POS_{dry}$ ) of the neat PG 64-22 binder with granite-I (974.92 kPa) increased (39.7%) as a result of addition of 20% S-RAP binder to the blend. The  $POS_{dry}$  values of the PG 64-22 binder blend containing 0.5% WMA additive and 0.5% ASA with granite-I, were found to be 10% less (significantly the same) and 37% high than that of the neat binder. It shows that the adhesion of the asphalt binder and aggregate in dry condition can be affected by the binder type and aggregate mineralogy.

Also, from Table 4.6 and Figure 4-16, it is evident that the moisture-conditioned pull-off strength ( $POS_{wet}$ ) of the neat PG 64-22 binder with granite-I (468.15 kPa) was found to be significantly the same as a result of addition of 20% S-RAP binder to the blend. Also, the  $POS_{wet}$  values of the PG 64-22 binder blends containing 0.5% WMA additive with granite-I, was found to be 54% higher than that of the neat binder. However, addition of 0.5% ASA in the PG 64-22 neat binder with granite-I was found to have significantly same  $POS_{wet}$  values. In other words, addition of amine-based WMA additive increased the adhesion of the PG 64-22 binder to granite-I after moisture conditioning with significant increase in the  $POS_{wet}$  values compared to that of neat PG 64-22 binder. The pull-off strength ratio (PSR) calculated by dividing  $POS_{wet}$  to  $POS_{dry}$  for each asphalt



binder blend-aggregate system tested was utilized to analyze effect of moisture conditioning. From Table 4-6, and Figure 4-16, it was found that the PSR value of neat PG 64-22 asphalt binder (0.48) with granite-I was found to be decreased after addition of 20% S-RAP to the binder blend. Also, the binder blend containing ASA (0.34) did not significantly improved the adhesion. However, PSR values calculated for binder blends containing WMA additive was found to be 0.82, exhibiting significant improvement.

Therefore, it can be concluded that the amine-based additive (WMA) significantly improved the resistance of the tested PG 64-22 asphalt binder with granite-I aggregate. The mode of failure recorded by visual observation and calculation of the adhesive and cohesive areas from pictures taken from the failure surfaces after BBS tests are presented in Figure 4-14. From Table 4-6, the failure mode for all blends of the unconditioned PG 64-22 binder-granite-I samples were found to be cohesive (i.e., adhesive POS > cohesive POS). However, the pull-off failure mode of the neat 64-22 binder and blends containing 20% S-RAP, and 0.5% WMA additive, and 0.5% ASA with granite-I aggregate mainly changed to adhesive failure, after moisture-conditioning of the samples. In other words, moisture-conditioning had an adverse effect on the adhesion of binder and aggregates.

#### *4.2.1.11 Moisture-induced damage evaluation in granite-I aggregate with PG 64-34 binder*

The Table 4-6 shows that the dry pull-off strength ( $POS_{dry}$ ) of the neat PG 64-34 binder with granite-I (506.08 kPa) significantly increased (41.7%) after addition of 20% S-RAP binder to the blend. The  $POS_{dry}$  values of the PG 64-34 binder blends containing 0.5%

WMA additive and 0.5% ASA, however, with granite-I were found to be 24.4% high and 15% less than that of the neat binder. It is clear that the selection of the additive type should be made based on both the aggregate type and binder properties to have better durability. From Table 4-6 and Figure 4-16, it is very interesting to know that that the moisture-conditioned pull-off strength ( $POS_{wet}$ ) of the neat PG 64-34 binder with granite-I (366.11 kPa) was found to be decreased by 21.6%, increased by 23.54%, and increased by 50.3% with addition of 20% S-RAP binder, 0.5% WMA additive, and 0.5% ASA respectively in the binder blend with granite-I. In other words, addition of amine-based WMA additive and ASA to the binder increased the adhesion of the PG 64-34 binder to granite-I after moisture conditioning with significant increase in the  $POS_{wet}$  values compared to that of neat PG 64-34 binder.

The pull-off strength ratio (PSR) was desirable to be higher in order to have a better resistance to moisture-induced damage. From Table 4-6 and Figure 4-16 it is clear that the PSR value of neat PG 64-34 asphalt binder (0.72) with granite-I significantly improved to 1.28 by adding 0.5% ASA to the binder blend. However, PSR values calculated for binder blends containing 20% S-RAP binder, and binder blend containing WMA additive did not increased the PSR values. Therefore, it is credible to say that the amine-based ASA significantly improved the resistance of the tested PG 64-34 asphalt binder with granite-I aggregate. The examples of mode of failure are presented in Figure 4-14. From Table 4-6, it is evident that the failure mode for all blends of the unconditioned PG 64-34 binder-granite-I samples were found to be cohesive (i.e., adhesive  $POS >$  cohesive  $POS$ ). However, the pull-off failure mode of the neat PG 64-34

binder and blends containing 20% S-RAP and 0.5% WMA additive with granite-I aggregate mainly changed to adhesive failure, after moisture-conditioning of the samples. Therefore, it can be said that moisture-conditioning had a detrimental effect on the adhesion of binder and aggregates. However, addition of the ASA to PG 64-34 binder resulted in a cohesive failure after moisture conditioning, indicating an improved adhesion with granite-I as a result of using ASA in binder blend.

#### *4.2.1.12 Moisture-induced damage evaluation in granite-I aggregate with PG 70-28 binder*

From Table 4-6 it is clearly seen that the dry pull-off strength ( $POS_{dry}$ ) of the neat PG 70-28 binder with granite-I (841.85 kPa) significantly increased (20.8%) as a result of addition of 20% S-RAP binder to the blend. The  $POS_{dry}$  values of the PG 70-28 binder blends containing 0.5% WMA additive and 0.5% ASA with granite-I, however, were found to be significantly the same as that of the neat binder. It is apparent to say that the adhesion of the asphalt binder and aggregate in dry condition can be affected by the binder type and aggregate mineralogy. Therefore, selection of the additive type should be made based on the aggregate type and binder properties to have a better durability with respect to adhesion. Table 4.6 and Figure 4-16, shows that the moisture-conditioned pull-off strength ( $POS_{wet}$ ) of the neat PG 70-28 binder with granite-I (384.73 kPa) was found to be increased by 54.7% as a result of addition of 20% S-RAP binder to the blend. Also, the  $POS_{wet}$  values of the PG 70-28 binder blends containing 0.5% WMA additive and 0.5% ASA with granite-I, were found to be 31.2% higher and 54.8% higher than that of the neat binder. In other words, addition of amine-based additives (ASA, and WMA), and

S-RAP binder increased the adhesion of the PG 70-28 binder to granite-I after moisture conditioning with significant increase in the  $POS_{wet}$  values compared to that of neat PG 70-28 binder. In order to compare the effect of moisture-conditioning on the POS values, pull-off strength ratio (PSR) calculated by dividing  $POS_{wet}$  to  $POS_{dry}$  for each asphalt binder blend-aggregate system tested herein. From Table 4-6 and Figure 4-16 it was found that the PSR value of neat PG 70-28 asphalt binder (0.46) with granite-I significantly improved by adding 20% S-RAP, 0.5% ASA, and 0.5%WMA additive. From Table 4-6, Figure 4-14 it is visible that the failure mode for all blends of the unconditioned PG 70-28 binder-granite-I samples were found to be cohesive (i.e., adhesive  $POS >$  cohesive  $POS$ ). However, the pull-off failure mode of the neat 70-28 binder and blends containing 20% S-RAP, 0.5% WMA additive, and 0.5% ASA each with granite-I aggregate mainly changed to adhesive failure, after moisture-conditioning of the samples. The evaluation of asphalt binder-aggregate pull-off strength based on the higher to lower pull-off strength ratio (PSR) is presented in Table 4-7.

Table 4-7 Resistance to moisture-induced damage based on average PSR

Aggregate type	Binder Type	Additive	Average PSR	Rank	Aggregate type	Binder Type	Additive	Average PSR	Rank
Granite-I	PG 64-34	ASA	1.28	1	Granite-II	PG 70-28	S-RAP	0.69	21
Granite-II	PG 58-28	WMA	1.25	2	Quartzite	PG 58-28	Neat	0.65	22
Quartzite	PG 58-28	ASA	1.20	3	Granite-II	PG 70-28	Neat	0.65	22
Granite-II	PG 64-34	ASA	1.16	4	Quartzite	PG 70-28	S-RAP	0.65	23
Granite-I	PG 58-28	WMA	1.09	5	Granite-I	PG 70-28	WMA	0.64	24
Quartzite	PG 70-28	WMA	1.06	6	Granite-I	PG 70-28	ASA	0.60	25
Granite-II	PG 70-28	WMA	1.04	7	Quartzite	PG 64-22	Neat	0.60	25
Quartzite	PG 64-34	ASA	1.04	7	Granite-I	PG 70-28	S-RAP	0.59	26
Quartzite	PG 64-34	WMA	0.96	8	Granite-II	PG 64-22	ASA	0.58	27
Quartzite	PG 58-28	WMA	0.92	9	Quartzite	PG 64-22	ASA	0.58	27
Quartzite	PG 70-28	Neat	0.91	10	Quartzite	PG 64-34	Neat	0.56	28
Granite-II	PG 58-28	ASA	0.90	11	Granite-II	PG 64-22	Neat	0.56	28
Granite-I	PG 58-28	Neat	0.89	12	Granite-II	PG 64-34	Neat	0.56	28
Quartzite	PG 64-22	WMA	0.87	13	Granite-II	PG 64-34	S-RAP	0.56	28
Granite-I	PG 64-22	WMA	0.82	14	Granite-II	PG 64-22	S-RAP	0.50	29
Granite-II	PG 64-22	WMA	0.79	15	Granite-I	PG 64-22	Neat	0.48	30
Quartzite	PG 64-34	S-RAP	0.79	15	Granite-II	PG 58-28	Neat	0.48	30
Granite-II	PG 64-34	WMA	0.77	16	Granite-II	PG 58-28	S-RAP	0.46	31
Granite-II	PG 70-28	ASA	0.77	16	Granite-I	PG 70-28	Neat	0.46	31
Quartzite	PG 70-28	ASA	0.76	17	Quartzite	PG 64-22	S-RAP	0.44	32
Granite-I	PG 58-28	ASA	0.75	18	Granite-I	PG 64-34	S-RAP	0.40	33
Granite-I	PG 64-34	Neat	0.72	19	Granite-I	PG 64-22	S-RAP	0.34	34
Granite-I	PG 64-34	WMA	0.72	19	Granite-I	PG 64-22	ASA	0.34	34
Quartzite	PG 58-28	S-RAP	0.70	20	Granite-I	PG 58-28	S-RAP	0.22	35

## CHAPTER 5 CONCLUSIONS AND RECOMMENDATIONS

### 5.1 Conclusions

Based on the tests conducted on the three mixes, namely HMA-Lime, HMA-RAP, and C-WMA, the following conclusions were drawn.

1. The asphalt mixes, namely HMA-Lime, HMA-RAP, and C-WMA met the minimum tensile strength ratio (TSR) requirement of 0.80 set by the Superpave<sup>®</sup> mix design for screening the mixes for their susceptibility to moisture-induced damage.
2. The critical strain energy release rate of moisture-conditioned samples of HMA-Lime mix was found to be lower than minimum value,  $0.5 \text{ kJ/m}^2$  set by ASTM D8044-16 standard. In other words, HMA-Lime may be susceptible to cracking as a result of moisture-induced damage. However, the C-WMA and HMA-RAP samples were found to pass the minimum critical strain energy release rate requirement of  $0.5 \text{ kJ/m}^2$ , indicating the possibility of a better resistance to cracking after moisture conditioning when compared with HMA-RAP. However, energy release ratio (ERR) of the each mix was found to be greater than one, an indicator of no reduction in fracture energy as a result of moisture conditioning.
3. The fatigue index ratio (FIR) values obtained by conducting IDT test on each mix were found to be greater than one, indicating no reduction in fracture energy as a result of moisture conditioning. However, the fracture toughness was found to decrease in HMA-Lime due to moisture conditioning.

4. The toughness index ratio (TIR) obtained from IDT test was found to be less than one in HMA-Lime with a decrease in the fracture toughness in moisture-conditioned samples. However, TIR of HMA-RAP, and C-WMA mixes were found to be greater than one, an indicator of no effect on fracture toughness as a result of moisture conditioning.
5. The ITS and FI values were found to be significantly correlated ( $R^2 = 0.9525$ ) for both dry and moisture-conditioned samples. The coefficient of determination was found to be 0.8043 and 0.9525 for the dry and moisture-conditioned samples.

Based on the binder bond strength (BBS) tests conducted on asphalt binder-aggregate systems, the following conclusions were drawn.

1. The pull-off strength ratio (PSR) obtained from BBS tests showed that the PG 64-34 binder containing 0.5% ASA with granite-I, and PG 58-28 binder containing 0.5% WMA additive with granite-II had the highest resistance to moisture-induced damage among the tested asphalt binder-aggregate combinations. The PG 58-28 binder containing 20% RAP with granite-I was found to have the lowest PSR value compared to other asphalt binder-aggregate systems.
2. Adhesive failure was observed in all moisture-conditioned asphalt binder-aggregate samples containing 20% S-RAP. Addition of 20% S-RAP to the neat asphalt binder increased the PSR (increased adhesion) value of the

asphalt binder-aggregate samples prepared by both PG 64-34 and PG 70-28 binders with quartzite aggregate.

3. Addition of 0.5% amine-based WMA additive to the neat binder increased the PSR (improved adhesion) of the asphalt binder-aggregate samples prepared with PG 58-28, PG 64-22, and PG 70-28 binders with granite-II, quartzite and granite-I aggregates, respectively. However, addition of 0.5% amine-based WMA additive to neat PG 64-34 binder with quartzite aggregate resulted in an improved adhesion compared to that of the neat binder.
4. Addition of 0.5% ASA to the neat binder increased the PSR (improved adhesion) of the asphalt binder-aggregate samples prepared by PG 58-28 and PG 64-34 binders with granite-II, and quartzite aggregates, respectively. Also, addition of 0.5% ASA to PG 64-34, and PG 70-28 binders with granite-I aggregate improved their adhesion. Cohesive failure was observed in the PG 64-34 binder with granite-I, and PG 58-28, PG 64-22 and PG 64-34 with quartzite.

## 5.2 Recommendations

A number of recommendations for the future research were made based on the findings of this study, as follows:

1. A new pass/fail criterion required for screening the mixes using BBS test is suggested as PSR values obtained from BBS testing were found to be less than 0.8 (rounded) in all aggregates with neat binders except PG 58-28 binder with granite-I, and PG 70-28 binder with granite-I.



2. Field testing/laboratory testing of asphalt mix is suggested with the same asphalt binder-aggregate combinations used in the research to develop a correlation between TSR of asphalt mix and PSR of asphalt binder-aggregate combinations.

## APPENDIX A

**Summary of  $G_{mm}$  test result**

S.N.	Type of asphalt mix	Average $G_{mm}$	COV
1	HMA-Lime	2.461	0.12
2	HMA-RAP	2.488	0.13
3	C-WMA	2.453	0.11

**Summary of  $G_{mb}$  test result and AV calculation in TSR specimens**

Asphalt mix type	Name of the TSR specimen	$G_{mb}$	AV (%)
<b>HMA-Lime</b>	B1-M1-T2-S1	2.29	6.9
	B1-M1-T2-S2	2.284	7.2
	B1-M1-T2-S3	2.295	6.7
	B1-M1-T2-S4	2.281	7.3
	B1-M1-T2-S5	2.295	6.7
	B1-M1-T2-S6	2.283	7.2
	B1-M1-T2-S7	2.296	6.7
	B1-M1-T2-S8	2.285	7.2
<b>HMA-RAP</b>	B2-M2-T2-S1	2.312	7.1
	B2-M2-T2-S2	2.310	7.2
	B2-M2-T2-S3	2.305	7.4
	B2-M2-T2-S4	2.310	7.2
	B2-M2-T2-S5	2.310	7.2
	B2-M2-T2-S6	2.306	7.3
	B2-M2-T2-S7	2.306	7.3
	B2-M2-T2-S8	2.311	7.1
<b>C-WMA</b>	B3-M3-T2-S1	2.294	6.5
	B3-M3-T2-S2	2.285	6.8
	B3-M3-T2-S3	2.273	7.3
	B3-M3-T2-S4	2.283	6.9
	B3-M3-T2-S5	2.287	6.8
	B3-M3-T2-S6	2.280	7.1
	B3-M3-T2-S7	2.280	7.1
	B3-M3-T2-S8	2.286	6.8

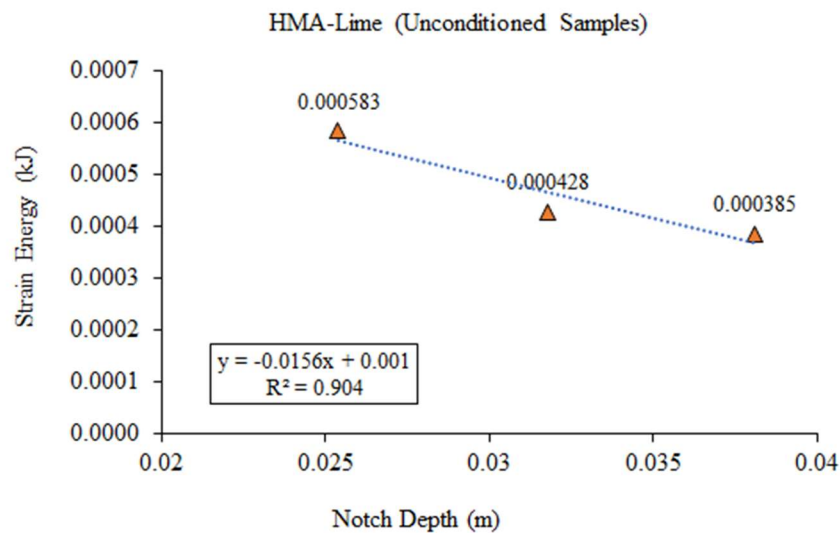
Summary of  $G_{mb}$  test result and AV calculation of SCB specimens prepared by HMA

Asphalt mix type	Name of the SCB specimen	$G_{mb}$	AV (%)
<b>HMA-Lime</b>	B1-M1-T1-S1-25.4 mm	2.284	7.2
	B1-M1-T1-S1-31.75 mm	2.276	7.5
	B1-M1-T1-S1-38.1 mm	2.285	7.2
	B1-M1-T1-S2-25.4 mm	2.280	7.4
	B1-M1-T1-S2-31.75 mm	2.295	6.7
	B1-M1-T1-S2-38.1 mm	2.283	7.2
	B1-M1-T1-S3-25.4 mm	2.282	7.3
	B1-M1-T1-S3-31.75 mm	2.277	7.5
	B1-M1-T1-S3-38.1 mm	2.296	6.7
	B1-M1-T1-S4-25.4 mm	2.277	7.5
	B1-M1-T1-S4-31.75 mm	2.289	7
	B1-M1-T1-S4-38.1 mm	2.292	6.9
	B1-M1-T1-S5-25.4 mm	2.286	7.1
	B1-M1-T1-S5-31.75 mm	2.283	7.2
	B1-M1-T1-S5-38.1 mm	2.280	7.4
	B1-M1-T1-S6-25.4 mm	2.287	7.1
	B1-M1-T1-S6-31.75 mm	2.284	7.2
	B1-M1-T1-S6-38.1 mm	2.280	7.4
<b>HMA-RAP</b>	B2-M2-T1-S1-25.4 mm	2.314	7
	B2-M2-T1-S1-31.75 mm	2.314	7
	B2-M2-T1-S1-38.1 mm	2.32	6.8
	B2-M2-T1-S2-25.4 mm	2.313	7
	B2-M2-T1-S2-31.75 mm	2.303	7.4
	B2-M2-T1-S2-38.1 mm	2.311	7.1
	B2-M2-T1-S3-25.4 mm	2.307	7.3
	B2-M2-T1-S3-31.75 mm	2.301	7.5
	B2-M2-T1-S3-38.1 mm	2.316	6.9
	B2-M2-T1-S4-25.4 mm	2.324	6.6
	B2-M2-T1-S4-31.75 mm	2.316	6.9
	B2-M2-T1-S4-38.1 mm	2.302	7.5
	B2-M2-T1-S5-25.4 mm	2.301	7.5
	B2-M2-T1-S5-31.75 mm	2.301	7.5
	B2-M2-T1-S5-38.1 mm	2.304	7.4
	B2-M2-T1-S6-25.4 mm	2.301	7.5
	B2-M2-T1-S6-31.75 mm	2.303	7.4
	B2-M2-T1-S6-38.1 mm	2.314	7

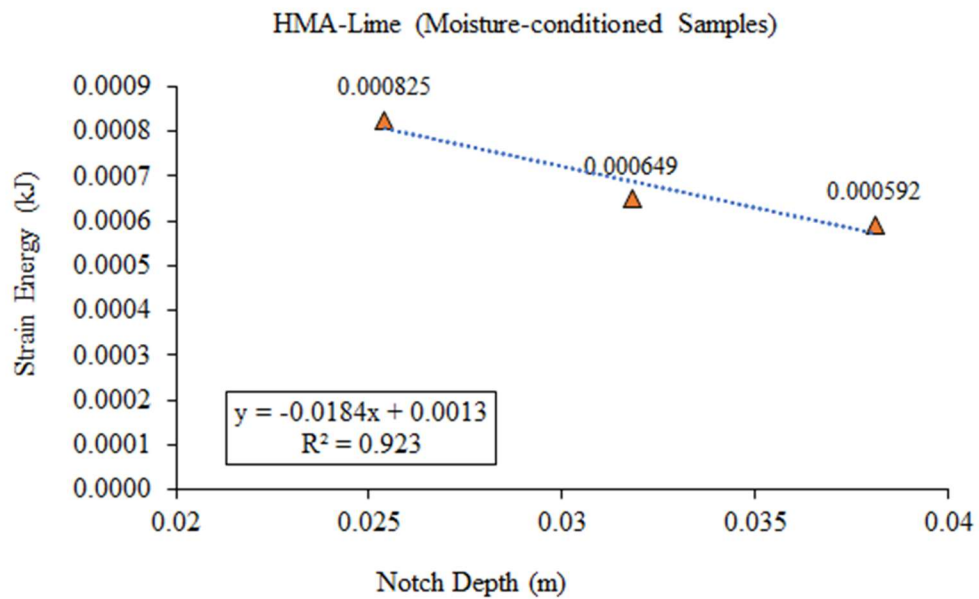
Asphalt mix type	Name of the SCB specimen	G <sub>mb</sub>	AV (%)
<b>C-WMA</b>	B3-M3-T1-S1-25.4 mm	2.269	7.5
	B3-M3-T1-S1-31.75 mm	2.291	6.6
	B3-M3-T1-S1-38.1 mm	2.285	6.8
	B3-M3-T1-S2-25.4 mm	2.291	6.6
	B3-M3-T1-S2-31.75 mm	2.274	7.3
	B3-M3-T1-S2-38.1 mm	2.283	6.9
	B3-M3-T1-S3-25.4 mm	2.268	7.5
	B3-M3-T1-S3-31.75 mm	2.273	7.3
	B3-M3-T1-S3-38.1 mm	2.289	6.7
	B3-M3-T1-S4-25.4 mm	2.294	6.5
	B3-M3-T1-S4-31.75 mm	2.28	7.1
	B3-M3-T1-S4-38.1 mm	2.282	7
	B3-M3-T1-S5-25.4 mm	2.274	7.3
	B3-M3-T1-S5-31.75 mm	2.274	7.3
	B3-M3-T1-S5-38.1 mm	2.279	7.1
	B3-M3-T1-S6-25.4 mm	2.273	7.3
	B3-M3-T1-S6-31.75 mm	2.286	6.8
	B3-M3-T1-S6-38.1 mm	2.288	6.7

## APPENDIX B

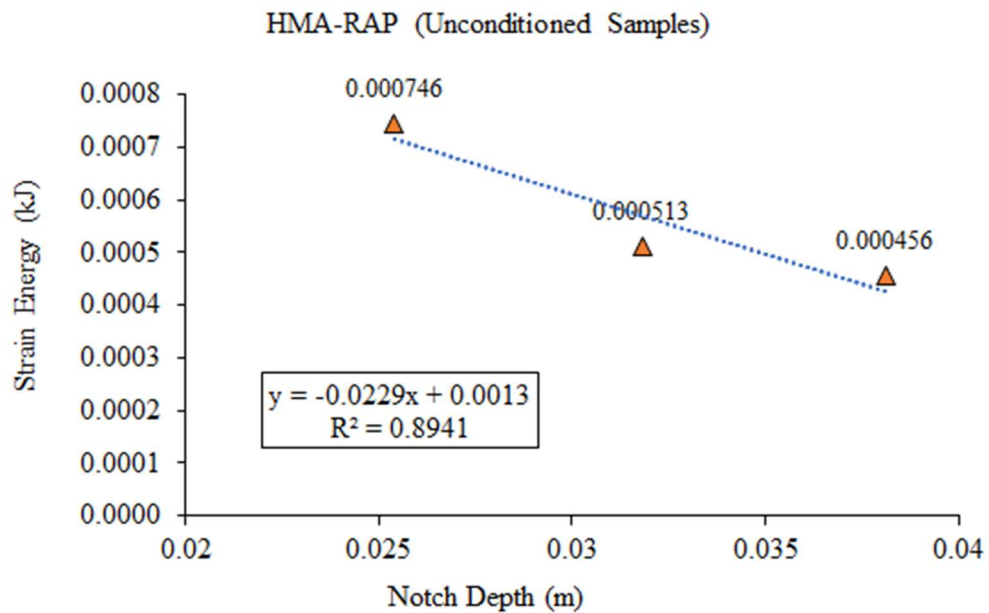
Variation of strain energy with notch depth in unconditioned HMA-Lime



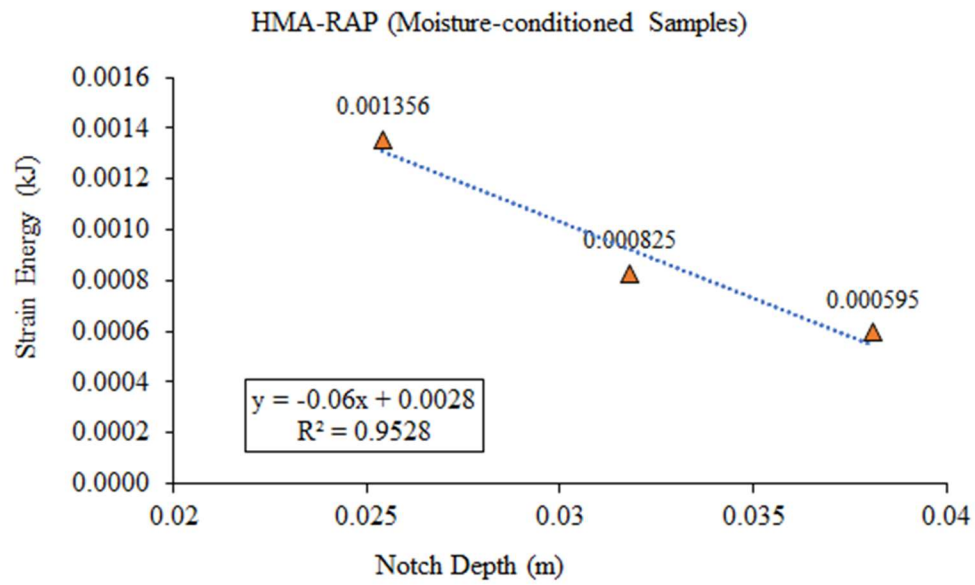
Variation of strain energy with notch depth in moisture-conditioned HMA-Lime samples



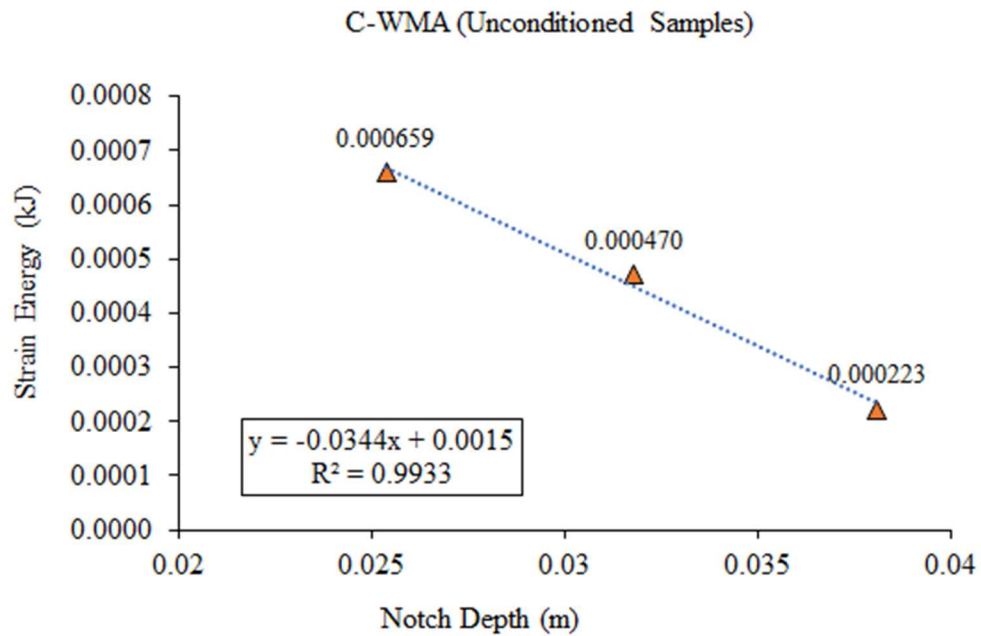
Variation of strain energy with notch depth in unconditioned HMA-RAP samples



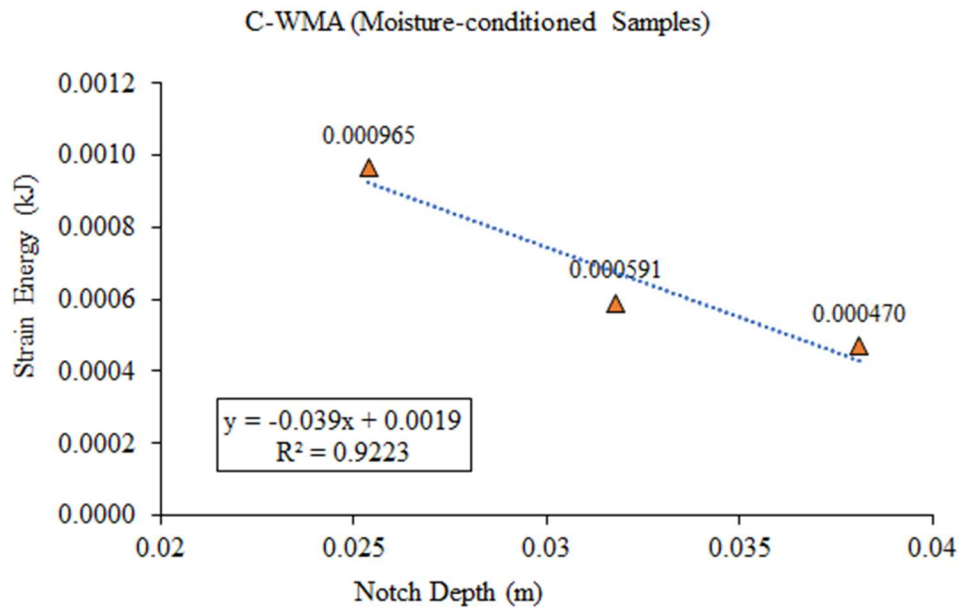
Variation of strain energy with notch depth in moisture-conditioned HMA-RAP samples



Variation of strain energy with notch depth in unconditioned C-WMA samples



Relation between strain energy and notch depth in moisture-conditioned C-WMA samples




### APPENDIX C

- Two sample two-tailed t-test (difference in mean), F test (difference in variance)
- Unpaired (two groups tested once), F (ratio of larger variance to small variance)
- $F > F_{\text{critical}}$  for the degree of freedom (4)/unequal variance, p value < 0.05

- Unequal variance: degree of freedom = 
$$\frac{\left(\frac{s_1^2}{n_1} + \frac{s_2^2}{n_2}\right)^2}{\frac{\left(\frac{s_1^2}{n_1}\right)^2}{n_1 - 1} + \frac{\left(\frac{s_2^2}{n_2}\right)^2}{n_2 - 1}}$$

- Equal variance:  $sp^2 = \frac{(n_1 - 1)s_1^2 + (n_2 - 1)s_2^2}{n_1 + n_2 - 2}$

$$\bullet \quad t_{equal} = \frac{((\bar{X1}) - (\bar{X2})) - (\mu1 - \mu2)}{\sqrt{\left(\frac{sp^2}{n1}\right) + \left(\frac{sp^2}{n2}\right)}}, \quad t_{unequal} = \frac{((\bar{X1}) - (\bar{X2})) - (\mu1 - \mu2)}{\sqrt{\left(\frac{s1^2}{n1}\right) + \left(\frac{s2^2}{n2}\right)}}$$

D=Significantly different average pull-off strength S=Significantly same average pull-off strength				Gravel															
Statistical significance 				Unconditioned															
				PG 58-28				PG 64-22				PG 64-34				PG 70-28			
				Neat	RAP	WMA	ASA	Neat	RAP	WMA	ASA	Neat	RAP	WMA	ASA	Neat	RAP	WMA	ASA
Gravel	Unconditioned	PG 58-28	Neat	S	S	D	S	S	D	D	D	D	S	D	D	D	D	S	S
			RAP	S	S	D	S	S	D	D	D	D	D	D	D	S	D	S	S
			WMA	D	D	S	D	D	D	D	D	S	D	D	D	D	D	D	D
			ASA	S	S	D	S	D	D	D	D	D	S	S	D	D	D	S	D
		PG 64-22	Neat	S	S	D	D	S	D	S	D	D	D	D	D	S	D	S	S
			RAP	D	D	D	D	D	S	D	S	D	D	D	D	D	D	D	D
			WMA	D	D	D	D	S	D	S	D	D	D	D	D	S	S	S	S
			ASA	D	D	D	D	D	D	D	S	D	D	D	D	D	D	D	D
		PG 64-34	Neat	D	D	S	D	D	D	D	D	S	D	D	S	D	D	D	D
			RAP	S	D	D	S	D	D	D	D	D	S	S	D	D	D	S	D
			WMA	D	D	D	S	D	D	D	D	D	S	S	D	D	D	D	D
			ASA	D	D	D	D	D	D	D	D	S	D	D	S	D	D	D	D
		PG 70-28	Neat	D	S	D	D	S	D	S	D	D	D	D	D	S	D	S	S
			RAP	D	D	D	D	D	D	S	D	D	D	D	D	D	S	D	D
			WMA	S	S	D	S	S	D	S	D	D	S	D	D	S	D	S	S
			ASA	S	S	D	D	S	D	S	D	D	D	D	D	S	D	S	S

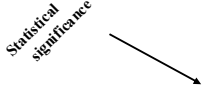


D=Significantly different average pull-off strength S=Significantly same average pull-off strength				Gravel															
Statistical significance				Moisture Conditioned															
				PG 58-28				PG 64-22				PG 64-34				PG 70-28			
				Neat	RAP	WMA	ASA	Neat	RAP	WMA	ASA	Neat	RAP	WMA	ASA	Neat	RAP	WMA	ASA
Gravel	Unconditioned	PG 58-28	Neat	D	D	D	D	D	S	S	D	D	D	D	D	D	S	S	D
			RAP	D	D	D	D	D	S	S	D	D	D	D	D	D	S	S	D
			WMA	D	D	D	D	S	D	D	D	D	D	S	S	S	D	D	D
			ASA	D	D	S	S	D	S	S	S	D	D	D	D	D	S	D	S
		PG 64-22	Neat	D	D	D	D	D	D	S	D	D	D	D	D	D	D	S	D
			RAP	D	D	D	D	D	D	D	D	D	D	D	D	D	D	D	D
			WMA	D	D	D	D	D	D	D	D	D	D	D	D	D	D	S	D
			ASA	D	D	D	D	D	D	D	D	D	D	D	D	D	D	D	D
		PG 64-34	Neat	D	D	D	D	S	D	D	D	D	D	S	S	S	D	D	D
			RAP	D	D	S	S	D	S	S	S	D	D	D	D	D	S	D	S
			WMA	D	D	S	S	D	S	S	S	D	D	D	D	D	S	D	S
			ASA	D	D	D	D	S	D	D	D	D	D	S	S	D	D	D	D
		PG 70-28	Neat	D	D	D	D	D	D	D	D	D	D	D	D	D	D	S	D
			RAP	D	D	D	D	D	D	D	D	D	D	D	D	D	D	D	D
			WMA	D	D	D	D	D	S	S	D	D	D	D	D	D	S	S	D
			ASA	D	D	D	D	D	D	D	D	D	D	D	D	D	D	S	D

D=Significantly different average pull-off strength S=Significantly same average pull-off strength				Quartzite															
Statistical significance				Unconditioned															
				PG 58-28				PG 64-22				PG 64-34				PG 70-28			
				Neat	RAP	WMA	ASA	Neat	RAP	WMA	ASA	Neat	RAP	WMA	ASA	Neat	RAP	WMA	ASA
Gravel	Unconditioned	PG 58-28	Neat	S	S	D	D	D	D	S	D	D	D	D	D	S	D	S	D
			RAP	S	D	D	D	D	D	S	D	D	D	D	D	S	D	S	D
			WMA	D	D	D	S	D	D	D	D	S	D	S	S	D	D	D	D
			ASA	D	S	S	S	D	D	D	D	D	S	S	D	D	D	S	D
		PG 64-22	Neat	S	D	D	D	S	D	S	D	D	D	D	D	S	D	S	S
			RAP	D	D	D	D	D	D	D	D	D	D	D	D	D	D	D	D
			WMA	D	D	D	D	S	D	S	D	D	D	D	D	D	D	D	S
			ASA	D	D	D	D	D	S	D	S	D	D	D	D	D	S	D	D
		PG 64-34	Neat	D	D	D	D	D	D	D	D	S	D	D	S	D	D	D	D
			RAP	D	S	S	S	D	D	D	D	D	S	S	D	D	D	S	D
			WMA	D	S	S	S	D	D	D	D	D	S	S	D	D	D	D	D
			ASA	D	D	D	D	D	D	D	D	S	D	D	S	D	D	D	D
		PG 70-28	Neat	S	D	D	D	D	D	S	D	D	D	D	D	S	D	S	S
			RAP	D	D	D	D	S	D	D	D	D	D	D	D	D	D	D	D
			WMA	S	S	D	D	D	D	S	D	D	D	D	D	S	D	S	S
			ASA	S	D	D	D	D	D	S	D	D	D	D	D	S	D	S	S

D=Significantly different average pull-off strength S=Significantly same average pull-off strength				Quartzite															
Statistical significance				Moisture Conditioned															
				PG 58-28				PG 64-22				PG 64-34				PG 70-28			
				Neat	RAP	WMA	ASA	Neat	RAP	WMA	ASA	Neat	RAP	WMA	ASA	Neat	RAP	WMA	ASA
Gravel	Unconditioned	PG 58-28	Neat	D	D	D	S	D	D	S	D	D	D	D	D	S	S	S	S
			RAP	D	D	D	S	D	D	D	D	D	D	D	D	D	S	S	D
			WMA	S	S	S	D	S	S	D	D	D	S	D	S	D	D	D	D
			ASA	D	D	S	S	S	D	S	S	D	D	D	D	S	S	D	S
		PG 64-22	Neat	D	D	D	D	D	D	S	D	D	D	D	D	S	S	S	D
			RAP	D	D	D	D	D	D	D	D	D	D	D	D	D	D	D	D
			WMA	D	D	D	D	D	D	D	D	D	D	D	D	D	D	S	D
			ASA	D	D	D	D	D	D	D	D	D	D	D	D	D	D	D	D
		PG 64-34	Neat	S	S	D	D	D	S	D	D	D	S	D	S	D	D	D	D
			RAP	D	D	D	S	S	D	S	S	D	D	D	D	S	S	D	S
			WMA	D	D	D	S	S	D	D	S	D	D	D	D	D	D	D	S
			ASA	D	S	D	D	D	D	D	D	D	S	D	S	D	D	D	D
		PG 70-28	Neat	D	D	D	D	D	D	D	D	D	D	D	D	D	S	S	D
			RAP	D	D	D	D	D	D	D	D	D	D	D	D	D	D	D	D
			WMA	D	D	D	S	D	D	S	D	D	D	D	D	S	S	S	D
			ASA	D	D	D	D	D	D	D	D	D	D	D	D	D	S	S	D


D=Significantly different average pull-off strength S=Significantly same average pull-off strength				Granite															
Statistical significance				Unconditioned															
				PG 58-28				PG 64-22				PG 64-34				PG 70-28			
				Neat	RAP	WMA	ASA	Neat	RAP	WMA	ASA	Neat	RAP	WMA	ASA	Neat	RAP	WMA	ASA
Gravel	Unconditioned	PG 58-28	Neat	S	S	D	D	D	D	D	D	D	S	D	D	S	D	S	D
			RAP	S	S	D	D	D	D	S	D	D	D	D	D	S	D	S	D
			WMA	D	D	D	D	D	D	D	D	S	D	D	D	D	D	D	D
			ASA	S	S	S	S	D	D	D	D	D	S	S	D	D	D	S	D
		PG 64-22	Neat	S	S	D	D	S	D	S	D	D	S	D	D	S	D	S	S
			RAP	D	D	D	D	D	S	D	S	D	D	D	D	D	D	D	D
			WMA	D	S	D	D	S	D	S	D	D	D	D	D	S	D	S	S
			ASA	D	D	D	D	D	D	D	D	D	D	D	D	D	D	D	D
		PG 64-34	Neat	D	D	D	D	D	D	D	D	S	D	D	S	D	D	D	D
			RAP	S	S	S	S	D	D	D	D	D	S	S	D	D	D	S	D
			WMA	D	S	S	S	D	D	D	D	D	D	S	D	D	D	D	D
			ASA	D	D	D	D	D	D	D	D	S	D	D	S	D	D	D	D
		PG 70-28	Neat	D	S	D	D	D	D	S	D	D	D	D	D	S	D	S	S
			RAP	D	D	D	D	S	D	D	D	D	D	D	D	D	S	D	S
			WMA	S	S	D	D	D	D	S	D	D	S	D	D	S	D	S	D
			ASA	D	S	D	D	D	D	S	D	D	D	D	D	S	D	S	S

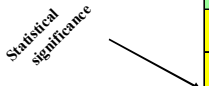
D=Significantly different average pull-off strength S=Significantly same average pull-off strength				Granite															
Statistical significance 				Moisture Conditioned															
				PG 58-28				PG 64-22				PG 64-34				PG 70-28			
				Neat	RAP	WMA	ASA	Neat	RAP	WMA	ASA	Neat	RAP	WMA	ASA	Neat	RAP	WMA	ASA
Gravel	Unconditioned	PG 58-28	Neat	D	D	S	D	D	D	S	D	D	D	D	D	D	D	D	D
			RAP	D	D	D	D	D	D	S	D	D	D	D	D	D	D	D	D
			WMA	D	D	D	S	S	D	D	D	D	D	D	D	D	D	S	D
			ASA	S	D	S	D	D	D	S	D	D	D	D	D	D	S	D	S
		PG 64-22	Neat	D	D	S	D	D	D	S	D	D	D	D	D	D	D	D	D
			RAP	D	D	D	D	D	D	D	D	D	D	D	D	D	D	D	D
			WMA	D	D	D	D	D	D	D	D	D	D	D	D	D	D	D	D
			ASA	D	D	D	D	D	D	D	D	D	D	D	D	D	D	D	D
		PG 64-34	Neat	D	D	D	S	S	S	D	S	D	D	S	D	D	D	S	D
			RAP	S	D	S	D	D	D	S	D	D	D	D	D	D	D	D	S
			WMA	S	D	D	D	D	D	S	D	D	D	D	D	D	S	D	S
			ASA	D	D	D	S	S	S	D	S	D	D	S	D	S	D	S	D
		PG 70-28	Neat	D	D	D	D	D	D	D	D	D	D	D	D	D	D	D	D
			RAP	D	D	D	D	D	D	D	D	D	D	D	D	D	D	D	D
			WMA	D	D	S	D	D	D	S	D	D	D	D	D	D	D	D	D
			ASA	D	D	D	D	D	D	S	D	D	D	D	D	D	D	D	D

D=Significantly different average pull-off strength S=Significantly same average pull-off strength				Gravel															
Statistical significance 				Unconditioned															
				PG 58-28				PG 64-22				PG 64-34				PG 70-28			
				Neat	RAP	WMA	ASA	Neat	RAP	WMA	ASA	Neat	RAP	WMA	ASA	Neat	RAP	WMA	ASA
Gravel	Moisture Conditioned	PG 58-28	Neat	D	D	D	D	D	D	D	D	D	D	D	D	D	D	D	D
			RAP	D	D	D	D	D	D	D	D	D	D	D	D	D	D	D	D
			WMA	D	D	D	S	D	D	D	D	D	S	S	D	D	D	D	D
			ASA	D	D	D	S	D	D	D	D	D	S	S	D	D	D	D	D
		PG 64-22	Neat	D	D	S	D	D	D	D	D	S	D	D	S	D	D	D	D
			RAP	S	S	D	S	D	D	D	D	D	S	S	D	D	D	S	D
			WMA	S	S	D	S	S	D	D	D	D	S	S	D	D	D	S	D
			ASA	D	D	D	S	D	D	D	D	D	S	S	D	D	D	D	D
		PG 64-34	Neat	D	D	D	D	D	D	D	D	D	D	D	D	D	D	D	D
			RAP	D	D	D	D	D	D	D	D	D	D	D	D	D	D	D	D
			WMA	D	D	S	D	D	D	D	D	S	D	D	S	D	D	D	D
			ASA	D	D	S	D	D	D	D	D	S	D	D	S	D	D	D	D
		PG 70-28	Neat	D	D	S	D	D	D	D	D	S	D	D	D	D	D	D	D
			RAP	S	S	D	S	D	D	D	D	D	S	S	D	D	D	S	D
			WMA	S	S	D	D	S	D	S	D	D	D	D	D	S	D	S	S
			ASA	D	D	D	S	D	D	D	D	D	S	S	D	D	D	D	D

D=Significantly different average pull-off strength S=Significantly same average pull-off strength				Gravel															
				Moisture Conditioned															
				PG 58-28				PG 64-22				PG 64-34				PG 70-28			
				Neat	RAP	WMA	ASA	Neat	RAP	WMA	ASA	Neat	RAP	WMA	ASA	Neat	RAP	WMA	ASA
Gravel	Moisture Conditioned	PG 58-28	Neat	S	S	D	D	D	D	D	D	D	S	D	D	D	D	D	D
			RAP	S	S	D	D	D	D	D	D	D	S	D	D	D	D	D	D
			WMA	D	D	S	S	D	S	S	S	D	D	D	D	D	S	D	S
			ASA	D	D	S	S	D	S	S	S	D	D	D	D	S	S	D	S
		PG 64-22	Neat	D	D	D	D	S	D	D	D	D	D	S	S	S	D	D	D
			RAP	D	D	S	S	D	S	S	S	D	D	D	D	D	S	D	S
			WMA	D	D	S	S	D	S	S	S	D	D	D	D	D	S	D	S
			ASA	D	D	S	S	D	S	S	S	D	D	D	D	D	S	D	S
		PG 64-34	Neat	D	D	D	D	D	D	D	D	S	D	D	D	D	D	D	D
			RAP	S	S	D	D	D	D	D	D	D	S	D	D	D	D	D	D
			WMA	D	D	D	D	S	D	D	D	D	D	S	S	S	D	D	D
			ASA	D	D	D	D	S	D	D	D	D	D	S	S	S	D	D	D
		PG 70-28	Neat	D	D	D	S	S	D	D	D	D	D	S	S	S	D	D	D
			RAP	D	D	S	S	D	S	S	S	D	D	D	D	D	S	D	S
			WMA	D	D	D	D	D	D	D	D	D	D	D	D	D	D	S	D
			ASA	D	D	S	S	D	S	S	S	D	D	D	D	D	S	D	S

D=Significantly different average pull-off strength S=Significantly same average pull-off strength				Quartzite															
				Unconditioned															
				PG 58-28				PG 64-22				PG 64-34				PG 70-28			
				Neat	RAP	WMA	ASA	Neat	RAP	WMA	ASA	Neat	RAP	WMA	ASA	Neat	RAP	WMA	ASA
Gravel	Moisture Conditioned	PG 58-28	Neat	D	D	D	D	D	D	D	D	D	D	D	D	D	D	D	D
			RAP	D	D	D	D	D	D	D	D	D	D	D	D	D	D	D	D
			WMA	D	S	S	S	D	D	D	D	D	S	S	D	D	D	D	D
			ASA	D	D	S	S	D	D	D	D	D	S	S	D	D	D	D	D
		PG 64-22	Neat	D	D	D	S	D	D	D	D	S	D	D	S	D	D	D	D
			RAP	S	S	D	D	D	D	D	D	D	S	D	D	D	D	S	D
			WMA	S	S	S	D	D	D	D	D	D	S	S	D	S	D	S	D
			ASA	D	S	D	D	D	D	D	D	D	S	S	D	D	D	D	D
		PG 64-34	Neat	D	D	D	D	D	D	D	D	D	D	D	D	D	D	D	D
			RAP	D	D	D	D	D	D	D	D	D	D	D	D	D	D	D	D
			WMA	D	D	D	S	D	D	D	D	S	D	S	S	D	D	D	D
			ASA	D	D	D	S	D	D	D	D	S	D	S	S	D	D	D	D
		PG 70-28	Neat	D	D	S	S	D	D	D	D	S	D	S	S	D	D	D	D
			RAP	S	S	S	S	D	D	D	D	D	S	S	D	D	D	S	D
			WMA	S	D	D	D	D	D	S	D	D	D	D	D	S	D	S	S
			ASA	D	S	S	S	D	D	D	D	D	S	S	D	D	D	D	D

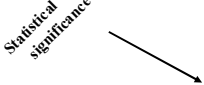
D=Significantly different average pull-off strength S=Significantly same average pull-off strength				Quartzite															
Statistical significance 				Moisture Conditioned															
				PG 58-28				PG 64-22				PG 64-34				PG 70-28			
				Neat	RAP	WMA	ASA	Neat	RAP	WMA	ASA	Neat	RAP	WMA	ASA	Neat	RAP	WMA	ASA
Gravel	Moisture Conditioned	PG 58-28	Neat	D	D	D	D	D	D	D	D	D	D	D	D	D	D	D	D
			RAP	D	D	D	D	D	D	D	D	D	D	D	D	D	D	D	D
			WMA	D	D	S	S	S	S	D	S	D	D	S	D	D	D	D	S
			ASA	D	D	S	S	S	S	D	S	D	D	S	D	D	D	D	S
		PG 64-22	Neat	S	S	S	D	D	S	D	D	D	S	D	S	D	D	D	D
			RAP	D	D	D	S	S	D	S	S	D	D	D	D	S	S	D	S
			WMA	D	D	D	S	S	D	S	S	D	D	D	D	S	S	D	S
			ASA	D	D	D	S	S	D	D	S	D	D	D	D	S	S	D	S
		PG 64-34	Neat	D	D	D	D	D	D	D	D	S	D	D	D	D	D	D	D
			RAP	D	D	D	D	D	D	D	D	D	D	D	D	D	D	D	D
			WMA	S	S	S	D	D	S	D	D	D	S	D	S	D	D	D	D
			ASA	S	S	S	D	S	S	D	D	D	S	S	S	D	D	D	D
		PG 70-28	Neat	S	S	S	D	S	S	D	D	D	S	S	S	D	D	D	D
			RAP	D	D	D	S	S	D	S	S	D	D	D	D	S	S	D	S
			WMA	D	D	D	D	D	D	D	D	D	D	D	D	D	S	S	D
			ASA	D	D	S	S	S	D	D	S	D	D	D	D	S	S	D	S

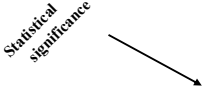
D=Significantly different average pull-off strength S=Significantly same average pull-off strength				Granite															
Statistical significance 				Unconditioned															
				PG 58-28				PG 64-22				PG 64-34				PG 70-28			
				Neat	RAP	WMA	ASA	Neat	RAP	WMA	ASA	Neat	RAP	WMA	ASA	Neat	RAP	WMA	ASA
Gravel	Moisture Conditioned	PG 58-28	Neat	D	D	D	D	D	D	D	D	D	D	D	S	D	D	D	D
			RAP	D	D	D	D	D	D	D	D	D	D	D	D	D	D	D	D
			WMA	D	D	S	S	D	D	D	D	D	D	S	D	D	D	D	D
			ASA	D	D	S	S	D	D	D	D	D	D	S	D	D	D	D	D
		PG 64-22	Neat	D	D	D	D	D	D	D	D	S	D	D	D	D	D	D	D
			RAP	S	S	S	S	D	D	D	D	D	S	S	D	D	D	S	D
			WMA	S	S	S	S	D	D	D	D	D	S	S	D	D	D	S	D
			ASA	D	S	S	S	D	D	D	D	D	S	S	D	D	D	D	D
		PG 64-34	Neat	D	D	D	D	D	D	D	D	D	D	D	D	D	D	D	D
			RAP	D	D	D	D	D	D	D	D	D	D	D	D	D	D	D	D
			WMA	D	D	D	D	D	D	D	D	S	D	D	S	D	D	D	D
			ASA	D	D	D	D	D	D	D	D	S	D	D	D	D	D	D	D
		PG 70-28	Neat	D	D	D	D	D	D	D	D	S	D	S	D	D	D	D	D
			RAP	S	S	S	S	D	D	D	D	D	S	S	D	D	D	S	D
			WMA	D	S	D	D	D	D	S	D	D	D	D	D	S	D	S	D
			ASA	D	D	S	S	D	D	D	D	D	S	S	D	D	D	D	D

D=Significantly different average pull-off strength S=Significantly same average pull-off strength				Granite															
Statistical significance				Moisture Conditioned															
				PG 58-28				PG 64-22				PG 64-34				PG 70-28			
				Neat	RAP	WMA	ASA	Neat	RAP	WMA	ASA	Neat	RAP	WMA	ASA	Neat	RAP	WMA	ASA
Gravel	Moisture Conditioned	PG 58-28	Neat	D	D	D	D	D	D	D	D	S	D	D	D	S	D	D	D
			RAP	D	D	D	D	D	D	D	D	S	D	D	D	S	D	D	D
			WMA	S	D	S	D	D	D	S	D	D	D	D	D	D	S	D	S
			ASA	S	D	D	D	D	D	S	D	D	D	D	S	D	S	D	S
		PG 64-22	Neat	D	D	D	S	S	S	D	S	D	D	S	D	D	D	S	D
			RAP	S	D	S	D	D	D	S	D	D	D	D	D	D	D	D	D
			WMA	S	D	S	D	D	D	S	D	D	D	D	D	D	D	D	D
			ASA	S	D	S	D	D	D	S	D	D	D	D	D	D	D	D	D
		PG 64-34	Neat	D	D	D	D	D	D	D	D	D	D	D	D	D	D	D	D
			RAP	D	D	D	D	D	D	D	D	S	D	D	D	S	D	D	D
			WMA	D	D	D	S	S	S	D	S	D	D	S	S	D	D	S	D
			ASA	D	D	D	S	S	S	D	D	D	D	S	S	D	D	S	D
		PG 70-28	Neat	D	D	D	S	S	S	D	D	D	D	D	S	D	S	S	S
			RAP	S	D	S	D	D	D	S	D	D	D	D	D	S	D	S	S
			WMA	D	D	D	D	D	D	S	D	D	D	D	D	D	D	D	D
			ASA	S	D	S	D	D	D	S	D	D	D	D	D	S	D	S	S

D=Significantly different average pull-off strength S=Significantly same average pull-off strength				Gravel															
Statistical significance				Unconditioned															
				PG 58-28				PG 64-22				PG 64-34				PG 70-28			
				Neat	RAP	WMA	ASA	Neat	RAP	WMA	ASA	Neat	RAP	WMA	ASA	Neat	RAP	WMA	ASA
Quartzite	Unconditioned	PG 58-28	Neat	S	S	D	D	S	D	D	D	D	D	D	D	S	D	S	S
			RAP	S	D	D	S	D	D	D	D	D	S	S	D	D	D	S	D
			WMA	D	D	D	S	D	D	D	D	D	S	S	D	D	D	D	D
			ASA	D	D	S	S	D	D	D	D	D	S	S	D	D	D	D	D
		PG 64-22	Neat	D	D	D	D	S	D	S	D	D	D	D	D	D	S	D	D
			RAP	D	D	D	D	D	D	D	S	D	D	D	D	D	D	D	D
			WMA	S	S	D	D	S	D	S	D	D	D	D	D	S	D	S	S
			ASA	D	D	D	D	D	D	D	S	D	D	D	D	D	D	D	D
		PG 64-34	Neat	D	D	S	D	D	D	D	D	S	D	D	S	D	D	D	D
			RAP	D	D	D	S	D	D	D	D	D	S	S	D	D	D	D	D
			WMA	D	D	S	S	D	D	D	D	D	S	S	D	D	D	D	D
			ASA	D	D	S	D	D	D	D	D	S	D	D	S	D	D	D	D
		PG 70-28	Neat	S	S	D	D	S	D	D	D	D	D	D	D	S	D	S	S
			RAP	D	D	D	D	D	D	D	S	D	D	D	D	D	D	D	D
			WMA	S	S	D	S	S	D	D	D	D	S	D	D	S	D	S	S
			ASA	D	D	D	D	S	D	S	D	D	D	D	D	S	D	S	S



D=Significantly different average pull-off strength S=Significantly same average pull-off strength				Quartzite															
Statistical significance 				Moisture Conditioned															
				PG 58-28				PG 64-22				PG 64-34				PG 70-28			
				Neat	RAP	WMA	ASA	Neat	RAP	WMA	ASA	Neat	RAP	WMA	ASA	Neat	RAP	WMA	ASA
Quartzite	Unconditioned	PG 58-28	Neat	D	D	D	S	D	D	S	D	D	D	D	D	D	S	S	D
			RAP	D	D	D	S	D	D	S	S	D	D	D	D	S	S	D	S
			WMA	D	D	S	S	S	S	D	D	D	D	S	D	D	D	D	S
			ASA	S	S	S	S	S	S	D	S	D	S	S	S	D	D	D	S
		PG 64-22	Neat	D	D	D	D	D	D	D	D	D	D	D	D	D	D	D	D
			RAP	D	D	D	D	D	D	D	D	D	D	D	D	D	D	D	D
			WMA	D	D	D	D	D	D	S	D	D	D	D	D	D	S	S	D
			ASA	D	D	D	D	D	D	D	D	D	D	D	D	D	D	D	D
		PG 64-34	Neat	S	S	S	D	D	S	D	D	D	S	D	S	D	D	D	D
			RAP	D	D	D	S	S	D	D	S	D	D	D	D	D	D	D	S
			WMA	S	D	S	S	S	S	D	S	D	S	S	S	D	D	D	S
			ASA	S	S	S	D	D	S	D	D	D	S	D	S	D	D	D	D
		PG 70-28	Neat	D	D	D	D	D	D	D	D	D	D	D	D	D	S	S	D
			RAP	D	D	D	D	D	D	D	D	D	D	D	D	D	D	D	D
			WMA	D	D	D	S	D	D	S	D	D	D	D	D	S	S	S	S
			ASA	D	D	D	D	D	D	D	D	D	D	D	D	D	D	S	D

D=Significantly different average pull-off strength S=Significantly same average pull-off strength				Granite															
Statistical significance 				Unconditioned															
				PG 58-28				PG 64-22				PG 64-34				PG 70-28			
				Neat	RAP	WMA	ASA	Neat	RAP	WMA	ASA	Neat	RAP	WMA	ASA	Neat	RAP	WMA	ASA
Quartzite	Unconditioned	PG 58-28	Neat	S	S	D	D	D	D	S	D	D	D	D	D	S	D	S	D
			RAP	S	S	S	S	D	D	D	D	D	S	S	D	D	D	S	D
			WMA	D	D	S	S	D	D	D	D	D	D	S	D	D	D	D	D
			ASA	D	D	S	S	D	D	D	D	S	D	S	D	D	D	D	D
		PG 64-22	Neat	D	D	D	D	S	D	S	D	D	D	D	D	D	S	D	S
			RAP	D	D	D	D	D	S	D	S	D	D	D	D	D	D	D	D
			WMA	S	S	D	D	D	D	S	D	D	S	D	D	S	D	S	S
			ASA	D	D	D	D	D	D	D	S	D	D	D	D	D	S	D	S
		PG 64-34	Neat	D	D	D	D	D	D	D	D	S	D	D	D	D	D	D	D
			RAP	D	S	S	S	D	D	D	D	D	D	S	D	D	D	D	D
			WMA	D	D	S	S	D	D	D	D	S	D	S	D	D	D	D	D
			ASA	D	D	D	D	D	D	D	D	S	D	D	S	D	D	D	D
		PG 70-28	Neat	S	S	D	D	D	D	S	D	D	D	D	D	S	D	S	D
			RAP	D	D	D	D	D	D	D	D	D	D	D	D	D	D	D	D
			WMA	S	S	D	D	D	D	S	D	D	S	D	D	S	D	S	D
			ASA	D	S	D	D	D	D	S	D	D	D	D	D	S	D	S	S




D=Significantly different average pull-off strength S=Significantly same average pull-off strength  Statistical significance				Granite															
				Moisture Conditioned															
				PG 58-28				PG 64-22				PG 64-34				PG 70-28			
				Neat	RAP	WMA	ASA	Neat	RAP	WMA	ASA	Neat	RAP	WMA	ASA	Neat	RAP	WMA	ASA
Quartzite	Unconditioned	PG 58-28	Neat	D	D	D	D	D	D	S	D	D	D	D	D	D	D	D	D
			RAP	S	D	S	D	D	D	S	D	D	D	D	D	D	D	D	D
			WMA	D	D	D	D	D	D	S	D	D	D	D	D	D	S	D	S
			ASA	S	D	D	S	D	D	D	D	D	D	D	S	D	S	S	S
		PG 64-22	Neat	D	D	D	D	D	D	D	D	D	D	D	D	D	D	D	D
			RAP	D	D	D	D	D	D	D	D	D	D	D	D	D	D	D	D
			WMA	D	D	D	D	D	D	S	D	D	D	D	D	D	D	D	D
			ASA	D	D	D	D	D	D	D	D	D	D	D	D	D	D	D	D
		PG 64-34	Neat	D	D	D	S	S	S	D	S	D	D	S	D	D	D	S	D
			RAP	S	D	S	D	D	D	S	D	D	D	D	D	D	S	D	S
			WMA	S	D	D	D	D	D	D	D	D	D	S	D	S	S	S	S
			ASA	D	D	D	S	S	S	D	S	D	D	S	S	D	D	S	D
		PG 70-28	Neat	D	D	D	D	D	D	S	D	D	D	D	D	D	D	D	D
			RAP	D	D	D	D	D	D	D	D	D	D	D	D	D	D	D	D
			WMA	D	D	S	D	D	D	S	D	D	D	D	D	D	D	D	D
			ASA	D	D	D	D	D	D	D	D	D	D	D	D	D	D	D	D

D=Significantly different average pull-off strength S=Significantly same average pull-off strength  Statistical significance				Gravel															
				Unconditioned															
				PG 58-28				PG 64-22				PG 64-34				PG 70-28			
				Neat	RAP	WMA	ASA	Neat	RAP	WMA	ASA	Neat	RAP	WMA	ASA	Neat	RAP	WMA	ASA
Quartzite	Moisture Conditioned	PG 58-28	Neat	D	D	S	D	D	D	D	D	S	D	D	D	D	D	D	D
			RAP	D	D	S	D	D	D	D	D	S	D	D	S	D	D	D	D
			WMA	D	D	S	S	D	D	D	D	D	D	D	D	D	D	D	D
			ASA	S	S	D	S	D	D	D	D	D	S	S	D	D	D	S	D
		PG 64-22	Neat	D	D	S	S	D	D	D	D	D	S	S	D	D	D	D	D
			RAP	D	D	S	D	D	D	D	D	S	D	D	D	D	D	D	D
			WMA	S	D	D	S	S	D	D	D	D	S	D	D	D	D	S	D
			ASA	D	D	D	S	D	D	D	D	D	S	S	D	D	D	D	D
		PG 64-34	Neat	D	D	D	D	D	D	D	D	D	D	D	D	D	D	D	D
			RAP	D	D	S	D	D	D	D	D	S	D	D	S	D	D	D	D
			WMA	D	D	D	D	D	D	D	D	D	D	D	D	D	D	D	D
			ASA	D	D	S	D	D	D	D	D	S	D	D	S	D	D	D	D
		PG 70-28	Neat	S	D	D	S	S	D	D	D	D	S	D	D	D	D	S	D
			RAP	S	S	D	S	S	D	D	D	D	S	D	D	S	D	S	S
			WMA	S	S	D	D	S	D	S	D	D	D	D	S	D	S	S	S
			ASA	S	D	D	S	D	D	D	D	D	S	S	D	D	D	D	D

D=Significantly different average pull-off strength S=Significantly same average pull-off strength  Statistical significance				Gravel															
				Moisture Conditioned															
				PG 58-28				PG 64-22				PG 64-34				PG 70-28			
				Neat	RAP	WMA	ASA	Neat	RAP	WMA	ASA	Neat	RAP	WMA	ASA	Neat	RAP	WMA	ASA
Quartzite	Moisture Conditioned	PG 58-28	Neat	D	D	D	D	S	D	D	D	D	D	S	S	S	D	D	D
			RAP	D	D	D	D	S	D	D	D	D	D	S	S	S	D	D	D
			WMA	D	D	S	S	S	D	D	D	D	D	S	S	S	D	D	S
			ASA	D	D	S	S	D	S	S	S	D	D	D	D	D	S	D	S
		PG 64-22	Neat	D	D	S	S	D	S	S	S	D	D	D	S	S	S	D	S
			RAP	D	D	S	S	S	D	D	D	D	D	S	S	S	D	D	D
			WMA	D	D	D	D	D	S	S	D	D	D	D	D	D	S	D	D
			ASA	D	D	S	S	D	S	S	S	D	D	D	D	D	S	D	S
		PG 64-34	Neat	D	D	D	D	D	D	D	D	S	D	D	D	D	D	D	D
			RAP	D	D	D	D	S	D	D	D	D	D	S	S	S	D	D	D
			WMA	D	D	S	S	D	D	D	D	D	D	D	S	S	D	D	D
			ASA	D	D	D	D	S	D	D	D	D	D	S	S	S	D	D	D
		PG 70-28	Neat	D	D	D	D	D	S	S	S	D	D	D	D	D	S	D	S
			RAP	D	D	D	D	D	S	S	S	D	D	D	D	D	S	S	S
			WMA	D	D	D	D	D	D	D	D	D	D	D	D	D	D	S	D
			ASA	D	D	S	S	D	S	S	S	D	D	D	D	D	S	D	S


D=Significantly different average pull-off strength S=Significantly same average pull-off strength  Statistical significance				Quartzite															
				Unconditioned															
				PG 58-28				PG 64-22				PG 64-34				PG 70-28			
				Neat	RAP	WMA	ASA	Neat	RAP	WMA	ASA	Neat	RAP	WMA	ASA	Neat	RAP	WMA	ASA
Quartzite	Moisture Conditioned	PG 58-28	Neat	D	D	D	S	D	D	D	D	S	D	S	S	D	D	D	D
			RAP	D	D	D	S	D	D	D	D	S	D	D	S	D	D	D	D
			WMA	D	D	S	S	D	D	D	D	S	D	S	S	D	D	D	D
			ASA	S	S	S	S	D	D	D	D	D	S	S	D	D	D	S	D
		PG 64-22	Neat	D	D	S	S	D	D	D	D	D	S	S	D	D	D	D	D
			RAP	D	D	S	S	D	D	D	D	S	D	S	S	D	D	D	D
			WMA	S	S	D	D	D	D	S	D	D	D	D	D	D	D	S	D
			ASA	D	S	D	S	D	D	D	D	D	S	S	D	D	D	D	D
		PG 64-34	Neat	D	D	D	D	D	D	D	D	D	D	D	D	D	D	D	D
			RAP	D	D	D	S	D	D	D	D	S	D	S	S	D	D	D	D
			WMA	D	D	S	S	D	D	D	D	D	D	S	D	D	D	D	D
			ASA	D	D	D	S	D	D	D	D	S	D	S	S	D	D	D	D
		PG 70-28	Neat	D	S	D	D	D	D	D	D	D	D	D	D	D	D	S	D
			RAP	S	S	D	D	D	D	S	D	D	D	D	D	S	D	S	D
			WMA	S	D	D	D	D	D	S	D	D	D	D	D	S	D	S	S
			ASA	D	S	S	S	D	D	D	D	D	S	S	D	D	D	S	D

D=Significantly different average pull-off strength S=Significantly same average pull-off strength				Quartzite															
Statistical significance 				Moisture Conditioned															
				PG 58-28				PG 64-22				PG 64-34				PG 70-28			
				Neat	RAP	WMA	ASA	Neat	RAP	WMA	ASA	Neat	RAP	WMA	ASA	Neat	RAP	WMA	ASA
Quartzite	Moisture Conditioned	PG 58-28	Neat	S	S	S	D	S	S	D	D	D	S	S	S	D	D	D	D
			RAP	S	S	S	D	D	S	D	D	D	S	D	S	D	D	D	D
			WMA	S	S	S	D	S	S	D	D	D	S	S	S	D	D	D	D
			ASA	D	D	D	S	S	D	S	S	D	D	D	D	S	S	D	S
		PG 64-22	Neat	S	D	S	S	S	S	D	S	D	S	S	D	D	D	D	S
			RAP	S	S	S	D	S	S	D	D	D	S	S	S	D	D	D	D
			WMA	D	D	D	S	D	D	S	D	D	D	D	D	S	S	S	S
			ASA	D	D	D	S	S	D	D	S	D	D	D	D	S	S	D	S
		PG 64-34	Neat	D	D	D	D	D	D	D	D	S	D	D	D	D	D	D	D
			RAP	S	S	S	D	S	S	D	D	D	S	S	S	D	D	D	D
			WMA	S	D	S	D	S	S	D	D	D	S	S	S	D	D	D	D
			ASA	S	S	S	D	D	S	D	D	D	S	S	S	D	D	D	D
		PG 70-28	Neat	D	D	D	S	D	D	S	S	D	D	D	D	S	S	D	S
			RAP	D	D	D	S	D	D	S	S	D	D	D	D	S	S	S	S
			WMA	D	D	D	D	D	D	S	D	D	D	D	D	D	S	S	D
			ASA	D	D	D	S	S	D	S	S	D	D	D	D	S	S	D	S



[illegible]

[illegible]

D=Significantly different average pull-off strength S=Significantly same average pull-off strength				Granite															
				Unconditioned															
<div>Statistical significance</div> 				PG 58-28				PG 64-22				PG 64-34				PG 70-28			
				Neat	RAP	WMA	ASA	Neat	RAP	WMA	ASA	Neat	RAP	WMA	ASA	Neat	RAP	WMA	ASA
				Neat	RAP	WMA	ASA	Neat	RAP	WMA	ASA	Neat	RAP	WMA	ASA	Neat	RAP	WMA	ASA
Granite	Unconditioned	PG 58-28	Neat	S	S	D	D	D	D	D	D	D	S	D	D	D	D	S	D
			RAP	S	S	S	D	D	D	S	D	D	S	D	D	S	D	S	D
			WMA	D	S	S	S	D	D	D	D	D	S	S	D	D	D	D	D
			ASA	D	D	S	S	D	D	D	D	D	D	S	D	D	D	D	D
		PG 64-22	Neat	D	D	D	D	S	D	D	D	D	D	D	D	D	S	D	S
			RAP	D	D	D	D	D	S	D	S	D	D	D	D	D	D	D	D
			WMA	D	S	D	D	D	D	S	D	D	D	D	D	S	D	S	S
			ASA	D	D	D	D	D	S	D	S	D	D	D	D	D	D	D	D
		PG 64-34	Neat	D	D	D	D	D	D	D	D	S	D	D	D	D	D	D	D
			RAP	S	S	S	D	D	D	D	D	D	S	S	D	D	D	S	D
			WMA	D	D	S	S	D	D	D	D	D	S	S	D	D	D	D	D
			ASA	D	D	D	D	D	D	D	D	D	D	D	S	D	D	D	D
		PG 70-28	Neat	D	S	D	D	D	D	S	D	D	D	D	D	S	D	S	S
			RAP	D	D	D	D	S	D	D	D	D	D	D	D	D	S	D	S
			WMA	S	S	D	D	D	D	S	D	D	S	D	D	S	D	S	D
			ASA	D	D	D	D	S	D	S	D	D	D	D	D	S	S	D	S

[illegible]

D=Significantly different average pull-off strength S=Significantly same average pull-off strength				Gravel															
Statistical significance				Unconditioned															
				PG 58-28				PG 64-22				PG 64-34				PG 70-28			
				Neat	RAP	WMA	ASA	Neat	RAP	WMA	ASA	Neat	RAP	WMA	ASA	Neat	RAP	WMA	ASA
Granite	Moisture Conditioned	PG 58-28	Neat	D	D	D	S	D	D	D	D	D	S	S	D	D	D	D	D
			RAP	D	D	D	D	D	D	D	D	D	D	D	D	D	D	D	D
			WMA	S	D	D	S	S	D	D	D	D	S	D	D	D	D	S	D
			ASA	D	D	S	D	D	D	D	D	S	D	D	S	D	D	D	D
		PG 64-22	Neat	D	D	S	D	D	D	D	D	S	D	D	S	D	D	D	D
			RAP	D	D	D	D	D	D	D	D	S	D	D	S	D	D	D	D
			WMA	S	S	D	S	S	D	D	D	D	S	S	D	D	D	S	S
			ASA	D	D	D	D	D	D	D	D	S	D	D	S	D	D	D	D
		PG 64-34	Neat	D	D	D	D	D	D	D	D	D	D	D	D	D	D	D	D
			RAP	D	D	D	D	D	D	D	D	D	D	D	D	D	D	D	D
			WMA	D	D	D	D	D	D	D	D	S	D	D	S	D	D	D	D
			ASA	D	D	D	D	D	D	D	D	D	D	D	D	D	D	D	D
		PG 70-28	Neat	D	D	D	D	D	D	D	D	D	D	D	S	D	D	D	D
			RAP	D	D	D	S	D	D	D	D	D	D	S	D	D	D	D	D
			WMA	D	D	S	D	D	D	D	D	S	D	D	S	D	D	D	D
			ASA	D	D	D	S	D	D	D	D	D	S	S	D	D	D	D	D

D=Significantly different average pull-off strength S=Significantly same average pull-off strength				Gravel															
Statistical significance				Moisture Conditioned															
				PG 58-28				PG 64-22				PG 64-34				PG 70-28			
				Neat	RAP	WMA	ASA	Neat	RAP	WMA	ASA	Neat	RAP	WMA	ASA	Neat	RAP	WMA	ASA
Granite	Moisture Conditioned	PG 58-28	Neat	D	D	S	S	D	S	S	S	D	D	D	D	D	S	D	S
			RAP	D	D	D	D	D	D	D	D	D	D	D	D	D	D	D	D
			WMA	D	D	S	D	D	S	S	S	D	D	D	D	D	S	D	S
			ASA	D	D	D	D	S	D	D	D	D	D	S	S	S	D	D	D
		PG 64-22	Neat	D	D	D	D	S	D	D	D	D	D	S	S	S	D	D	D
			RAP	D	D	D	D	S	D	D	D	D	D	S	S	S	D	D	D
			WMA	D	D	S	S	D	S	S	S	D	D	D	D	D	S	S	S
			ASA	D	D	D	D	S	D	D	D	D	D	S	D	D	D	D	D
		PG 64-34	Neat	S	S	D	D	D	D	D	D	D	S	D	D	D	D	D	D
			RAP	D	D	D	D	D	D	D	D	D	D	D	D	D	D	D	D
			WMA	D	D	D	D	S	D	D	D	D	D	S	S	D	D	D	D
			ASA	D	D	D	S	D	D	D	D	D	D	S	S	S	D	D	D
		PG 70-28	Neat	S	S	D	D	D	D	D	D	D	S	D	D	D	D	D	D
			RAP	D	D	S	S	D	D	D	D	D	D	D	S	S	D	D	S
			WMA	D	D	D	D	S	D	D	D	D	D	S	S	S	D	D	D
			ASA	D	D	S	S	D	D	D	D	D	D	D	S	S	D	D	S



D=Significantly different average pull-off strength S=Significantly same average pull-off strength				Quartzite															
Statistical significance				Unconditioned															
				PG 58-28				PG 64-22				PG 64-34				PG 70-28			
				Neat	RAP	WMA	ASA	Neat	RAP	WMA	ASA	Neat	RAP	WMA	ASA	Neat	RAP	WMA	ASA
Granite	Moisture Conditioned	PG 58-28	Neat	D	S	D	S	D	D	D	D	D	S	S	D	D	D	D	D
			RAP	D	D	D	D	D	D	D	D	D	D	D	D	D	D	D	D
			WMA	D	S	D	D	D	D	D	D	D	S	D	D	D	D	S	D
			ASA	D	D	D	S	D	D	D	D	S	D	D	S	D	D	D	D
		PG 64-22	Neat	D	D	D	D	D	D	D	D	S	D	D	S	D	D	D	D
			RAP	D	D	D	D	D	D	D	D	S	D	D	S	D	D	D	D
			WMA	S	S	S	D	D	D	S	D	D	S	D	D	S	D	S	D
			ASA	D	D	D	D	D	D	D	D	S	D	D	S	D	D	D	D
		PG 64-34	Neat	D	D	D	D	D	D	D	D	D	D	D	D	D	D	D	D
			RAP	D	D	D	D	D	D	D	D	D	D	D	D	D	D	D	D
			WMA	D	D	D	D	D	D	D	D	S	D	D	S	D	D	D	D
			ASA	D	D	D	S	D	D	D	D	D	D	S	S	D	D	D	D
		PG 70-28	Neat	D	D	D	D	D	D	D	D	D	D	D	D	D	D	D	D
			RAP	D	D	S	S	D	D	D	D	D	S	S	D	D	D	D	D
			WMA	D	D	D	S	D	D	D	D	S	D	S	S	D	D	D	D
			ASA	D	D	S	S	D	D	D	D	D	S	S	D	D	D	D	D

D=Significantly different average pull-off strength S=Significantly same average pull-off strength				Quartzite															
Statistical significance				Moisture Conditioned															
				PG 58-28				PG 64-22				PG 64-34				PG 70-28			
				Neat	RAP	WMA	ASA	Neat	RAP	WMA	ASA	Neat	RAP	WMA	ASA	Neat	RAP	WMA	ASA
Granite	Moisture Conditioned	PG 58-28	Neat	D	D	D	S	S	D	D	S	D	D	D	D	S	S	D	S
			RAP	D	D	D	D	D	D	D	D	D	D	D	D	D	D	D	D
			WMA	D	D	D	S	D	D	S	S	D	D	D	D	S	S	D	S
			ASA	S	S	S	D	D	S	D	D	D	S	D	S	D	D	D	D
		PG 64-22	Neat	S	S	D	D	D	S	D	D	D	S	D	S	D	D	D	D
			RAP	D	S	S	D	D	S	D	D	D	S	D	S	D	D	D	D
			WMA	D	D	D	S	S	D	S	S	D	D	D	D	S	S	S	S
			ASA	D	S	D	D	D	D	D	D	D	S	D	S	D	D	D	D
		PG 64-34	Neat	D	D	D	D	D	D	D	D	D	D	D	D	D	D	D	D
			RAP	D	D	D	D	D	D	D	D	S	D	D	D	D	D	D	D
			WMA	D	S	D	D	D	D	D	D	D	S	D	S	D	D	D	D
			ASA	S	D	S	D	S	S	D	D	D	S	S	S	D	D	D	D
		PG 70-28	Neat	D	D	D	D	D	D	D	D	D	D	D	D	D	D	D	D
			RAP	D	D	S	S	S	S	D	D	D	S	D	D	D	D	D	S
			WMA	S	S	S	D	S	S	D	D	D	S	S	S	D	D	D	D
			ASA	D	D	S	S	S	S	D	S	D	S	S	D	D	D	D	S

D=Significantly different average pull-off strength S=Significantly same average pull-off strength				Granite															
Statistical significance				Unconditioned															
				PG 58-28				PG 64-22				PG 64-34				PG 70-28			
				Neat	RAP	WMA	ASA	Neat	RAP	WMA	ASA	Neat	RAP	WMA	ASA	Neat	RAP	WMA	ASA
Granite	Moisture Conditioned	PG 58-28	Neat	D	S	S	S	D	D	D	D	D	S	S	D	D	D	D	D
			RAP	D	D	D	D	D	D	D	D	D	D	D	D	D	D	D	D
			WMA	S	S	S	S	D	D	D	D	D	S	S	D	D	D	S	D
			ASA	D	D	D	D	D	D	D	D	S	D	D	D	D	D	D	D
		PG 64-22	Neat	D	D	D	D	D	D	D	D	S	D	D	S	D	D	D	D
			RAP	D	D	D	D	D	D	D	D	S	D	D	S	D	D	D	D
			WMA	S	S	S	S	D	D	D	D	D	S	S	D	S	D	S	D
			ASA	D	D	D	D	D	D	D	D	S	D	D	S	D	D	D	D
		PG 64-34	Neat	D	D	D	D	D	D	D	D	D	D	D	D	D	D	D	D
			RAP	D	D	D	D	D	D	D	D	D	D	D	D	D	D	D	D
			WMA	D	D	D	D	D	D	D	D	S	D	D	S	D	D	D	D
			ASA	D	D	D	D	D	D	D	D	S	D	S	D	D	D	D	D
		PG 70-28	Neat	D	D	D	D	D	D	D	D	D	D	D	S	D	D	D	D
			RAP	D	D	S	S	D	D	D	D	D	D	S	D	D	D	D	D
			WMA	D	D	D	D	D	D	D	D	S	D	D	S	D	D	D	D
			ASA	D	D	S	S	D	D	D	D	D	D	S	D	D	D	D	D

D=Significantly different average pull-off strength S=Significantly same average pull-off strength				Granite															
Statistical significance				Moisture Conditioned															
				PG 58-28				PG 64-22				PG 64-34				PG 70-28			
				Neat	RAP	WMA	ASA	Neat	RAP	WMA	ASA	Neat	RAP	WMA	ASA	Neat	RAP	WMA	ASA
Granite	Moisture Conditioned	PG 58-28	Neat	S	D	S	D	D	D	S	D	D	D	D	D	D	D	D	S
			RAP	D	S	D	D	D	D	D	D	D	D	D	D	D	D	D	D
			WMA	S	D	S	D	D	D	S	D	D	D	D	D	D	D	D	D
			ASA	D	D	D	S	S	S	D	S	D	D	S	D	D	D	S	D
		PG 64-22	Neat	D	D	D	S	S	S	D	S	D	D	S	D	D	D	S	D
			RAP	D	D	D	S	S	S	D	S	D	D	S	D	D	D	S	D
			WMA	S	D	S	D	D	D	S	D	D	D	D	D	D	D	D	D
			ASA	D	D	D	S	S	S	D	S	D	D	S	D	S	D	S	D
		PG 64-34	Neat	D	D	D	D	D	D	D	D	S	D	D	D	S	D	D	D
			RAP	D	D	D	D	D	D	D	D	S	D	D	D	D	D	D	D
			WMA	D	D	D	S	S	S	D	S	D	D	S	D	D	D	S	D
			ASA	D	D	D	D	D	D	D	D	D	D	S	D	S	S	S	S
		PG 70-28	Neat	D	D	D	D	D	D	D	S	S	D	D	D	S	D	D	D
			RAP	D	D	D	D	D	D	D	D	D	D	D	S	D	S	D	S
			WMA	D	D	D	S	S	S	D	S	D	D	S	S	D	D	S	D
			ASA	S	D	D	D	D	D	D	D	D	D	S	D	S	D	S	S

## REFERENCES

- AASHTO. (2010). Resistance of Compacted Hot Mix Asphalt (HMA) to Moisture-Induced Damage. In: American Association of State Highway and Transportation Officials (AASHTO), Washington, DC, USA.
- AASHTO. (2011). Determining Asphalt Binder Bond Strength by Means of the Bitumen Bond Strength (BBS) Test In: American Association of State Highway and Transportation Officials (AASHTO), Washington, DC, USA.
- AASHTO. (2012). Superpave Volumetric Mix Design. In: American Association of State Highway and Transportation Officials (AASHTO), Washington, DC, USA.
- AASHTO. (2013a). Standard method of test for determining the fracture energy of asphalt mixtures using the semicircular bend geometry (SCB). In: American Association of State Highway and Transportation Officials (AASHTO), Washington, DC, USA.
- AASHTO. (2013b). Theoretical maximum specific gravity (Gmm) and density of hot mix asphalt (HMA). In: American Association of State Highway and Transportation Officials (AASHTO), Washington, DC, USA.
- AASHTO. (2016). Standard method of test for bulk specific gravity (Gmb) of compacted hot mix asphalt (HMA) using saturated surface-dry specimens. In: American Association of State Highway and Transportation Officials (AASHTO), Washington, DC, USA.
- Abuawad, I. M. A., Al-Qadi, I. L., & Trepanier, J. S. (2015). Mitigation of moisture damage in asphalt concrete: Testing techniques and additives/modifiers effectiveness. *Construction and Building Materials*, 84, 437-443. doi:10.1016/j.conbuildmat.2015.03.001
- Ahmad, J., Yusoff, N. I. M., Hainin, M. R., Abd Rahman, M. Y., & Hossain, M. (2014). Investigation into hot-mix asphalt moisture-induced damage under tropical climatic conditions. *Construction and Building Materials*, 50, 567-576. doi:10.1016/j.conbuildmat.2013.10.017
- Ahmad, M., Mannan, U. A., Islam, M. R., & Tarefder, R. A. (2017). Chemical and mechanical changes in asphalt binder due to moisture conditioning. *Road Materials and Pavement Design*, 1-14. doi:10.1080/14680629.2017.1299631
- Alavi, M. Z., Hajj, E. Y., Hanz, A., & Bahia, H. U. (2012). Evaluating Adhesion Properties and Moisture Damage Susceptibility of Warm-Mix Asphalts Bitumen Bond Strength and Dynamic Modulus Ratio Tests. *Transportation Research Record*(2295), 44-53. doi:10.3141/2295-06
- Amelian, S., Abtahi, S. M., & Hejazi, S. M. (2014). Moisture susceptibility evaluation of asphalt mixes based on image analysis. *Construction and Building Materials*, 63, 294-302. doi:10.1016/j.conbuildmat.2014.04.012
- Apeagyei, A. K., Grenfell, J. R. A., & Airey, G. D. (2015). Influence of aggregate absorption and diffusion properties on moisture damage in asphalt mixtures. *Road Materials and Pavement Design*, 16, 404-422. doi:10.1080/14680629.2015.1030827
- Asphalt-Magazine. (2018). *How much does density matter ?* , Retrieved from <http://www.pavementinteractive.org/stripping/>

- ASTM. (2016). D 8044-16 Standard Test Method for Evaluation of Asphalt Mixture Cracking Resistance using the Semi-Circular Bend Test (SCB) at Intermediate Temperatures<sup>1</sup>. In *ASTM International*, 100 barr harbor Drive, PO Box C700, West Conshohocken, PA 19428-2959, United States.
- Barman, M., Ghabchi, R., Singh, D., Zaman, M., & Commuri, S. (2018). An alternative analysis of indirect tensile test results for evaluating fatigue characteristics of asphalt mixes. *Construction and Building Materials*, 166, 204-213. doi:<https://doi.org/10.1016/j.conbuildmat.2018.01.049>
- Barnes, C. L., & Trottier, J. F. (2010). Evaluating laboratory-induced asphalt concrete moisture damage using surface waves. *International Journal of Pavement Engineering*, 11(6), 489-497. doi:Pii 919193463 10.1080/10298430903578929
- Behiry, A. E. A. E.-M. (2013). Laboratory evaluation of resistance to moisture damage in asphalt mixtures. *Ain Shams Engineering Journal*, 4(3), 351-363. doi:<https://doi.org/10.1016/j.asej.2012.10.009>
- Bennert, T., Maher, A., & Sauber, R. (2011). Influence of Production Temperature and Aggregate Moisture Content on the Initial Performance of Warm-Mix Asphalt. *Transportation Research Record*(2208), 97-107. doi:10.3141/2208-13
- Bhasin, A., Masad, E., Little, D., & Lytton, R. (2006). *Limits on Adhesive Bond Energy for Improved Resistance of Hot-Mix Asphalt to Moisture Damage* (Vol. 1970).
- Canestrari, F., Ferrotti, G., Cardone, F., & Stimilli, A. (2014). Innovative Testing Protocol for Evaluation of Binder-Reclaimed Aggregate Bond Strength. *Transportation Research Record: Journal of the Transportation Research Board*, 2444, 63-70. doi:10.3141/2444-07
- Caro, S., Masad, E., Bhasin, A., & Little, D. (2010). Coupled Micromechanical Model of Moisture-Induced Damage in Asphalt Mixtures. *Journal of Materials in Civil Engineering*, 22(4), 380-388. doi:10.1061/(ASCE)MT.1943-5533.0000031
- Caro, S., Masad, E., Bhasin, A., & Little, D. N. (2008). Moisture susceptibility of asphalt mixtures, Part 1: mechanisms. *International Journal of Pavement Engineering*, 9(2), 81-98. doi:10.1080/10298430701792128
- Chen, X. W., & Huang, B. S. (2008). Evaluation of moisture damage in hot mix asphalt using simple performance and superpave indirect tensile tests. *Construction and Building Materials*, 22(9), 1950-1962. doi:10.1016/j.conbuildmat.2007.07.014
- Cho, D. W., & Kim, K. (2010). The mechanisms of moisture damage in asphalt pavement by applying chemistry aspects. *Ksce Journal of Civil Engineering*, 14(3), 333-341. doi:10.1007/s12205-010-0333-z
- Cong, P. L., Zhang, Y. H., & Liu, N. (2016). Investigation of the properties of asphalt mixtures incorporating reclaimed SBS modified asphalt pavement. *Construction and Building Materials*, 113, 334-340. doi:10.1016/j.conbuildmat.2016.03.059
- Copeland, A. R., Youtcheff, J., & Shenoy, A. (2007). Moisture sensitivity of modified asphalt binders - Factors influencing bond strength. *Transportation Research Record*(1998), 18-28. doi:10.3141/1998-03
- Cucalon, L. G., Kassem, E., Little, D. N., & Masad, E. (2017). Fundamental evaluation of moisture damage in warm-mix asphalts. *Road Materials and Pavement Design*, 18, 258-283. doi:10.1080/14680629.2016.1266765

- Cui, X. Z., Zhang, J., Zhang, N., Zhou, Y. X., Gao, Z. J., & Sui, W. (2015). Laboratory simulation tests of effect of mechanical damage on moisture damage evolution in hot-mix asphalt pavement. *International Journal of Pavement Engineering*, 16(8), 699-709. doi:10.1080/10298436.2014.943221
- Das, P. K., Baaj, H., Kringos, N., & Tighe, S. (2015). Coupling of oxidative ageing and moisture damage in asphalt mixtures. *Road Materials and Pavement Design*, 16, 265-279. doi:10.1080/14680629.2015.1030835
- Fakhri, M., & Ahmadi, A. (2017a). Evaluation of fracture resistance of asphalt mixes involving steel slag and RAP: Susceptibility to aging level and freeze and thaw cycles. *Construction and Building Materials*, 157, 748-756. doi:10.1016/j.conbuildmat.2017.09.116
- Fakhri, M., & Hosseini, S. A. (2017b). Laboratory evaluation of rutting and moisture damage resistance of glass fiber modified warm mix asphalt incorporating high RAP proportion. *Construction and Building Materials*, 134, 626-640. doi:10.1016/j.conbuildmat.2016.12.168
- Ghabchi, R., Singh, D., & Zaman, M. (2014). Evaluation of moisture susceptibility of asphalt mixes containing RAP and different types of aggregates and asphalt binders using the surface free energy method. *Construction and Building Materials*, 73, 479-489. doi:<https://doi.org/10.1016/j.conbuildmat.2014.09.042>
- Ghabchi, R., Singh, D., & Zaman, M. (2015). Laboratory evaluation of stiffness, low-temperature cracking, rutting, moisture damage, and fatigue performance of WMA mixes. *Road Materials and Pavement Design*, 16(2), 334-357. doi:10.1080/14680629.2014.1000943
- Ghabchi, R., Singh, D., Zaman, M., & Hossain, Z. (2016). Laboratory characterisation of asphalt mixes containing RAP and RAS. *International Journal of Pavement Engineering*, 17(9), 829-846. doi:10.1080/10298436.2015.1022778
- Gong, W. Y., Tao, M. J., Mallick, R. B., & El-Korchi, T. (2012). Investigation of Moisture susceptibility of Warm-Mix Asphalt Mixes Through Laboratory Mechanical Testing. *Transportation Research Record*(2295), 27-34. doi:10.3141/2295-04
- HMA Construction*. (2001). Retrieved from Lexington, KY:
- Hossain, M. I., & Tarefder, R. A. (2014). Quantifying moisture damage at mastic-aggregate interface. *International Journal of Pavement Engineering*, 15(2), 174-189. doi:10.1080/10298436.2013.812212
- Huang, B., Shu, X., Dong, Q., & Shen, J. (2010). Laboratory Evaluation of Moisture Susceptibility of Hot-Mix Asphalt Containing Cementitious Fillers. *Journal of Materials in Civil Engineering*, 22(7), 667-673. doi:10.1061/(ASCE)MT.1943-5533.0000064
- Huang, B. S., Shu, X., & Zuo, G. (2013). Using notched semi circular bending fatigue test to characterize fracture resistance of asphalt mixtures. *Engineering Fracture Mechanics*, 109, 78-88. doi:10.1016/j.engfracmech.2013.07.003
- Jahromi, S. G. (2009). Estimation of resistance to moisture destruction in asphalt mixtures. *Construction and Building Materials*, 23(6), 2324-2331. doi:10.1016/j.conbuildmat.2008.11.007

- Kakar, M. R., Hamzah, M. O., & Valentin, J. (2015). A review on moisture damages of hot and warm mix asphalt and related investigations. *Journal of Cleaner Production*, 99, 39-58. doi:10.1016/j.jclepro.2015.03.028
- Kanitpong, K., & Bahia, H. (2005). Relating adhesion and cohesion of asphalts to the effect of moisture on laboratory performance of asphalt mixtures. *Bituminous Binders 2005*(1901), 33-43. doi:Doi 10.3141/1901-05
- Kim, M., Mohammad, L. N., Challa, H., & Elseifi, M. A. (2015). A simplified performance-based specification for asphalt pavements. *Road Materials and Pavement Design*, 16, 168-196. doi:10.1080/14680629.2015.1077005
- Kim, Y. R. (2011). Cohesive zone model to predict fracture in bituminous materials and asphaltic pavements: state-of-the-art review. *International Journal of Pavement Engineering*, 12(4), 343-356. doi:10.1080/10298436.2011.575138
- Kim, Y. R., Lutfi, J. S., Bhasin, A., & Little, D. N. (2008). Evaluation of moisture damage mechanisms and effects of hydrated lime in asphalt mixtures through measurements of mixture component properties and performance testing. *Journal of Materials in Civil Engineering*, 20(10), 659-667. doi:10.1061/(Asce)0899-1561(2008)20:10(659)
- Kim, Y. R., Zhang, J., & Ban, H. (2012). Moisture damage characterization of warm-mix asphalt mixtures based on laboratory-field evaluation. *Construction and Building Materials*, 31, 204-211. doi:10.1016/j.conbuildmat.2011.12.085
- Kringos, N., & Scarpas, A. (2007). *Simulation of combined physical-mechanical moisture induced damage in asphaltic mixes*. Paper presented at the International Conference on Advanced Characterisation of Pavement and Soil Engineering Materials, June 20, 2007 - June 22, 2007, Athens, Greece.
- Kringos, N., & Scarpas, A. (2008a). Physical and mechanical moisture susceptibility of asphaltic mixtures. *International Journal of Solids and Structures*, 45(9), 2671-2685. doi:10.1016/j.ijsolstr.2007.12.017
- Kringos, N., Scarpas, A., Copeland, A., & Youtcheff, J. (2008b). Modelling of combined physical-mechanical moisture-induced damage in asphaltic mixes Part 2: moisture susceptibility parameters. *International Journal of Pavement Engineering*, 9(2), 129-151. doi:10.1080/10298430701792227
- Kringos, N., Scarpas, T., Kasbergen, C., & Selvadurai, P. (2008c). Modelling of combined physical-mechanical moisture-induced damage in asphaltic mixes, Part 1: governing processes and formulations. *International Journal of Pavement Engineering*, 9(2), 115-128. doi:10.1080/10298430701792185
- LaCroix, A., Regimand, A., & James, L. (2016). Proposed Approach for Evaluation of Cohesive and Adhesive Properties of Asphalt Mixtures for Determination of Moisture Sensitivity. *Transportation Research Record*(2575), 61-69. doi:10.3141/2575-07
- Lee, J. S., Lee, J. J., Kwon, S. A., & Kim, Y. R. (2013). Use of Cyclic Direct Tension Tests and Digital Imaging Analysis to Evaluate Moisture Susceptibility of Warm-Mix Asphalt Concrete. *Transportation Research Record*(2372), 61-71. doi:10.3141/2372-08

- Lopez-Montero, T., & Miro, R. (2016). Differences in cracking resistance of asphalt mixtures due to ageing and moisture damage. *Construction and Building Materials*, 112, 299-306. doi:10.1016/j.conbuildmat.2016.02.199
- Lu, Q., T Harvey, J., & L Monismith, C. (2007). *Investigation of Conditions for Moisture Damage in Asphalt Concrete and Appropriate Laboratory Test Methods: Summary Version*. Retrieved from
- Lu, Y., & Wang, L. B. (2017). Atomistic modelling of moisture sensitivity: a damage mechanisms study of asphalt concrete interfaces. *Road Materials and Pavement Design*, 18, 200-214. doi:10.1080/14680629.2017.1329875
- Mallick, R. B., Pelland, R., & Hugo, F. (2005). Use of accelerated loading equipment for determination of long term moisture susceptibility of hot mix asphalt. *International Journal of Pavement Engineering*, 6(2), 125-136. doi:10.1080/10298430500158984
- Mogawer, W., Austerman, A., Mohammad, L., & Kutay, M. E. (2013). Evaluation of high RAP-WMA asphalt rubber mixtures. *Road Materials and Pavement Design*, 14, 129-147. doi:10.1080/14680629.2013.812846
- Mogawer, W. S., Austerman, A. J., & Bahia, H. U. (2011). Evaluating the Effect of Warm-Mix Asphalt Technologies on Moisture Characteristics of Asphalt Binders and Mixtures. *Transportation Research Record*(2209), 52-60. doi:10.3141/2209-07
- Mohammad, L. N., Kim, M., & Elseifi, M. (2012, 2012//). *Characterization of Asphalt Mixture's Fracture Resistance Using the Semi-Circular Bending (SCB) Test*. Paper presented at the 7th RILEM International Conference on Cracking in Pavements, Dordrecht.
- Moraes, R., Velasquez, R., & Bahia, H. U. (2011). Measuring the Effect of Moisture on Asphalt-Aggregate Bond with the Bitumen Bond Strength Test. *Transportation Research Record*(2209), 70-81. doi:10.3141/2209-09
- Nazirizad, M., Kavussi, A., & Abdi, A. (2015). Evaluation of the effects of anti-stripping agents on the performance of asphalt mixtures. *Construction and Building Materials*, 84, 348-353. doi:10.1016/j.conbuildmat.2015.03.024
- Ozer, H., Al-Qadi, I. L., Lambros, J., El-Khatib, A., Singhvi, P., & Doll, B. (2016). Development of the fracture-based flexibility index for asphalt concrete cracking potential using modified semi-circle bending test parameters. *Construction and Building Materials*, 115, 390-401. doi:10.1016/j.conbuildmat.2016.03.144
- Pavement-Interactive. (2018). Stripping Retrieved from <http://www.pavementinteractive.org/stripping/>
- Saha, G., & Biligiri, K. P. (2016a). Fracture properties of asphalt mixtures using semi-circular bending test: A state-of-the-art review and future research. *Construction and Building Materials*, 105, 103-112. doi:10.1016/j.conbuildmat.2015.12.046
- Saha, G., & Biligiri, K. P. (2016b). Homothetic behaviour investigation on fracture toughness of asphalt mixtures using semicircular bending test. *Construction and Building Materials*, 114, 423-433. doi:<https://doi.org/10.1016/j.conbuildmat.2016.03.169>
- Singh, D., Chitragar, S. F., & Ashish, P. K. (2017). Comparison of moisture and fracture damage resistance of hot and warm asphalt mixes containing reclaimed pavement



- materials. *Construction and Building Materials*, 157, 1145-1153.  
doi:10.1016/j.conbuildmat.2017.09.176
- Tarefder, R. A., & Ahmad, M. (2015). Evaluating the Relationship between Permeability and Moisture Damage of Asphalt Concrete Pavements. *Journal of Materials in Civil Engineering*, 27(5). doi:Artn 04014172  
10.1061/(Asce)Mt.1943-5533.0001129
- Tarefder, R. A., & Ahmad, M. (2017). Evaluation of pore structure and its influence on permeability and moisture damage in asphalt concrete. *International Journal of Pavement Engineering*, 18(3), 274-283. doi:10.1080/10298436.2015.1065995
- Tarefder, R. A., & Yousefi, S. S. (2012). Laboratory evaluation of moisture damage in asphalt. *Canadian Journal of Civil Engineering*, 39(1), 104-115.  
doi:10.1139/L11-114
- Varveri, A., Avgerinopoulos, S., & Scarpas, A. (2016). Experimental evaluation of long- and short-term moisture damage characteristics of asphalt mixtures. *Road Materials and Pavement Design*, 17(1), 168-186.  
doi:10.1080/14680629.2015.1066705
- Varveri, A., Huang, A., Benedetto, S. D., & Herve. (2015). Moisture damage in asphaltic mixtures. *Advances in road materials : road and pavement construction*, 303-344.
- Wasiuddin, N. L. M., Zaman, M. M., & D'Rear, E. A. (2008). Effect of Sasobit and Aspha-Min on Wettability and Adhesion Between Asphalt Binders and Aggregates. *Transportation Research Record*(2051), 80-89. doi:10.3141/2051-10
- Wasiuddin, N. M., Saltibus, N. E., & Mohammad, L. N. (2011). Novel Moisture-Conditioning Method for Adhesive Failure of Hot- and Warm-Mix Asphalt Binders. *Transportation Research Record*(2208), 108-117. doi:10.3141/2208-14
- Wasiuddin, N. M., Zaman, M. M., & O'Rear, E. A. (2010). Polymeric Aggregate Treatment Using Styrene-Butadiene Rubber (SBR) for Moisture-Induced Damage Potential. *International Journal of Pavement Research and Technology*, 3(1), 1-9.  
doi:10.6135/ijprt.org.tw/2010.3(1).1
- Weldegiorgis, M. T., & Tarefder, R. A. (2015). Towards a Mechanistic Understanding of Moisture Damage in Asphalt Concrete. *Journal of Materials in Civil Engineering*, 27(3). doi:Artn 04014128  
10.1061/(Asce)Mt.1943-5533.0001062
- Wen, H. F., Wu, S. H., Mohammad, L. N., Zhang, W. G., Shen, S. H., & Faheem, A. (2016). Long-Term Field Rutting and Moisture Susceptibility Performance of Warm-Mix Asphalt Pavement. *Transportation Research Record*(2575), 103-112.  
doi:10.3141/2575-11
- Xiao, F. P., Jordan, J., & Amirkhanian, S. N. (2009). Laboratory Investigation of Moisture Damage in Warm-Mix Asphalt Containing Moist Aggregate. *Transportation Research Record*(2126), 115-124. doi:10.3141/2126-14
- Yang, S., Braham, A., Wang, L. F., & Wang, Q. K. (2016). Influence of aging and moisture on laboratory performance of asphalt concrete. *Construction and Building Materials*, 115, 527-535. doi:10.1016/j.conbuildmat.2016.04.063
- Zhang, J. Z., Airey, G. D., Grenfell, J., & Apeagyei, A. K. (2017). Moisture damage evaluation of aggregate-bitumen bonds with the respect of moisture absorption,



tensile strength and failure surface. *Road Materials and Pavement Design*, 18(4), 833-848. doi:10.1080/14680629.2017.1286441